2-1-2011

Development of prototype gold nanoparticle-dased immunoassays for the detection of plasmodium falciparum hsp70

Bassem Samy Guirgis

The American University in Cairo

School of Sciences and Engineering

Development of Prototype Gold Nanoparticle-Based Immunoassays for the detection of *Plasmodium falciparum* Hsp70

A Thesis Submitted to

The Biotechnology Graduate Program

in partial fulfilment of the requirements for

the degree of Master of Science in Biotechnology

By: Bassem Samy Guirgis

Bachelor of Pharmaceutical Sciences-Ain Shams University

Under the supervision of: Prof. Hassan M. E. Azzazy and Prof. Ricardo Franco

Fall 2010

The American University in Cairo

Development of Prototype Gold Nanoparticle-Based Immunoassays for the detection of *Plasmodium falciparum* Hsp70

A Thesis Submitted by Bassem Samy Guirgis

To the Biotechnology Graduate Program, Fall 2010

in partial fulfilment of the requirements for the degree of Master of Science in Biotechnology has been approved by:

Prof. Hassan M.E. Azzazy

Thesis Committee Chair / Advisor

Affiliation: Associate Dean for Graduate Studies & Research; School of Sciences & Engineering; The American University In Cairo.

Prof. Ricardo Franco

Co-advisor

Affiliation: Assistant Professor of Chemistry at the Faculdade de Ciências e Tecnologia, Universidade Nova de Lisboa, Portugal

Prof. Miguel Prudêncio

Thesis Committee Reader / External examiner

Affiliation: Staff Scientist of the Malaria division of Instituto de Medicina Molecular, Portugal

Prof. Suher Zada

Thesis Committee Reader / Internal examiner

Affiliation: Professor, Biology department; The American University In Cairo.

Prof. Salah El Sheikh

Observer

Affiliation: Professor and associate chair, Department of Physics; The American University In Cairo.

Program Director Date

Dean Date

ACKNOWLEDGMENTS

I would like to acknowledge my advisor Professor Hassan Azzazy (Associate Dean for Graduate Studies & Research; School of Sciences & Engineering; The American University In Cairo) for upgrading my writing as well as experimental skills and who was always with me throughout the previous 3 years. I would also like to acknowledge my co-advisor Professor Ricardo Franco (Assistant Professor of Chemistry at the Faculdade de Ciências e Tecnologia, Universidade Nova de Lisboa, Portugal) who has helped me do my experimental part of my thesis in Portugal. I would also acknowledge Inês Gomes (Post Doc) who worked with me throughout the whole experimental project. Miguel Prudêncio (Staff Scientist of the Malaria division of Instituto de Medicina Molecular) and Claudia Sa e Cunha (Post Doc; Unidade de Malaria; Portugal) took me through the biological part of my thesis. I would acknowledge my Egyptian (Sherif Shawky and Mai Mansour) as well as my protégées colleagues (Joao Cortez and Inês Osorio) who were always hand in hand with me through my studies. The study was supported by FLAD (Luso-American Foundation) and FCT/MCTES: REQUIMTE; PTDC/BIO/66514/2006, PTDC/SAU-BEB/66511/2006 and PTDC/QUI/64484/2006. STRC has provided me the graduate scholarship that helped a lot to reach what I have reached so far. Last but not least, I would acknowledge my mother that supported me financially and emotionally throughout the years.

ABSTRACT

The American University in Cairo

Development of Prototype Gold Nanoparticle-Based Immunoassays for the detection of *Plasmodium falciparum* Hsp70

By: Bassem Samy Guirgis

Under the supervision of: Prof. Hassan M. E. Azzazy and Prof. Ricardo Franco

Biomedical nanotechnology is providing revolutionary opportunities for the rapid and simple diagnosis of many infectious diseases. About half of the world's population are at risk of infection with malaria and diagnostic assays available either lack sensitivity and specificity or require expensive equipment, expertise or costly infrastructure; that are not usually available in countries where the disease is endemic. Thus, there is an urgent need to develop rapid, sensitive, and inexpensive diagnostic tests for malaria for both high- and low-resource settings. In this study, we developed two prototype gold nanoparticle (AuNP)-based immunoassays for the detection of *Plasmodium falciparum* Heat Shock Protein 70 (*Pf*Hsp70) antigen. *Pf*Hsp70 is a heat shock protein that has recently attracted attention as a novel therapeutic target. Monoclonal antibody (2E6) against *Pf*Hsp70 was produced and purified using immunoaffinity chromatography. Proof-of-concept for using Hsp70 as a diagnostic target was carried out by comparing the pellet of saponin-treated red blood cells of infected mice with that of non-infected mice or healthy humans, by Western blot. His-tagged-*Pf*Hsp70 antigen was expressed from a genetically modified *E. coli* system and purified by affinity chromatography. For the development of the immunoassays, conjugation of mercaptoundecanoic acid (MUA) capped AuNPs with 2E6 was performed in presence and absence of protein cross-linkers. Characterization of the obtained bio-nanoconjugate (BNC) was performed using UV-visible spectrophotometry, agarose gel electrophoresis and ζ-potential measurements. Stability of the BNC against high salt concentrations and pH changes was also assessed. Based on the described antibody/antigen system, two prototype immuno-competitive assays were developed in two distinct formats, namely, (i) a colorimetric chip assay, and (ii) a fluorescent quenching competitive assay. Proof-of-concept of chip assay allowed the comparison between conjugates prepared with and without NHS/EDC and it was found that non-NHS/EDC conjugates were more active. A fluorescence quenching competitive prototype assay was also developed which had a

limit of detection of 87 ng/mL (1.16 pM). As Hsp70 is a rather ubiquitous protein, other *Plasmodium* specific proteins that are secreted into the plasma of malaria patients will be identified in the future in the search of new diagnostic targets. Also further developments of the fluorescence quenching competitive assay will involve the use of cubical and decahedral AuNPs in order to try to increase the sensitivity of the assay as compared to spherical AuNPs.

TABLE OF CONTENTS

LIST OF FIGURES

LIST OF TABLES

APPENDIX

LIST OF ABBREVIATIONS

ACTs: Artemisinin-based combination therapies

AMA: Apical membrane antigen

ASV: Anodic stripping voltammetry

AuNP: Gold nanoparticle

BCA: Bicinchoninic acid.

BNC: Bio-nanoconjugate

BSA: Bovine serum albumin

CSP: Circumsporozoite protein

cTnT: Cardiac troponin T

EBA: Erythrocyte-binding antigen

EDC: 1-Ethyl-3-[3-dimethylaminopropyl] carbodiimide hydrochloride

EXP: Exported protein

FITC: Fluorescein isothiocyanate

FT: Flow through

GFR: Glomerular filtration rate

GLURP: Glutamate-rich protein

HBsAg: Hepatitis B surface antigen

HRP: Horseradish peroxidase

HRP-2: Histidine rich protein-2

ICP: Inductive Coupled Plasma

IPTG: Isopropyl β-D-1-thiogalactopyranoside

LB: Luria Broth

LOD: Limit of detection

LSA: Liver stage antigens

MSP: Merozoite surface proteins

MUA: Mercaptoundecanoic acid

NHS: N-hydroxysuccinimide

*Pb*Hsp70: *Plasmodium berghei* heat shock protein 70

PBS: Phosphate buffer saline

PCR: Polymerase chain reaction

*Pf*EMP1: Erythrocyte protein 1 antigen

*Pf*Hsp70: *Plasmodium falciparum* heat shock protein 70

pLDH: *Plasmodium* lactate dehydrogenase

PMSF: Phenyl methyl sulphonyl fluoride

RBCs: Red blood cells

RDTs: Rapid diagnostic tests

SDS-PAGE: Sodium dodecyl sulfate polyacrylamide gel electrophoresis

SPIA: Sol particle immunoassays

SPR: Surface Plasmon Resonance

SSP: Sporozoite surface protein

TEM: Transmission Electron Microscopy

CHAPTER 1. INTRODUCTION

Malaria is a protozoan infection transmitted via female *Anopheles* mosquito bites. It is one of the most common infections worldwide and about half of the world's population live in malaria-endemic areas including regions in Asia, Central and South America, Africa, Oceania, and the Caribbean islands[1]. In 2008, 247 million malaria cases were diagnosed that resulted in the death of about one million patients, mainly African children. It is reported that in Africa, malaria results in the death of a child every 45 sec[2]. Malaria infection rates are increasing worldwide and imported malaria has increased by 400% in industrialized countries in the last 20 years[3].

Patients may be infected with one or more of the 4 main species of *Plasmodium (P.)*; namely *P. falciparum, P. vivax, P. ovale* and *P. malariae*[1-2]. *P. falciparum* and *P. vivax* are the most common[2]. *P. falciparum* is the most fatal species and is the predominant species in Africa, Papua New Guinea and parts of Asia. *P. vivax* is rarely fatal but can cause severe symptoms and is most common in Central America, the Indian subcontinent, and China. *P malariae* is less common and the majority of cases are reported in sub-Saharan Africa. *P. ovale* is the rarest species, with the majority of cases reported in sub-Saharan West Africa[1].

The most common symptoms of malaria include fever (more than 92% of cases), chills (79%), headaches (70%), and diaphoresis (64%)[4]. Other symptoms include dizziness, malaise, myalgia, abdominal pain, nausea, vomiting, mild diarrhea and dry cough[4]. Common signs include fever, tachycardia, jaundice, pallor, orthostatic hypotension, hepatomegaly and splenomegaly. *P. falciparum* malaria may lead to severe complications including cerebral malaria, pulmonary edema, acute renal failure, severe anaemia, and/or bleeding, acidosis and hypoglycaemia. These complications can lead to death within hours or days from the start of symptoms[4].

The life cycle of *P. falciparum* can be divided into asexual reproduction in mammalians and sexual reproduction in female *Anopheles* mosquito (figure 1)[5-6]. In mammals (including humans), the life cycle starts with a bite of the individual by an infected mosquito. Sporozoites are released from the saliva of the mosquito into the patient's blood and then migrate to the liver. In liver cells (hepatocytes), asexual reproduction occurs leading to the production of merozoites that are released into the blood stream with the rupture of infected hepatocytes. Merozoites invade red blood

cells (RBCs) and start the erythrocytic cycle in which asexual replication occurs. Release of merozoites from infected ruptured RBCs allow invasion of more RBCs. This cycle keeps on repeating and after some time, some of the merozoites start to form male and female sexual forms in the patient blood. During the feeding of a female *Anopheles* mosquito, these sexual forms are taken up by the mosquito leading to the formation of the zygote in the midgut of the mosquito. The zygote formed matures to generate ookinetes that divide within oocysts (on external gut wall) to generate thousands of sporozoites. Sporozoites then migrate to the salivary gland ready to be injected with the next mosquito blood meal[5-6].

To reduce the risk of infection transmission, vector control is mandatory. This can be accomplished by using insecticide-treated nets, indoor residual insecticidal sprays, as well as other approaches including the reduction of standing water habitats where mosquitoes breed. Many drugs can be used for the treatment of malaria allowing shortening of infection duration, prevention of complications and avoiding deaths[2]. According to the WHO, the best available medication for malaria treatment (especially *P. falciparum*) is the use of the so called artemisinin-based combination therapies (ACTs)[2].

Until the present day, no completely effective vaccine is available, although many trials have been reported[2]. Many attempts to develop a vaccine against malaria has been reported but failure to fully develop a vaccine for malaria is suggested to be due to complexity of the parasite (expresses more than 5000 proteins during its life cycle), complexity in the interaction between parasite biology and host immunity, and finally scarcity in dedicated resources and global cooperation[7]. Vaccines developed so far target either the pre-erythrocytic, the asexual erythrocytic or the sexual stages of the parasite or others[8]. Pre-erythrocytic vaccine is potentially useful for travellers. The theory is inducing the development of antibodies that either neutralize sporozoites (preventing them from infecting hepatocytes) or triggering a cell-mediated immune resulting in death of infected hepatocytes. These include circumsporozoite protein (CSP) vaccines that incorporates CSP protein that is expressed at the surface of the sporozoite and of the infected hepatocyte[8]. During clinical trials on volunteers, the only CSP vaccine that was effective was RTS,S (C-terminal parts of the CS protein bound to S protein of HBV) when combined with a suitable adjuvant

(GlaxoSmithKline proprietary AS02A composed of MPL, QS21 and an oil-in-water emulsion) that resulted in 50% protection during Phase IIa and 30-60% in field trials[7]. Currently, a Phase III trial is being undergone for the RTS,S vaccine[8]. The second class of CSP vaccines are plasmid DNA vaccines and live recombinant vaccines that encode CSP protein. Although in mouse models, Plasmid DNA vaccines allowed for efficient humoral and cellular immune responses, it didn't provide efficient protection in humans. In addition, multiple-antigen DNA vaccine were also developed such as MuStDO-5 that encodes CSP, liver stage antigens 1 and 3 (LSA-1 and -3), exported protein 1 (EXP1), and the sporozoite surface protein 2 (SSP2). Although in mice and rabbits MuStDO-5 was found to be safe and well tolerated, it only showed weak immunogenicity in primates with no evidence of protection (Phase IIa)[8].

Asexual blood-stage (erythrocytic stage) vaccines have been developed as potentially useful for countries where malaria is endemic. The theory is inducing the development of antibodies that either inactivate merozoites or will recognize malarial antigens present on the surface of infected RBCs leading to antibody-dependent cellular cytotoxicity, complement lysis and/or trigger T-cell responses, inhibiting the development of parasites within RBCs[8]. The most advanced erythrocytic stage vaccine is based on the use of merozoite surface proteins 1 (MSP-1), 2 (MSP-2) and 3 (MSP-3), the apical membrane antigen 1 (AMA-1) and the glutamate-rich protein (GLURP). A successful vaccine was MSP-1 formulated in AS02 adjuvant that was found to be safe and immunogenetic in humans. Similarly, AMA-1 protein formulated in AS02 adjuvant caused protection against malaria in rodents and non human primates. Another successful vaccine was PfCP-2.9 that is a fusion antigen of MSP-1/AMA-1 formulated with Montanide ISA adjuvant[8]. This vaccine showed good immunogenicity in both rabbits and non-human primates. MSP-3 based vaccine was found to be safe and to successfully induce long-lasting antibodies that display antibody-dependent cellular inhibition activity in mice (phase I). Sexual stage have been developed that are potentially useful to reduce transmission of the parasite to hosts. Candidates include *P. falciparum* and *P. Vivax* ookinete surface antigens (Pfs25; Pfs28 and Pvs25; Pvs28). Phase I study for Pvs25 showed modest immunogenicity[8].

Other antigens are still being tested as efficient vaccines including MSP-4, -5, -8 and -9, erythrocyte-binding antigen (EBA-175), pregnancy-associated malaria, the erythrocyte protein 1 (*Pf*EMP1) antigen and *Pf*Hsp70[8-9]. Finally a different approach is to use attenuated parasite (such as attenuated sporozoites) to induce immunity. Whole irradiated sporozoites (Sanaria) is in its phase I[10]. Challenges in producing attenuated vaccines include producing sporozoites in large amounts, quality control during production, process monitoring, stability and the price of the product[8].

Regarding malaria diagnosis, available methods either lack sensitivity and specificity or require expensive equipment, expertise or costly infrastructure; that are not usually available in countries where the disease is endemic. Thus it is clear that there is a need for a sensitive and cost effective method to test for malaria. It is important to note that it is estimated that with the aid of proper diagnosis, more than 100,000 deaths may be sparred and about 400 million unnecessary treatments may be averted [3]. Also finding novel diagnostic targets for *P. falciparum* may help in developing more sensitive tests.

The present study investigated the possibility of using *Pf*Hsp70 as a diagnostic target for malaria and the development of two prototype AuNP-based assays for its detection. *Pf*Hsp70 is a member of the heat shock protein family that is produced by the parasite to protect from stress during its stay within the different hosts. Hsp70 mainly act as molecular chaperones, binding to proteins in their non-native forms and helping their refolding to native forms [11]. Also it was found that Hsp70 helps in the assembly or disassembly of multiprotein complexes, protein translocation, protein degradation, signal transduction and prion replication[12]. *Pf*Hsp70 is expressed in all asexual blood stages of the parasite[11].

As expected from its name, *Pf*Hsp70 is heat-inducible, meaning that it is expressed at higher levels when the parasite is exposed to elevated temperatures protecting the parasite against patients fever [13]. The underlying mechanism is that at high temperatures, the transcriptional factor “heat-shock factor”(HSF) binds more efficiently to heat-shock elements (HSE; conserved regions upstream the gene coding for Hsp70) leading to higher gene expression[13].

The structure of *Pf*Hsp70 is similar to that of eukaryotic Hsp70, presenting three domains namely; N-terminal ATPase domain (45 kDa), a central substrate binding domain (15 kDa) and a C-terminal domain (10 kDa) (figure 2) [13-14]. Malaria Hsps are antigenic to human probably due to non-homologous sequences at the C-terminus of the proteins[13].

Gold nanoparticles (AuNP) display unique physical properties due to their nano-size. AuNPs have intense absorbance and scattering properties due to Surface Plasmon Resonance (SPR). When an oscillating electric field interacts with the free conductive band of electrons at the surface of the AuNP, collective dipolar oscillation of the electrons occurs. This is called Surface Plasmon[15] (figure 3). SPR occurs when the frequency of the exciting light is similar to that of the Surface Plasmon. The absorption cross-section of AuNPs was found to be 10^4 to 10^5 folds higher than that of the strongest absorbing Rhodamine-6G dye molecule. Regarding the scattering of AuNP, 80 nm AuNP was found to have 10^5 folds higher scattering than fluorescein[15]. When AuNPs come close together, Plasmon-Plasmon coupling occurs leading to energy loss and a shift in the absorbance peak maximum to a longer wavelength and thus a change in color from red to blue[15].

Another advantage of AuNPs is that their optical properties can be tuned by varying both their size and shape. For example, small particles (such as 20 nm) show SPR absorption with negligible scattering properties[15]. However, larger particles (such as 80 nm) have high scattering properties and thus they are chosen in scattering based assays[15]. AuNPs can also be easily synthesized in different size ranges (9-120 nm) and conjugated to biomolecules (protein and oligonucleotides)[16]. These unique properties allow AuNP-based assays to be highly sensitive, and many can be used in point of care testing kits providing fast, simple and relatively inexpensive detection.

Immunological AuNP-based assays can be classified according to signal detection techniques into visual (dipsticks and sol particle immunoassays), spectrophotometric, fluorescence quenching , immuno-PCR, scattering, scanometric, chemiluminescence, real-time refractometric, surface-enhanced raman scattering and electronic detection based assays [17].

In the present study two prototype AuNP-based assays for the detection of the malarial antigen, *Pf*Hsp70 were developed. The first is a competitive-based chip assay that allows for the rapid and simple qualitative detection of malarial antigens and can be used as a field assay. The second is a fluorescence quenching competitive assay that is sensitive, rapid and simple to perform. The assay can be used in advanced laboratories and has the potential for quantitative detection of malarial antigens.

CHAPTER 2. LITERATURE REVIEW

2.1 Existing Malaria diagnostic assays

Diagnostic tests available for malaria either lack sensitivity and specificity or require expensive equipment, expertise or costly infrastructure; that are not usually available in countries where the disease is endemic. Malaria diagnostic tests include direct methods that detect the parasite or parasitic components such as light microscopical analysis, immunochromatographic assays and nucleic acid detection tests and indirect tests such as flow cytometry and laser desorption mass spectroscopy. Light microscopical analysis is still considered the standard method for malarial diagnosis. It simply involves direct visualization of malaria parasites in Giemsa-stained blood samples allowing the detection as well as the differentiation between *Plasmodium spp* (figure 4)[18]. Light microscopical analysis may also allow the determination of parasitemia level. This method has a low direct cost ranging from 0.4-0.7 US$ per slide. However, it is labour intensive and requires technical expertise, with a low turn-around time (the process is slow)[3,19-20]. The sensitivity of the light microscopy method is reported to range from 50-100 parasites per μL in routine labs; however in expert labs the sensitivity may reach 10 parasites per μL^{3}. Thus, much simpler and easier to interpret methods with higher turn-around time have been developed including immunochromatographic assays or what is also named rapid diagnostic tests (RDTs). These include dipsticks and cassettes that allow the detection of different malarial antigens including parasite histidine rich protein (HRP-2), lactate dehydrogenase (pLDH), and aldolase[3]. The sensitivity of this method may be comparable to that of microscopy (100 parasites per μL) but it is much simpler and easier, requiring minimal infrastructure and expertise[3]. However, the sensitivity of such tests may be dramatically affected by in field conditions such as heat and humidity[21]. These tests may also give false positives due to cross reactivity with rheumatoid factor that is present in high titre in blood of patients suffering from certain diseases such as rheumatoid arthritis[22].

HRP-2 is an antigen present only in *P. falciparum* and rapid tests testing HRP-2 were found to be most sensitive for the detection of *P falciparum*[3]. However, the two main drawbacks of HRP-2-based RDTs are that, on one hand, the positivity may remain even 3 weeks after disease resolution and on the other hand, this antigen is

only expressed in *P. falciparum* and thus this RDT cannot be used for the detection of other *Plasmodium spp*[3]. The latter drawback has been overcome by using RDTs utilizing both HRP-2 and aldolase. Aldolase is a pan antigen (present in the different *Plasmodium spp*) and thus assays utilizing both aldolase and HRP-2 can detect both *falciparum* and *n*on-*falciparum* species. However, the sensitivity and specificity for detecting non-*falciparum* infection is low for aldolase based assays (46 - 93% for *P. vivax* and 7 - 80% for *P. ovale* or *P. malariae*)[3,23].

pLDH is a species-specific antigen utilized in RDTs and thus can be used for the differentiation between the diff *P. spp*. However, tests based on pLDH have a lower sensitivity in detecting *P. falciparum* infection (sensitivity of pLDH tests is 67% *vs* 93% for HRP-2 based tests) compared to HRP-2-based tests[3, 24]. The sensitivity of pLDH for non-*falciparum* species is however superior to aldolase-based tests (*P. vivax* 62 - 95% and for *P. ovale* and *P. malariae* 36 - 95%) [3,23]. pLDH level changes proportional to the parasitemia level and thus pLDH based assays can be utilized for therapeutic monitoring[3].

A more sensitive method for the detection of malarial infection is the detection of parasitic nucleic acid via PCR. This method is very sensitive allowing the detection of 1-5 parasites per μL and can be used to differentiate between malarial species. Although this method allows for high throughput analysis, method standardization as well as rapid detection, the capital and operating costs are high. Advanced infrastructure and trained personnel are also crucial to prevent contamination[3,25-26].

The second group of tests that can also be used to detect malarial infection are the indirect tests such as flow cytometry and laser desorption mass spectrometry. Flow cytometry can be used to detect hemozoin within phagocytes[3,27-29]. Hemozoin is produced within RBC infected cells where malaria digests hemoglobin and promotes its crystallization, forming hemozoin that is stored in acidic vacuoles. The detection of hemozoin is thus an indirect marker of malaria infection which can be accomplished by measuring the depolarization of laser in a flow cytometer channel[3]. This method uses standard hematology analyzers and is thus potentially useful for diagnosing clinically un-suspected imported malaria. However, this technology is expensive and diagnosis should be confirmed via other methods[3]. Another technique to measure hemozoin is laser desorption mass spectroscopy. When hemozoin crystals absorb

ultraviolet photons, intact heme is released giving spectra of the parent molecule as well as its molecular ion fragments. In non-infected blood samples, heme bound to haemoglobin is not rapidly ionized and thus is not detected[3]. The sensitivity of this method is 10 parasites per μL[30]. The method is rapid, easy to use and requires low sample volume. However, the cost of the equipment is very high and until now this method cannot differentiate between the different *P. sp* [3]. Table 1 summarizes the advantages and disadvantages of the different diagnostic assays available for malaria.

It is thus clear that there is still a need for the development of a diagnostic assay for the detection of malaria antigens that is sensitive, rapid, simple and cost effective.

2.2 AuNP-based immunoassays

Immunological AuNP-based assays can be classified according to signal detection techniques into visual (dipsticks and solution phase), fluorescence quenching, scattering and electronic detection based assays and others as mentioned earlier (under introduction)[17]. Tanaka *et al*.[31] developed a sol particle visual immunoassay for the determination of cystatin C (endogenous marker of glomerular filtration rate (GFR)). In the presence of cystatin C, aggregation of antibody conjugated-AuNPs occur leading to change in color and shift in absorption peak maxima. Detection limit was reported to be 0.2 mg/L and linearity was achieved in the range between 0.2 to 8 mg/L[31]. Liu *et al*. [32]developed a scattering-based homogenous immunoassay for the detection of mouse IgG. In the presence of mouse IgG antibody, aggregation occurs to anti-mouse conjugated AuNPs. Aggregation can then be detected and quantified using dynamic light scattering. The detection limit reported was 0.5 ng/ml[32]. Shen *et al.* [33]developed an immunoassay based on the electrochemical properties of AuNPs. The assay utilizes anodic stripping voltammetry (ASV) for the detection of hepatitis B surface antigen (HBsAg). Magnetic nanoparticle-labelled anti-HBsAg and AuNP-labelled with a matched pair of anti-HBsAg were added to a sample having HBsAg. After incubation, the sandwiched complex was magnetically separated, washed and enhanced by adding copper enhancer solution (copper sulphate plus ascorbic acid). The sandwiched complex (with copper deposited on the surface of AuNPs) was separated and copper solubilised using nitric acid. The concentration of copper ions released was then measured using ASV. Concentration of copper ions measured

corresponded to the concentration of the HBsAg present in the sample. The detection limit of the assay was reported to be 87 pg/ml and the dynamic range lied between 0.1 to 1500 ng/ml[33].

Since this study involved the development of AuNP-based competitive chip as well as fluorescence quenching immunoassay, literature review will focus more on assays based on these platforms. Competitive as well as sandwich based colorimetric chip assays have been developed for the detection of several toxins and antigens including *P. spp* antigens[3]. Commercially available dipsticks are available that detect one or a combination of the three antigens (HRP-2, pLDH and aldolase) mentioned previously under introduction[34].

Regarding fluorescence quenching AuNP-based immunoassays, studies have reported the development of competitive and sandwich based assays for the detection of different antigens, markers or drugs[35-39]. The developed sandwich immunoassays were either in solution phase or immobilized on a support. Ao and collaborators[35] developed a solution based sandwich fluoroimmunoassay for the detection of alpha fetoprotein, in which magnetic nanoparticles were labelled with a polyclonal antibody and the AuNPs were labelled with monoclonal antibodies. Alpha-fetoprotein was sandwiched between the two antibody-functionalized nanoparticles. The immunocomplex was easily separated from the surrounding solution using a magnetic field [35]. The remaining supernatant which contains free gold probes (in case of positive sample there will be less than in case of the negative sample) was allowed to quench the fluorescence of fluorescein isothiocyanate (FITC). Fluorescence of FITC at 516 nm was then measured which was proportional to the amount of alpha-fetoprotein present in sample. The reported detection limit was 0.17 nM and the measurement range was from 15 to 400 ng/mL[35]. Recently, Mayilo *et al.* developed another sandwich fluoroimmunoassay in solution form for the detection of cardiac troponin T (cTnT)[36]. Two monoclonal antibodies were used in this study, the first and second antibodies were labelled with AuNPs and fluorescent dyes, respectively. In the presence of antigen, the distance between the fluorescent dye and the AuNP decreased leading to fluorescence quenching. The limit of detection in this study was 0.02 nM (0.7 ng/mL)[36]. An example of an immobilized sandwich fluoroimmunoassay is that developed by Peng *et al.* [37] for the detection of IgG. IgG was captured by a primary

antibody immobilized to polystyrene microwells, followed by the addition of a secondary AuNP-labelled antibody. The formed immunocomplex was then dissociated and the supernatant was added to a solution of fluorescein. If the sample was positive, then the level of AuNP-labelled secondary antibody immobilized to the microtiter plates will be high and so will be the amount of AuNPs in the supernatant after dissociation. Thus the fluorescence quenching of fluorescein will be high as determined by measurements at 517 nm. An inverse proportional relationship was achieved between the logarithmic value of IgG concentration and fluorescence intensity at 517 nm. The detection limit reported was 4.7 ng/mL and the dynamic range was 10 - 5,000 ng/mL [37].

Other studies have reported competitive surface and solution based immunofluorometric assays. Matveeva *et al.* [38] has developed a surface based competitive fluoroimmunoassay. In this study, AuNPs were covalently linked to indium tin oxide coated glass slide and antibodies against the analyte were non-covalently bound to the AuNPs. Then an analyte-fluorophore conjugate was added and the fluorescence emission value was low due to quenching by AuNPs. The sample containing unlabelled analyte was then added that competed with the immobilized analyte-fluorophore conjugate and fluorescence emission was restored. To further increase the fluorescence enhancement, the supernatant containing the displaced analyte-fluorophore conjugate was allowed to react with another surface having immobilized silver shelled AuNPs that are bound to anti-fluorophore antibodies. When the analyte-fluorophore conjugate were bound to this surface via anti-fluorophore antibodies, the signal was enhanced by the effect of the silver shelled AuNP (fluorescence emission was 7 - 8 times that of gold surface). Mayilo S *et al* [39] developed a homogenous solution based competitive immunoassay for the detection of the hapten digoxigenin. In this study, digoxigenin in the analyte competes with Cy3B (fluorophore)-labelled digoxigenin for antibody-conjugated-AuNP (bionanoconjugates; BNCs) binding sites. In case of positive samples, BNC binds to digoxigenin in the sample and thus Cy3B-labelled digoxigenin is inhibited from binding and low quenching occurs. In blank samples, Cy3B-labelled digoxigenin binds easily to the BNC and strong quenching occurs. Linearity was reported in the range from 0.5-3 ng/mL. The limit of detection (LOD) and limit of quantitation were

0.2 and 0.6 ng/mL, respectively. In this study, Mayilo S *et al's* [39] method was modified to detect *Pf*Hsp70 antigen and the principle of the assay is shown in figure 5.

CHAPTER 3. MATERIALS AND METHODS

3.1 Production, purification and activity of anti-*Pf*Hsp70 monoclonal antibody (2E6)

3.1.1 Production of 2E6

All materials used in this study were purchased from Sigma Aldrich, Germany unless otherwise stated. A hybridoma culture was grown using standard scale up culturing conditions to produce 2.6 L of culture containing 2E6 monoclonal antibody (antibody against *Pf*Hsp70; IgG). Protein precipitation was performed using 50% w/v ammonium sulphate solution, by gradually adding an equal volume of ammonium sulphate saturated solution at 4^{o}C. This allowed the gradual precipitation of proteins. The precipitate was collected by centrifugation (10,000 rpm for 10 min at 4^{o}C) and then resuspended in phosphate buffer saline (PBS; about 40 mL) and excess salts were removed by 2x overnight dialysis (pore size 30 kDa) against 5L PBS. After dialysis, 100 mL of impure 2E6-containing solution was obtained. The solution was centrifuged at 10,000 rpm for 30 min at 4^{o}C to remove precipitates and the supernatant was concentrated to 35 mL by ultrafiltration using a "diaflo" (Amicon) system with gentle mixing at 4^{o}C (cut-off value of membrane was 30 kDa; Ultrafiltration membrane Millipore, Germany)[40].

3.1.2 Purification of 2E6 using affinity chromatography

Purification of 2E6 antibody was done in two steps: the first step using Protein G Sepharose 4 Fast Flow (GE; 17-0618-01, Germany) and the second step using PD SpinTrap G-25 columns (GE; 28-9031-34, Germany) according to manufacturer's protocols[41]. Protein G Sepharose 4 Fast Flow (1.6 mL) was added to a column support and was equilibrated with 5-10 column volumes of binding buffer (20 mM sodium phosphate; pH = 7). Then 1.6 mL of concentrated impure antibody solution (60 mg/mL of total protein determined using BCA test [see below]) was added to the column. The column was then washed with binding solution until UV absorbance at 280 nm reached baseline. Then 10 mL of elution buffer (glycine HCl 0.1 M pH = 2.7; Riedel-de-Haen, Germany) was added to the column to elute the antibody. The first 5 drops were discarded and the rest was collected into tubes containing 400 µL of Tris-HCl buffer (1 M pH = 9; neutralizing buffer) to neutralize the pH of the solution to prevent 2E6 antibody from being denatured by the low pH of the elution buffer. The

column was then regenerated by washing with 5 - 10 column volumes of binding buffer. This procedure was repeated till the whole 35 mL of impure 2E6 antibody were passed through the column. To dialyze the purified antibody, the eluted purified 2E6 antibody solution was concentrated using a "diaflo" ultrafiltration stirred cell (Amicon, 30 kDa; 4^{o}C) to yield a volume of 25 mL and buffer was replaced by adding an equal volume of fresh binding buffer and concentrating to half the volume. This procedure was repeated 4 times and the volume was finally adjusted to 25 mL.

Since the 2E6 antibody was only partially purified using Protein G Sepharose 4 Fast Flow (determined using SDS-PAGE [see below]), a second purification step was then performed using PD SpinTrap G-25 columns according to manufacturer instructions to further purify the 2E6 antibody[42]. Briefly, 600 µL of binding solution (see above) was added while the lower cap was on. The columns were centrifuged (Eppendorf 5810R) for 1 min at 825 rpm (after loosening the upper cap and removing the lower cap). Then 250 µL of partially purified 2E6 antibody (BCA: 4.2 mg/mL) was mixed with 300 µL of binding solution and the mixture was added to the spin column while the lower cap was on. Then the upper cap was screwed on and the column was mixed by inversion for 8 min. The columns were then centrifuged for 1 min at 825 rpm and washed twice using binding buffer by adding 600 µL binding buffer and centrifuging at 825 rpm for 1 min. Elution was performed twice by adding 400 µL of elution buffer, mixing by inversion for 1 min and centrifugation (825 rpm for 1 min) into collection tubes containing 30 µL of neutralizing solution. The columns were reused after washing 5 times with binding solution and storing in 20% ethanol at 4^{o}C. The collected solution was then concentrated to half volume using a "Centricon" ultrafiltration system (30 kDa; Amicons; 4,000 rpm) and the buffer was exchanged by adding equal volumes of binding buffer and concentrating for 5 cycles.

To determine the purity of 2E6 obtained after each purification step, samples were analyzed on a 12.5% SDS-PAGE (table 2). The samples were prepared by adding an equal volume of sample buffer (2 mL glycerol [Panreac, Germany]; 1 mL mercaptoethanol; 5.1 mL 10% SDS; 2.5 mL Tris 0.5 M pH 6.8; 2 mg bromophenol blue) and boiling at 100^{o}C for 7 min. Then 20 µL of samples were loaded and run at 180 mV for 50 min (BIO-RAD; USA). Running buffer used was prepared by diluting 10X running buffer (30.28 g Tris + 144.13 g glycine + 10 g SDS dissolved in 1 L

distilled water) in water. After running the gel, it was stained for 40 min in staining solution (0.5% Coomassie blue, 40% methanol, 10% acetic acid [Riedel-de-Haen, Germany] in aqueous solution) then destained in destaining solution (45% methanol, 7.5% acetic acid in aqueous solution) until protein bands were visible.

The concentration of the purified 2E6 antibody was determined by the Bicinchoninic Acid (BCA) method. The principle of the BCA assay is that at alkaline conditions, Cu^{2+} (provided in BCA solution B; Sigma, Germany) binds to peptide bonds of proteins and amino acids such as cysteine, tryptophan and tyrosine. This leads to the reduction of Cu^{2+} to Cu^{+}. Cu^{+} then binds to BCA molecule (provided in BCA solution A; Sigma, Germany) forming a complex with an intense purple color, the concentration of which can be determined by spectrophotometry and is proportional to the protein concentration[43] (figure 6). In our study, zero, 4, 8, 12, 16, 20, 24 µL of 1 mg/mL bovine serum albumin (BSA; protein standard micro standard, Sigma, Germany) were added to 7 tubes as a standard. To 6 other tubes, 10, 10, 20, 20, 30, 30 µL of 1 : 2 diluted purified 2E6 antibody (in 20 mM phosphate buffer; pH = 7.4; sodium phosphate mono and di basic; Riedel-de-Haen, Germany) were added. Then 1 mL of BCA mixture (14,706 µL of BCA reagent A + 294 µL of BCA reagent B) was added and the solution was mixed by vortexing. The solution was then incubated at 37^{o}C for 30 min and absorbance at 562 nm was measured using a UV-vis Varian Cary50 spectrophotometer (USA). After determining the concentration of 2E6 antibody, glycerol was added to give a final concentration of 10%, and the solution was aliquoted and stored at -20^{o}C.

3.1.3 Activity of 2E6 antibody

2E6 mouse monoclonal antibody activity was determined by incubating hepatocytes infected with *P. berghei* with the purified 2E6 antibody. Then AlexaFluor 555-labelled goat anti-mouse secondary antibody was added, and cell imaging was performed using a fluorescence microscope (Leica Microsystems; USA).

3.2 Hsp70 as a diagnostic target

3.2.1 Western blot analysis of plasma and whole blood of mice infected with *P. berghei*

Western blot analysis was performed on plasma and whole blood of mice infected with *P. berghei* using 2E6 as the primary antibody for the detection of *Pb*Hsp70 (*P. berghei* heat shock protein 70) antigen. First, a microscopical analysis was performed to determine parasitemia level. This was done by making an incision in the mouse tail, smearing a blood drop, allowing it to dry, fixing by methanol, leaving to dry, staining with Giemsa for 17 - 20 min, finally drying and examining under the microscope.

To perform Western blot analysis, blood was collected from both non-infected and *P. berghei* infected mice. First, mice were sacrificed using CO_2, incised to expose the heart and the heart was then opened to collect as much blood as possible using a tip and a collecting tube wetted with heparin-PBS to prevent blood clotting. Samples were then normalized so that the number of RBCs in non-infected and infected blood was similar. This was done by calculating the number of RBCs per mL using the following equation:

$$Average number\ of\ RBCs \times DF \times 10000 \quad (1)$$

where DF was the dilution factor in PBS. Then the volume of infected and non-infected blood having the same number of RBCs was withdrawn and each split into two; the first named “whole blood” and the second “plasma”. Plasma is the supernatant left after centrifuging whole blood at 3,000 rpm for 5 min at 4^{o}C. For each of the four samples (whole blood and plasma of both infected and non-infected), seven 1 : 5 dilutions in PBS were prepared. Equal volume of sample buffer (lamellae sample buffer; BIO-RAD, Germany) was added and the samples were heated at 100^{o}C for 7 min. Then 30 µL of each sample was loaded onto 10% SDS-PAGE (table 2) and run at 180 mV for 50 min (BIO-RAD). Running buffer was prepared by diluting 10X running buffer (30.28 g Tris + 144.13 g glycine + 10 g SDS dissolved in 1 L distilled water) in water.

The gel was then blotted onto nitrocellulose membranes by sandwiching the gel and a nitrocellulose membrane between 4 filter papers and 2 sponges (sponge/2 filter papers/gel/nitrocellulose membrane/2 filter papers/sponge) and all these components were clamped tightly together, while avoiding air bubbles. The system

was inserted into transfer buffer and an electrical field (nitrocellulose membrane faces positive anode) was applied at 300 mA for 60 min at 4°C (BIO-RAD). Transfer buffer (1X) needed for blotting was prepared by diluting 100 mL of 10X stock transfer buffer (3.03 g Tris; 14.4 g glycine in 1 L distilled water) with 700 mL water and 200 mL methanol. After blotting, membranes were washed with 0.05% PBST (250 µL Tween on 500 mL PBS) on a shaker at 50 rpm for 5 min. To ensure proper blotting, the membranes were stained with Ponceau stain. After the appearance of the protein bands, Ponceau stain was washed off using 0.05% PBST at 50 rpm for 5 min. For blocking, the membranes were immersed in blocking solution (5% w/v of non-fat dry milk in 0.05% PBST) and left overnight (shaken at 18 rpm at 4°C). After blocking, the membranes were washed (0.05% PBST; 50 rpm; 5 min) and then reacted with 2E6 primary antibody (1 : 400; diluted in 5% w/v of non-fat dry milk in PBST 0.05%) for 1hr (at 18 rpm). Washing 3 times for 5 minutes each using PBST 0.05% (50 rpm) was then done and horseradish peroxidase (HRP)-labelled secondary anti-mouse antibody (1 : 5,000; diluted in 5% w/v non-fat dry milk in PBST 0.05%) was added and incubated for 1 hr (shaken at 18 rpm). Washing was done 3 times for 5 min each using PBST 0.05% (50 rpm). Two mL of chemiluminescence substrate (after mixing 1 mL of substrate A and 1 mL of substrate B; SuperSignal West Pico Chemiluminescent Substrate, ThermoScientific; USA) was finally added to each membrane and left to react for 2 min at room temperature. The membrane was then wrapped in a plastic sheet and exposed to X-ray film for 2 min. The film was then developed using Curix 60 from Agfa (USA)[44-45].

3.2.2 Western blot analysis of saponin pellets of RBCs of non-infected mice, of mice infected with *P. berghei*, and of non-infected human

RBCs were separated from whole blood and treated with saponin and the pellet used to perform Western blot analysis. Whole blood was centrifuged for 5 min at 3,000 rpm at 4°C. The plasma was separated and the RBCs were washed twice with PBS (centrifuged for 5 min at 3,000 rpm at 4°C). To the RBCs, 1.5 mL of saponin (0.15% in PBS) was added and left for 5 min at room temperature with mixing. Then centrifugation was performed at 14,000 rpm for 5 min at 4°C. The supernatant was removed and named “RBC lysate”. The saponin pellet was washed with PBS 4 times (centrifugation at 13,500 rpm for 5 min at 4°C). The pellet was then resuspended in 50 µL PBS[44]. Non-infected human blood was also treated in the same manner, after

normalizing for the number of RBCs using the equation 1 (section 3.2.1). Plasma, RBC lysate and saponin pellets samples of non-infected mice, of mice infected with *P. berghei* and of non-infected human were run on SDS-PAGE and Western blot was performed as described in detail in section 3.2.1.

3.2.3 Western blot analysis of saponin pellet of RBCs of non-infected mice and of mice infected with *P. berghei*, using actin as loading control

As a control to the experiments, anti-actin primary antibody and anti-rabbit secondary antibody were added as a loading control. Samples were treated with saponin as described in section 3.2.2. After running the samples on SDS-PAGE gel and blotting and blocking the membranes (see section 3.2.1), membranes were cut just above the 50 kDa marker band. The upper part of the membrane, was then treated with 2E6 as primary antibody and anti-mouse antibody as secondary antibody as described earlier (section 3.2.1). The lower part of the membrane was treated with anti-actin antibody as primary antibody (1 : 500; diluted in 5% w/v non-fat dry milk in PBST 0.05%) and anti-rabbit antibody as secondary antibody (1 : 5,000; diluted in 5% w/v non-fat dry milk in PBST 0.05%) [46]. The rest of the steps were followed as described in section 3.2.1.

3.2.4 Western blot analysis of saponin pellet of RBCs of mice blood infected with *P. berghei* and of a human blood culture infected with *P. falciparum*

After optimizing Western blot conditions, analysis of human blood culture infected with *P. falciparum* was performed and compared with that of mice blood infected with *P. berghei. P. falciparum* was grown on a continuous culture prepared by diluting Albumax II stock solution (25 g Albumax II (Gibco); 0.1 g hypoxanthine; 1 g Glucose; 1.67 g $NaHCO_3$; 2.98 g HEPES; 500 µl gentamincin and 5.2 g RPMI 1640 [with L-glutamine; without $NaHCO_3$]) in 500 mL of RPMI 1640 [no L-glutamine; with $NaHCO_3$] and then adding 500 µL gentamycin (50 mg/mL stock), 5 mL of 200 mM L-glutamine and 12 mL 1 M HEPES. *P.* falciparum 3D7 (obtained from the previous growth) was then grown in a malaria culture medium at a hematocrit of 3 - 5%. RBCs and leucocytes needed for this culture were separated from buffy coats obtained from healthy volunteers by centrifugation using a Ficoll gradient. Both samples (human blood culture infected with *P. falciparum* and mice blood infected

with *P. berghei*) were saponin treated as described in section 3.2.2. Western blot analysis followed as described in sections 3.2.1 and 3.2.3 [44-46].

3.3 Conjugation of 2E6 antibodies to AuNPs

3.3.1 Synthesis of AuNPs

All glassware was soaked with Aqua Regia (HNO_3 [Panreac, Germany] and HCl in ratio 1 : 3) and left overnight. The next day, glassware was thoroughly rinsed with tap water till pH indicator gave pH = 6. The flasks were finally rinsed with Milli-Q water. To a 500 mL round bottom flask, 250 mL of $HAuCl_4$ (1 mM; prepared using gold (III) chloride solution in dilute HCl, 99.99%, Sigma Aldrich, Germany) were added, a condenser was adapted to the flask, and the solution was refluxed with stirring for 1 hr (starting from first condensation) using a sand bath. Then 25 mL of sodium citrate solution (38.8 mM; Sigma, Germany) were then added. The flask was again left to reflux for 15 minutes. Then the solution was allowed to cool and stored in dark until further use. The concentration of nanoparticles was determined by UV/vis spectrophotometry using Beer's law (extinction coefficient for the Plasmon band at 520 nm is 2.33 X 10^8)[47, 48].

3.3.2 Functionalization of AuNPs with mercaptoundecanoic acid and CALNN peptide

To 30 mL of the AuNP obtained in "3.3.1" (concentration 12.7 nM), 45 µL of mercaptoundecanoic acid (MUA; Sigma Aldrich, Germany) solution (1 mM in ethanol) was added so that the ratio in molarity of MUA to AuNP was 120 (this ratio was found to be optimum in previous studies in our lab; section 5.2). The solution was mixed and left overnight at 4^{o}C. The concentration was determined the next day as described in 3.3.1. Another functionalization was also tested by conjugating a CALNN peptide (Cysteine, Alanine, Leucine, Asparagine, Asparagine) which imparts a negative charge to the AuNPs, like MUA. AuNPs- CALNN were prepared by Dr. Pereira's group in Universidade do Porto.

3.3.3 Conjugation of 2E6 antibodies to AuNP-MUA

A 2 nM AuNP-MUA solution was prepared from stock solution by diluting with Milli-Q water. The pH was adjusted to 7.4 using 0.1 M NaOH (pronalab, Germany). Then to 5 mL of AuNP-MUA (2 nM; pH = 7.4), 2E6 antibody was added such that

the molar ratio of 2E6 to AuNP-MUA would be 70 (ratio = 70). Then 5 mL of 5 mM sodium phosphate buffer (pH = 7) was added. The mixture was mixed and left to incubate overnight at 4^{o}C. This allows for the electrostatic binding between 2E6 and AuNP-MUA to occur[49]. In trying to obtain more robust AuNP-2E6 conjugates, covalent linkage between 2E6 and AuNP-MUA was also tested through the use of N-hydroxysuccinimide / 1-Ethyl-3-[3-dimethylaminopropyl] carbodiimide hydrochloride (NHS/EDC) cross-linkers (NHS: Fluka, Germany). The same procedure was used as that for preparing non-NHS/EDC conjugates but instead of adding 5 mL of buffer alone (5 mM sodium phosphate buffer; pH = 7), NHS/EDC mixture in the same buffer was added. Concentration of NHS and EDC in the NHS/EDC mixture was 1.2 mM and 2.8 mM, respectively. The incubation was made for 2 hr at room temperature[50]. Preparation of conjugates was done in glass containers to prevent aggregation to the walls of plastic vials. Optimum pH values, ratios of 2E6 to AuNP-MUA and amounts of NHS/EDC needed for conjugation were all determined as described later in 3.4 and 3.5.

3.3.4 Conjugation of 2E6 to AuNP-CALNN

A 2 nM AuNP-CALNN solution was prepared from stock by diluting in Milli-Q water. pH was not adjusted, and then the same protocol as that for MUA particles was followed to prepare NHS/EDC linked conjugates. For non-NHS/EDC, sodium phosphate buffer (5 mM; pH = 7) was added first (to fix the pH to 7 since no adjustment in pH will be done to the AuNP-CALNN), then 2E6 solution and finally the AuNP-CALNN solution.

3.4 Characterization of BNCs

3.4.1 UV-visible spectroscopy

The first proof of 2E6 antibody conjugation to the AuNPs, was the observation of a shift in the absorbance peak maximum to a longer wavelength after 2E6 antibody conjugation[51]. Both NHS/EDC and non-NHS/EDC BNCs were prepared as described above (3.3.3). AuNP-MUA (1 nM; pH = 7.4; 1,000 μL) was prepared and 2E6 antibody was added at a molar ratio of 2E6 to AuNP-MUA of 100 (ratio = 100). Then either 500 μL of 5 mM sodium phosphate buffer (pH = 7), to prepare non-NHS/EDC BNCs; or NHS/EDC mixture in the same buffer (1.2 mM and 2.8 mM of NHS and EDC, respectively), to prepare NHS/EDC BNCs, was added. Non-NHS/EDC

conjugates were incubated at 4^{o}C overnight while NHS/EDC conjugates were incubated for only 2 hrs at room temperature. After incubation, the absorbance spectrum was analyzed.

3.4.2 Agarose gel electrophoresis

To determine whether or not the conjugates are uniform and non-aggregated, agarose gel electrophoresis was used. As a proof-of-concept, BSA BNCs were initially run on the gel. AuNP-MUA (5 nM) was prepared by diluting stock with Milli-Q water and pH was adjusted to 7.4 using 0.1 M NaOH. Different molar ratios of BSA to AuNP-MUA (1,000 µL) were prepared ranging from 0 - 4,000. To the mixture, 500 µL of 5 mM sodium phosphate buffer (pH = 7) was added and the volumes of the different ratios were made equal by adding the appropriate amount of buffer. After incubating the BNCs overnight at 4^{o}C, glycerol was added to the BNCs to a final concentration of 10% and 30 µL of the samples were loaded onto 1% agarose gel (ultra pure agarose, Invitrogen, Germany) prepared in sodium phosphate buffer (5 mM; pH = 7). Running buffer used was also sodium phosphate buffer (5 mM; pH = 7) and the electrophoresis was run at 70 mV (BIO-RAD; USA) [52].

After proof-of-concept of agarose gel electrophoresis using BSA non-NHS/EDC conjugates, 2E6 BNCs (with or without NHS/EDC) were prepared and run on agarose gel electrophoresis after determining the optimum amount of NHS/EDC needed for cross linking. To determine the optimum amount of NHS/EDC mixture needed for cross linking, different concentrations of NHS/EDC were prepared (concentration in NHS/EDC mixtures were: 0.6 mM and 1.4 mM; 1.2 mM and 2.8 mM; 3 mM and 7 mM; 6 mM and 14 mM of NHS and EDC, respectively). The concentration of AuNP-MUA used for preparing NHS/EDC BNCs was 1 nM and the pH was adjusted at 7.4 (2,000 µL). The molar ratio of 2E6 to AuNP-MUA was 250 and 1,000 µL of the different mixtures of NHS/EDC (0.6 mM and 1.4 mM; 1.2 mM and 2.8 mM; 3 mM and 7 mM; 6 mM and 14 mM of NHS and EDC, respectively) were then added. The BNCs were incubated at room temperature for 2 hrs then centrifuged at 7,000 rpm for 10 min. The supernatant (light pink in color) was removed to get rid of most of unconjugated 2E6 and the pellet was resuspended in 1,000 µL Milli-Q water. The solution was then concentrated using “Centricons” (Amicon, 30 kDa; centrifuged at 4,000 rpm) ultrafiltration system, for a final volume

of 50 μL. This concentration step was done to enhance color to be easily seen on the gel. Glycerol (final concentration 10%) was then added and samples were run on 1% agarose gel at 70 mV.

After optimizing the concentration of NHS/EDC, concentration of 1.2 mM and 2.8 mM of NHS and EDC, respectively, was chosen since it was the highest concentration that prepared stable, uniform and non-aggregated conjugates. Concentration of 0.6 mM and 1.4 mM of NHS and EDC, respectively, also produced stable conjugates but we preferred the 1.2 mM and 2.8 mM concentration to ensure that the concentration was not too low and that the reaction was complete. Conjugates with different molar ratios (from 5 - 70) of 2E6 to AuNP-MUA were prepared in the presence and absence of NHS/EDC. In this study, AuNP-MUA (2 nM; pH = 7.4; 2,000 μL) was used. Milli-Q water was used to make the volumes equal for conjugates with different ratios of 2E6 to AuNP-MUA. For non-NHS/EDC conjugates, 2,000 μL of buffer was added while for NHS/EDC conjugates a mixture of NHS/EDC (1.2 mM and 2.8 mM of NHS and EDC, respectively; 2,000 μL) was added. Conjugates were left to incubate (overnight at 4^{o}C for non-NHS/EDC and 2 hrs at room temperature for NHS/EDC conjugates). After incubation, conjugates were centrifuged at 6,000 - 7,000 rpm for 10 min and the pellet remaining after supernatant removal was resuspended in minimal volume of the remaining solution. Glycerol (final concentration 10%) was added and samples were run on 1% agarose gel at 70 mV.

For AuNP-CALNN particles, the optimum NHS/EDC concentration was also determined by the same procedure used for AuNP-MUA. Different concentrations of NHS/EDC were prepared (buffer only; 0.3 mM and 0.7 mM; 0.6 mM and 1.4 mM; 1.2 mM and 2.8 mM; 3 mM and 7 mM of NHS and EDC, respectively). The concentration of AuNP-CALNN used was 2 nM (2,000 μL) and the molar ratio of 2E6 to AuNP-CALNN was 100. To the mixtures, 2,000 μL of the different NHS/EDC concentrations was added. The BNCs were incubated at room temperature for 2 hrs for NHS/EDC conjugates but overnight incubation at 4^{o}C was performed for non-NHS/EDC conjugates. After incubation, conjugates were centrifuged at 7,000 rpm for 10 min. Supernatants were removed and pellets were resuspended in minimal volumes

of the remaining solution. Glycerol (final concentration 10%) was then added and the samples were run on 1% agarose gel at 70 mV.

3.4.3 Zeta (ζ)-potential

Non-NHS/EDC BNCs with different molar ratios (0 - 400) of 2E6 to AuNP-MUA were prepared (final concentration of AuNP-MUA 1 nM; pH = 7.4). Milli-Q water was used to make the volumes equal for conjugates with different ratios of 2E6 to AuNP-MUA. It is important to note that before diluting 2E6 antibody with 20mM sodium phosphate buffer (pH = 7.4), the buffer was filtered using a syringe disc filter (0.45 μm; Whatman, nylon 0.45 μm pore diameter, Germany). For NHS/EDC BNCs, the same ratios of 2E6 to AuNP-MUA were prepared to allow the comparison between non-NHS/EDC and NHS/EDC BNCs. AuNP-MUA (final concentration 1 nM; pH = 7.4) was used. Milli-Q water was also used to make the volumes equal for conjugates with different ratios of 2E6 to AuNP-MUA. Concentration of 1.2 mM and 2.8 mM of NHS and EDC, respectively, was used and the mixture was filtered using a syringe disc filter (0.45 μm) before use. Instead of adding 525 μL of the NHS/EDC solution (1.2 mM and 2.8 mM of NHS and EDC, respectively) to the BNCs, only 350 μL was added. Although adding 525 μL of the NHS/EDC to the BNCs would have allowed the optimum amount of NHS/EDC to be added (see sections 3.4.2 and 4.4.2), it could have led to the aggregation of BNCs having low molar ratios of 2E6 to AuNP-MUA. Thus it was decided to add a lower amount of NHS/EDC (equivalent to using 0.78 mM and 1.82 mM of NHS and EDC, respectively). This was also supported by the fact that a concentration as low as 0.6 mM and 1.4 mM of NHS and EDC, respectively, was proven to be as effective as the concentration of 1.2 mM and 2.8 mM of NHS and EDC, respectively (section 4.4.2). After incubating all BNCs overnight, ζ-potential was measured.

ζ-potential measurements were performed in a Zetasizer Nano-ZS from Malvern Instruments. A 4 mW He-Ne laser (633 nm) was used with a fixed 173 º (DLS) or 17 º (ζ-potential) scattering angle. All measurements were carried out at 25ºC. The zeta cell and caps were cleaned with Milli-Q water. One mL of sample was loaded into the disposable ζ-potential cuvette. The caps were then fitted and the cell was inserted into the machine. The software was adjusted as follows: Material: protein; dispersant: water; temperature: 25^{o}C; equilibration time: 900 sec;

measurement: monomodal; number of measurements: 4; number of runs: 100. Between samples, the cell was cleaned with at least 60 mL of Milli-Q water[53].

3.5 Stability of AuNP-MUA-2E6 conjugates

3.5.1 NaCl method

Both NHS/EDC (1.2 mM and 2.8 mM of NHS and EDC, respectively) and non-NHS/EDC BNCs with different molar ratios (0 - 70) of 2E6 to AuNP-MUA (2 nM; pH = 7.4; 2,000 µL) were prepared as described earlier (section 3.4.2). The conjugates were then centrifuged at 7,000 rpm for 10 min. The supernatant was removed and the pellet was resuspended in minimal volume of the remaining solution. Then to 30 µL of samples, 30 µL of 5 M NaCl (Panreac, Germany) were added at room temperature and left for 6 hrs. Visible absorbance spectra were then performed to determine the least amount of 2E6 antibody required to stabilize the BNCs against 5 M NaCl [54].

3.5.2 pH aggregation

The pH of 1 nM AuNP-MUA was changed using 0.1 M HCl or 0.1 M NaOH and the absorbance spectra were analyzed using visible spectroscopy. The same was done to non-NHS/EDC and NHS/EDC 2E6 BNCs. Five mL of AuNP-MUA (2 nM) were prepared and pH was adjusted to 7.4. Then to each of 2.5 mL of AUNP-MUA, 2E6 monoclonal antibody was added to give a molar ratio of 2E6 to AuNP-MUA of 70. Then 2.5 mL of either buffer (5 mM sodium phosphate buffer; pH = 7) or NHS/EDC mixture (1.2 mM and 2.8 mM of NHS and EDC, respectively) was added to prepare non-NHS/EDC and NHS/EDC BNCs, respectively. Incubation was performed overnight at 4^{o}C. It is important to note that the final concentration of AuNP-MUA in the BNCs was 1 nM allowing the comparison with naked AuNP-MUA particles (also 1 nM). The next day, pH of the conjugates was first decreased (using 0.1 M HCl) and then increased (using 0.1 M NaOH) on the same tube and absorbance was measured at different pH values (ranging from 1 - 11) [55].

3.6 *Pf*Hsp70 expression

3.6.1 Transformation of pQE30/*Pf*Hsp70 into RosettaBlue™ cells

Two hundred nanograms of pQE30/*Pf*Hsp70 plasmid, harbouring the *Pf*Hsp70 gene, were kindly provided by Prof. Gregory Blatch (Rhodes University, South Africa) in a paper dried drop format. The paper dried drop was submersed in 20 µL of autoclaved

water to give a final concentration of 10 ng/µL. Two µL of either pQE30/*Pf*Hsp70 plasmid (10 ng/µL), positive control ("Test Plasmid" supplied with cells) or autoclaved water (for negative control) were added to 20 µL of RosettaBlue™ cells (Novagen; 71058-4). Cells were then put on ice for 30 min before transformation by heat shock. The ice cold tubes were heated for 45 sec at 42^{o}C then placed on ice for 2 min. After heat shock, 80 µl SOC solution (supplied with cells) was added to each of the three tubes and the cells were incubated at 37°C for 60 min. SOC is a mixture of 2 g tryptone, 0.55 g Yeast extract, 1 mL 1 M NaCl, 0.25 mL 1 M KCl and 97 mL water that is autoclaved and cooled and to which 1 mL 1 M $MgCl_2$; 1 mL 1 M $MgSO_4$ and 1 mL 2 M glucose is added. Cells were then plated onto Luria Broth (LB) agar plates having both ampicillin and chloramphenicol with final concentrations of 100 µg/mL and 34 µg/mL, respectively; and left overnight to grow at 37^{o}C. Colonies on the plate were detected the next day indicating transformed cells[56-57].

To generate a transformant stock solution, colonies were inoculated in LB liquid media having both chloramphenicol and ampicillin (same ratio as plates) and incubated overnight at 37^{o}C allowing further bacterial growth. A negative control was performed substituting the cells with autoclaved water, to check for contaminations. The grown cells were then stocked in 30% glycerol at -80 ºC until further use. For expression studies, the stocked cells were streaked onto LB agar plates (containing chloramphenicol and ampicillin) and selected colonies were grown as described in the following section.

3.6.2 Expression of *Pf*Hsp70 under different induction conditions

For expression of *Pf*Hsp70, first a 50 mL preinoculum was prepared from which a larger culture (250 mL) was prepared. The 50 mL LB preinoculum (0.5 g bactotryptone [BD, Germany]; 0.25 g bactoyeast [BD, Germany]; 0.5 g NaCl; complete to 50 mL distilled water) contained 100 µL ampicillin (100 µg/mL), 125 µL of tetracycline (12.5 µg/mL) and 50 µL of chloramphenicol (34 µg/mL) plus a colony of transformed cells. Another flask was prepared as a blank having everything except the colony of transformed cells. After overnight incubation (210 rpm; 37^{o}C), blank was clear and the other flask was turbid from which 2.5 mL was added into each of three flasks having 250 mL fresh media having the same ratio of antibiotics. Flasks were named "no IPTG"; "IPTG 2hr" and "IPTG overnight". It is important to note

that aseptic conditions were followed throughout the transformation and expression procedures, including autoclaving the flasks, autoclaving the media before adding antibiotics and doing inoculations near a flame. The flasks were then incubated at 37^{o}C at 210 rpm. For each flask, 0.5 mL was withdrawn aseptically every 30 min until an optical density at 600 nm ($O.D_{600}$) reached 0.5 - 0.6. No addition was made to the flask labelled "no IPTG" and harvesting was done the following day. To the flask labelled "IPTG 2hr", 2.5 mL of 0.1 M Isopropyl β-D-1-thiogalactopyranoside (IPTG) was added and cells were further incubated for 2 hrs (210 rpm; 37^{o}C) before harvesting. For "IPTG overnight", 2.5 mL of 0.1M IPTG was added and incubation was done overnight (210 rpm; 37^{o}C) and cells were harvested the next day. For harvesting, a sample was withdrawn to determine final $O.D_{600}$ value and medium centrifuged at 10,000 rpm for 30 min. The supernatant was discarded and the pellet was weighed and then resuspended in lysis buffer (8 M urea [Panreac, Germany], 300 mM NaCl, 10 mM imidazole, 10 mM Tris pH 8.0, 1 mM phenyl methyl sulphonyl fluoride, and 1 mM lysozyme). The "no IPTG" flask pellet was resuspended in 10 mL; the "IPTG 2hr" pellet was resuspended in 4 mL and the "IPTG overnight" pellet was resuspended in 6 mL. The resuspended pellets were then frozen at -20^{o}C. Pellets obtained from cultures under different induction conditions were run on 10% SDS-PAGE, followed by Western blot analysis using 2E6 as primary antibody [57]. As a control, a 50 mL inoculum was prepared using the same protocol (same ratio of antibiotics as for the pre-inoculum) but using non-transformed RosettaBlue™ cells instead of transformed ones [57].

3.6.3 Expression of *Pf*Hsp70 under optimum conditions in a large scale

Eight flasks of 250 mL bacterial cultures were fermented, IPTG was used for induction of protein over-expression, and harvesting was done the following day. Instead of PMSF in lysis buffer, a protease inhibitor cocktail was used to reduce *Pf*Hsp70 degradation. This protease inhibitor cocktail solution was prepared by dissolving complete Protease Inhibitor Cocktail tablet (Roche Applied Science; 11 697 498 001) in 2 mL of Milli-Q water[57-58]. After harvesting, the total pellet was resuspended in 20 mL of lysis buffer which contained 800 µL of protease inhibitor cocktail solution.

3.7 Purification of *Pf*Hsp70 using Ni-NTA column

Since the expressed *Pf*Hsp70 has a 6xHis-tag at its N-terminus, Ni-NTA column was used as the method for its purification from the bacterial crude extract. The total resuspended pellet produced from the eight 250 mL culture flasks (20 mL) was thawed and homogenized by a homogenizer. Then a small amount of DNAse (Roche, Germany) was added to reduce viscosity before cell breakage by French-press. Bacteria were then lysed by passing the solution through a French pressure cell press (Thermo; Germany) at 2,000 psi gauge pressure (about 30,000-35,000 psi cell pressure). Pressure was applied three times to ensure cell destruction. Following cell lysis by French press, the solution was centrifuged at 5,000 rpm for 90 min to remove cell debris (pellet). To the supernatant, 25 µL of 10 mg/mL PMSF (in propanol) was added. Then 5 mL of Ni-NTA agarose (Qiagen; 30210) that was previously equilibrated with 60 mL lysis buffer (without lysozyme or PMSF) was mixed with supernatant at 4^{o}C for 2 hr. The solution was loaded onto column support and the solution passing through the column was named "flow through" (FT). Column washing was performed to remove non-specifically bound proteins, leaving only strongly bound proteins (those having His-tag) attached to the column. The washing buffer used was 300 mM NaCl, 10 mM imidazole, and 10 mM Tris (pH 8.0). Washing was continued till absorbance at 280 nm was lower than 0.1, assuring that no appreciable amount of protein material was present in the washes. *Pf*Hsp70 was then eluted from the column using 300 mM NaCl, 100 mM imidazole, and 10 mM Tris (pH 8.0) and the elute was collected till absorbance (at 280 nm) was lower than 0.1[57]. The eluted solution was then concentrated using 30 kDa "Centricon" ultrafiltration system (Amicon; 4,000 rpm) and buffer was exchanged by adding an equal volume of borate buffer (0.1 M borate pH = 8.3; 150 mM NaCl) and concentrating to half volume. This procedure was repeated 4 times. SDS-PAGE (10%) and BCA analysis were then performed to determine the purity and concentration of *Pf*Hsp70, respectively.

3.8 Labelling of *Pf*Hsp70 with Cy3B

For the fluorescence quenching competitive immunoassay, *Pf*Hsp70 needs to be labelled with Cy3B. Cy3B (1 mg; GE Healthcare; Germany) was dissolved in 200 µL Dimethyl sulfoxide (DMSO) to make a solution of 5 mg/mL. From this Cy3B solution, 5.1 µL were added to 710 µL of purified *Pf*Hsp70 (1.74 mg/mL; or 24 nmol/mL; section 3.7). This led to a molar ratio of Cy3B to *Pf*Hsp70 of 2 : 1. The

reaction was mixed in dark for one hour. To stop the reaction, 84.2 µL lysine (0.19 M) was added to give a final concentration of lysine of 0.02 M [39,59]. The reaction was mixed for an additional 10 min in dark. To remove most of lysine and the free unreacted excess dye, the solution was concentrated using "Centricons" (30 kDa; Amicon; 4,000 rpm) to half the volume. Then an equal volume of buffer (0.1 M borate pH = 8.3; 150 mM NaCl) was added. The solution was concentrated again and this procedure was repeated 4 - 6 times till the filtrate became nearly colorless to slightly pink. The solution was finally concentrated to 800 µL and absorbance spectrum was run and compared with spectrum of free Cy3B. The solution of labelled antigen was aliquoted and stored at -20^{o}C.

3.9 Chip assay

A chip assay was developed to prove that the activity and specificity of 2E6 was not affected by conjugation with AuNP-MUA (with or without NHS/EDC) and to determine whether the cross-linked or the non-cross-linked conjugate is more active, based on the intensity of the red color produced on the strips after normalization between both conjugates. A proof-of-concept of competitive chip assay was also performed.

First, BNCs (with or without NHS/EDC) for chip assay were prepared and pre-incubated with either buffer (as blank sample) or *Pf*Hsp70 solution (as a positive sample). NHS/EDC conjugates were prepared as described previously in section 3.3.3 (10 mL of 2 nM AuNP-MUA; molar ratio = 70; 1.2 mM and 2.8 mM of NHS and EDC, respectively) then centrifuged (7,000 rpm for 10 min) and the pellet was resuspended in 400 µL of 10 mg/mL BSA (in 0.1 M borate pH = 8.3; 150 mM NaCl) and left for 1hr, then centrifuged again and resuspended in 250 µL BSA. Then to half of these conjugates (125 µL), 100 µL concentrated *Pf*Hsp70 solution (1.74 mg/mL; obtained from section 3.7) was added (positive sample) and to the other half, 100 µL buffer (0.1 M borate pH = 8.3; 150 mM NaCl) was added (blank). Non-NHS/EDC conjugates were prepared as described previously in section 3.3.3 (10 mL of 2 nM AuNP-MUA; molar ratio = 70; buffer alone added instead of NHS/EDC); then the conjugates were centrifuged and pellet resuspended in 400 µL of 10 mg/mL BSA and left for 1hr, then centrifuged again and resuspended in 250 µL BSA, as in the case of NHS/EDC conjugates. To normalize samples, absorbance at peak maximum (530 nm)

of non-NHS/EDC conjugates was compared to that of NHS/EDC conjugates and thus the former conjugates were diluted (absorbance of NHS/EDC: 1.107; non-NHS/EDC: 1.226). From the 250 µL of non-NHS/EDC conjugates, 203 µL were pipetted and diluted to 250 µL by adding 47 µL of 10 mg/mL BSA. Thus now both the concentration and the volume of the two conjugates were exactly the same, allowing comparison between the two. Again to half of these conjugates (125 µL), 100 µL concentrated *Pf*Hsp70 (1.74 mg/mL) was added (positive sample), and to the other half, 100 µL buffer (0.1 M borate pH = 8.3; 150 mM NaCl) was added (blank). After adding the buffer or the *Pf*Hsp70 protein to either NHS/EDC or non-NHS/EDC conjugates, solutions were incubated for 1hr at room temperature.

To perform the chip assay, *Pf*Hsp70 antigen (7 µL of 1.74 mg/mL; section 3.7) was added to each of the 4 nitrocellulose strips as a drop. Then 3.5 µL of control non-transformed RosettaBlue™ cells (pellet produced from 50 mL culture, resuspended in lysis buffer; see section 3.6.2) was added to the opposite end of the nitrocellulose strips. Strips were allowed to dry for 1 hr at room temperature and then blocked by soaking in blocking solution (0.25 g of non-fat dry milk in 5 mL PBT [see below]). Blocking was performed for 1hr at room temperature. The strips were then washed once by soaking in PBT (50 mM phosphate buffer; 0.05% tween) for 2 min, and then the different conjugates (non-NHS/EDC or NHS/EDC preincubated with either buffer or pure *Pf*Hsp70) were added and incubated for 1 hr. After incubation, the strips were washed with PBT (for 15 min) and a photo was taken using a regular digital camera (Nikon) [54,60].

3.10 Fluorescence quenching competitive assay

As a proof-of-concept, AuNP-MUA particles were added to determine their quenching effect over Cy3B-labelled *Pf*Hsp70. To 193 µL of borate buffer (0.1 M sodium borate pH = 8.3; 150 mM NaCl), 7 µL of 1 : 25 dilution of Cy3B-*Pf*Hsp70 stock (see section 3.8; 1 : 714 dilution from stock) was added. Then 200 µL of AuNP-MUA was added to give a final concentration ranging from 0 - 2.75 nM (table 3). After the addition of AuNP-MUA, fluorescence emission was measured immediately using luminescence spectrometer LS45, Perkin Elmer (excitation wavelength 480 nm). Standard deviation of fluorescence emission values at 572 nm was 0.26 as determined by measuring buffer alone 4 times.

The fluorescence quenching competitive assay was developed for the detection of *Pf*Hsp70. In positive samples, *Pf*Hsp70 in borate buffer [0.1 M borate pH = 8.3; 150 mM NaCl] was pre-incubated with AuNP-MUA-2E6 and this mixture was added to Cy3B-labelled *Pf*Hsp70. Since the 2E6 is partially/fully saturated by unlabelled *Pf*Hsp70, binding to labelled antigen was inhibited and thus fluorescence was less quenched giving a high intensity value. In case of blank, the same procedure was followed but buffer was pre-incubated with AuNP-MUA-2E6 instead of *Pf*Hsp70 before adding to Cy3B-labelled *Pf*Hsp70. Thus the 2E6 binding sites were free (not bound to unlabelled antigen) and were thus able to bind to labelled antigen. Quenching occurred and fluorescence intensity was low (figure 5). In this experiment, for preparing BNCs, 29.5 mL of AuNP-MUA-2E6 (2 nM) was prepared and the molar ratio of 2E6 to AuNP-MUA was 70. No NHS/EDC mixture was added (since non-NHS/EDC BNCs are more active: see section 4.9). The conjugates were centrifuged at 7,000 rpm for 10 min and the pellet was resuspended in 600 µL BSA (10 mg/mL in borate buffer). The conjugates were incubated for 1 hr and then centrifuged at 7,000 rpm for 10 min and the pellet was resuspended in 600 µL borate buffer. The conjugates were centrifuged again at 7,000 rpm for 10 min and finally resuspended in 300 µL of borate buffer.

Two tubes were prepared for each sample. In tube 1, 193 µL borate buffer [0.1 M borate pH = 8.3; 150 mM NaCl]) was mixed with 7 µL of Cy3B-*Pf*Hsp70 (1 : 25). This was the same for all samples. In tube 2, 10 µL of AuNP-MUA-2E6 was mixed with different concentrations of *Pf*Hsp70 (final concentration of 8.7 µg/mL; 870 ng/mL; 87 ng/mL; 8.7 ng/mL; 870 pg/mL) and the volume was completed to 200 µL with borate buffer. After incubating tube 2 for 1 hr at room temperature, tubes 1 and 2 were mixed and fluorescence emission was measured immediately (excitation wavelength 480 nm). Standard deviation of fluorescence emission values at 574 nm was 0.67 as determined by measuring buffer alone 4 times [39].

CHAPTER 4. RESULTS

4.1 Production, purification and activity of anti-*Pf*Hsp70 antibody (2E6)

From 2.6 L hybridoma culture, 35 mL of concentrated impure 2E6 solution was obtained (60 mg/mL of total protein as determined using BCA test). Purification of antibody was performed in two steps, namely (i) Protein G Sepharose 4 Fast Flow; and (ii) PD SpinTrap G-25 columns. 2E6 obtained from Protein G Sepharose 4 Fast Flow was only partially purified as determined by SDS-PAGE (fig. 7). The reason for that might be that the protein G Sepharose 4 Fast Flow method needed further optimization, such as increasing the number of washes before elution. When the partially purified 2E6 was further purified using PD SpinTrap G-25 spin columns, pure 2E6 was obtained (fig. 7). The two bands on SDS-PAGE had calculated molecular weights of ~31 kDa and ~58 kDa, based on a calibration curve constructed with the migration distances of molecular markers (figure 8). After each batch purification of 2E6 using PD SpinTrap G-25 columns, the protein concentration was determined using BCA test. An example of one of the BCA results for the purified 2E6 antibody is shown in table 4 (concentration is 20.9 μM) and the standard curve is shown in figure 9. Regarding the activity of 2E6 antibody, fluorescence microscopy showed that 2E6 antibody was active.

4.2 Hsp70 as a diagnostic target

Since the present study involved the development of prototype immunoassays, the specific recognition of Hsp70 target in a clinical specimen by 2E6 had to proven. This was performed by Western blot analysis using 2E6 as the primary antibody.

4.2.1 Western blot analysis of plasma and whole blood of mice infected with *P. berghei*

Parasitemia (percentage of parasite-infected RBCs / 100 counted RBCs) was around 5% in all experiments (Dr.Claudia Sa e Cunha, PhD; Personal communication). Western blot analysis was performed using 2E6 antibody as the primary antibody for the detection of *Pb*Hsp70 in plasma and whole blood of mice infected with *P. berghei.* No difference was found when comparing plasma of *P. berghei* infected and non-infected blood (fig. 10). However, in the case of whole blood analysis, infected mice blood had an additional band at about 75 kDa (as expected for the presence of

*Pb*Hsp70) (fig. 11). Thus *Pb*Hsp70 seems not to be secreted into plasma but to be confined within the infected RBCs. Since several bands still appear in the negative whole blood sample, the antibody seems to bind non-specifically to other proteins that are mainly present in plasma, as can be concluded from the observation of the same bands in negative whole blood and in negative plasma. To overcome this drawback, RBCs were separated from whole blood and treated with saponin and the pellet after saponin treatment was compared between non-infected and infected samples. Saponin causes the rupture of RBCs and the release of RBC cytoplasmic content into lysate (supernatant). *Plasmodium* Hsp70 is localized within the parasitic membrane and is not exported into the RBC cytoplasm and thus should not be found in the lysate but should be seen in the pellet[44].

4.2.2 Western blot analysis of saponin pellets of RBCs of non-infected mice, of mice infected with *P. berghei*, and of non-infected human

RBCs of non-infected human, and of mice infected or non-infected with *P. berghei*, were treated for 5 min with saponin. Saponin pellets were then compared using Western blot analysis and as expected a band corresponding to *Pb*Hsp70 was only found in the infected RBCs lanes and not in the non-infected mice and human (fig. 12). Interestingly, no bands were detected in the non-infected human RBC saponin pellet even if undiluted. As a control to the experiments, actin was then used as a loading control. Actin is a protein that is present in RBC skeleton and thus if the same number of RBCs were lysed by saponin and loaded onto the SDS-PAGE, in case of non-infected mice and mice infected with *P. berghei*, the intensity of the band corresponding to actin should be similar[61]. Even when the bands of actin were of comparable intensity (RBC normalization was achieved), the non-infected mice RBC saponin pellet did not show a band corresponding to *Pb*Hsp70 while this band was present in the infected mice RBC saponin pellet (fig. 13).

4.2.3 Western blot analysis of saponin pellet of RBCs of mice blood infected with *P. berghei* and of human blood culture infected with *P. falciparum*

After establishing the proof-of-concept of using 2E6 to specifically recognize *Pb*Hsp70 in saponin pellet of RBCs of mice infected with *P. berghei*, recognition of *Pf*Hsp70 in *P. falciparum* infected human blood culture was tested as this system more closely mimics the human application of the immunoassays that are being

developed. As expected, the actin band intensities of saponin pellets of RBCs of mice blood infected with *P. berghei* and human blood culture infected with *P. falciparum* were similar (since they were normalized). The band intensity corresponding to *Pf*Hsp70 was much stronger than that of *Pb*Hsp70 indicating that 2E6 binds more to *Pf*Hsp70 than *Pb*Hsp70, as expected (fig.14).

4.3 AuNP synthesis and functionalization with MUA

The procedure followed for the synthesis of AuNPs produced nanoparticles of an average diameter of 17 nm. This was determined in a previous study using Transmission Electron Microscopy (TEM)[47]. Inductive Coupled Plasma (ICP) was used in a previous study for proof of functionalization of AuNP with MUA by the simultaneous detection of gold and sulphur[62].

4.4 Characterization of BNCs

4.4.1 UV-visible spectroscopy

As a proof of conjugation of AuNP-MUA with 2E6 to generate BNCs, absorbance spectroscopy was performed. 2E6 conjugation was clearly proven by a significant shift in plasmon resonance peak maximum to a longer wavelength, from 521 nm to 530 nm (figure 15).

4.4.2 Agarose gel electrophoresis

As a proof-of-concept, BSA BNCs were prepared with different ratios of BSA to AuNP-MUA and were run on agarose gels (figure 16). AuNPs-MUA and AuNPs-citrate aggregated in the wells possibly due to surface charge cancellation caused by the running buffer (5 mM sodium phosphate buffer; pH = 7). Since BSA conjugates carry a net negative charge (as determined by ζ-potential in a previous study performed in our lab), they should migrate towards the positive pole. It could be observed on the gel (figure 16) that as the molar ratio of BSA to AuNP-MUA increases, implying a larger size of the conjugate formed, the conjugate shows retarded migration on the gel. After proof-of-concept, 2E6 conjugates were prepared, with or without NHS/EDC, to determine which of the conjugates are more uniform and robust. First, the optimum concentration of NHS/EDC required for cross-linking was determined by preparing BNCs using different concentrations of NHS/EDC as described in detail under method section (3.4.2). After running samples on 1%

agarose gel, it was found that both 0.6 mM; 1.4 mM and 1.2 mM; 2.8 mM of NHS and EDC, respectively, were equally suited for preparing stable, uniform and non-aggregated conjugates (figure 17). Thus concentration of 1.2 mM and 2.8 mM of NHS and EDC, respectively, was chosen for further studies since it was the highest concentration of NHS/EDC to produce stable uniform conjugates. In case of concentration of 6 mM and 14 mM of NHS and EDC, respectively, it was clear that the BNCs were aggregated in the wells. BNCs with different 2E6 to AuNP-MUA molar ratios were then prepared with NHS/EDC (1.2 mM and 2.8 mM of NHS and EDC, respectively) or without NHS/EDC. After agarose gel electrophoresis, it could be noted that bands for the NHS/EDC conjugates were slightly more compact (figure 18), indicating that, as expected, NHS/EDC conjugation produced more uniform and robust AuNP-MUA-2E6 conjugates.

For AuNP-CALNN particles, the optimum NHS/EDC concentration was also determined by gel electrophoresis. NHS/EDC BNCs prepared using concentration of 3 mM and 7 mM of NHS and EDC, respectively, was found to be the most stable and uniform as seen as a compact band compared to conjugates prepared without or with other concentrations (ranging from 0.3 - 1.2 mM and 0.7 - 2.8 mM of NHS and EDC, respectively). See figure 19.

4.4.3 Zeta (ζ)-potential

Both non-NHS/EDC and NHS/EDC BNCs were prepared (AuNP-MUA 1 nM; molar ratios = 0 - 400; 0.78 mM and 1.82 mM of NHS and EDC, respectively [for NHS/EDC BNCs]) and ζ-potential measured.The ζ-potential for non-NHS/EDC BNCs showed an increase in ζ-potential with the increase in 2E6 to AuNP-MUA molar ratios till a ratio of about 70 where the ζ-potential was stabilized suggesting the stabilization of the number of antibodies that bind to the AuNP-MUA (figure 20). The binding constant for the conjugation process was determined to be $K_L = 0.023$, by the fitting of a Langmuir-type curve to the experimental data (equation 2).

$$\Delta\zeta = \frac{\Delta\zeta_{max} K_L R}{1 + K_L R} \qquad (2)$$

in which Δζ is the variation in the ζ-potential measured for a certain [2E6]/[AuNP-MUA] in relation to AuNP-MUA; Δζmax is the maximum value for

Δζ-potential as [2E6]/[AuNP-MUA] increases and K_L is a binding constant corresponding to the value of the inverse of the concentrations ratio, for one-half of Δζmax. For the NHS/EDC BNCs, the ζ-potential increase was sharper, *i.e.*, the binding constant for antibody binding was higher (K_L = 0.161). This behavior is expected since NHS/EDC cross-linking contributes to a tighter conjugation, thus BNCs can be totally covered with antibody with lower amounts of antibody than their non-crosslinked counterparts. In other words, NHS/EDC helps more antibody to be conjugated to the AuNP-MUA for conjugates having low 2E6 to AuNP-MUA molar ratios. The ζ-potential plateau value for NHS/EDC BNCs was 30. At high 2E6 to AuNP-MUA molar ratios, more 2E6 antibodies seemed to bind to AuNP-MUA when no NHS/EDC cross-linking agent was present, as can be observed by the higher ζ-potential plateau value for the non-NHS/EDC samples.

4.5 Stability of AuNP-MUA-2E6 BNCs

4.5.1 NaCl method

To determine the minimum amount of 2E6 that is necessary to stabilize the BNCs, an equal volume of 5 M NaCl was added to the BNCs and the absorbance was measured after 6 hrs to allow time for aggregation to occur. As shown by the absorbance spectra (figures 21 and 22), the minimum molar ratio of 2E6 to AuNP-MUA to stabilize against 5 M NaCl for both non-NHS/EDC and the NHS/EDC conjugates was 20. NHS/EDC conjugates seemed to be slightly more stable against 5 M NaCl than non-NHS/EDC conjugates (for molar ratios ≥ 15), as expected.

4.5.2 pH aggregation

AuNP-MUA nanoparticles (1 nM) were aggregated at pH ≤ 4 (figure 23). 2E6 BNCs with or without NHS/EDC were prepared (final AuNP-MUA concentration 1 nM; molar ratio = 70; 1.2 mM and 2.8 mM of NHS and EDC, respectively [for NHS/EDC BNCs]) and pH was adjusted at different values and the absorbance was measured (pH was first decreased and then increased in the same tube). Both non-NHS/EDC and NHS/EDC conjugates had similar behaviour, with minimal aggregation throughout the pH range (pH = 1 - 11) tested. This result was dramatically different from the result obtained for naked AuNP-MUA particles and thus pH aggregation was a further proof of conjugation (figures 24, 25, 26, 27).

4.6 *Pf*Hsp70 expression

4.6.1 Transformation of pQE30/*Pf*Hsp70 into RosettaBlue™ cells

Successful transformation of the pQE30/*Pf*Hsp70 plasmid into RosettaBlue™ cells was confirmed by the presence of colonies of transformed cells onto LB agar plates containing both ampicillin and chloramphenicol. Positive control (transforming a "test plasmid" with ampicillin resistance instead of pQE30/*Pf*Hsp70) but not negative control (autoclaved water instead of plasmid added) showed colonies of transformed cells. Figure 28 shows colonies on LB plates (containing both ampicillin and chloramphenicol) representing RosettaBlue™ cells transformed with either pQE30/*Pf*Hsp70 or positive control plasmid but no colonies seen for untransformed negative control.

4.6.2 Expression of *Pf*Hsp70 under different induction conditions

For *Pf*Hsp70 expression, a 50 mL pre-inoculum was prepared using a colony of RosettaBlue™ cells transformed with pQE30/*Pf*Hsp70, from which three 250 mL cultures was fermented. Samples were withdrawn during bacterial culture and $O.D_{600}$ was measured. O.D values increased indicating bacterial growth till O.D value ranging from 0.5 - 0.6. At that time point, the three cultures were exposed to different induction and harvesting conditions ("no IPTG"; "IPTG 2hr" and "IPTG overnight"; see 3.6.2). Figure 29 shows a curve of $O.D_{600}$ against time for the different induction conditions. After harvesting, SDS-PAGE and Western blot analysis were performed for pellets after resuspension in lysis buffer for the different induction conditions (figure 30). SDS-PAGE was performed to determine the presence of *Pf*Hsp70 in the resuspended pellet before purification and to compare between the different induction conditions. Western blot analysis was performed to confirm SDS-PAGE result and to determine the presence of truncation and degradation products within the impure bands. Since harvesting after 2 hrs led to low yield it was not practically feasible to use this induction pattern in the following scale up experiment. "IPTG overnight" culture seemed to produce slightly more pure *Pf*Hsp70 than "no IPTG" culture. This was concluded as the ratio of the intensity of the *Pf*Hsp70 protein band (75 kDa) to other lower bands (protein impurities or degradation and truncation products of *Pf*Hsp70) was higher for "IPTG overnight" compared to "no IPTG", as shown by SDS-PAGE (figure 30). Thus in the following scale up procedure, cultures were induced with IPTG and harvesting was done the next day. Western blot analysis

showed that within the impure bands appearing on SDS-PAGE, two bands bind to 2E6 antibody (at *ca*. 35 kDa and 50 kDa), originating from possible degradation or truncation products of *Pf*Hsp70 (figure 30). Figure 31 shows SDS-PAGE as well as Western blot analysis of transformed and non-transformed RosettaBlue™ cells. As seen on SDS-PAGE, there was a band in the non-transformed cells very close to *Pf*Hsp70 band (present in transformed cells) that was suggested to be DnaK (Hsp70 of *E. coli*, expressed by RosettaBlue™ cells)[39]. Western blot analysis gave a much clearer result where a band was seen at 75 kDa (accompanied by bands of possible degradation or truncation products at *ca*. 35 kDa and 50 kDa) for transformed cells but no bands for non-transformed cells (figure 31).

4.7 Purification of *Pf*Hsp70 using Ni-NTA column

After cell harvesting, resuspended pellet was homogenised and lysed by French-press and purified using Ni-NTA agarose column. Samples before and after purification by Ni-NTA column together with washes and flow through were all run on 10% SDS-PAGE (fig. 32). The sample that eluted from the Ni-NTA column still contained impurities (bands at molecular weights different from the 75 kDa) including bands from the possible degradation or truncation products at *ca*. 30 - 35 kDa and 45 - 50 kDa. The bands from impurities are nevertheless less intense (less amount) than the band corresponding to *Pf*Hsp70. The second intense band was a band at 30 - 35 kDa that was verified by Western blot analysis before to be a degradation or truncation product of *Pf*Hsp70. Although being only partially purified, the protein was labelled with Cy3B. This is because *Pf*Hsp70 comprises the highest amount and that the other strong band is the degradation or truncation product that can still bind to 2E6 (according to Western blot) and thus is suitable for the fluorescence quenching competitive assay. Further purification of this partially purified protein, using a second purification method was suggested, but was not followed since the yield would have been dramatically affected. Thus we decided to continue with the partially purified sample. The total concentration of *Pf*Hsp70 was then determined by BCA to be 1.74 mg/mL.

4.8 Labelling of *Pf*Hsp70 with Cy3B

The partially purified *Pf*Hsp70 was labelled with Cy3B. The easiest proof of labelling is the fact that labelled *Pf*Hsp70 is more than 75 kDa and thus does not pass with the

filtrate during Centricon washing (membrane cut-off: 30 kDa). However, free dye can easily pass since it is very small in size (mwt 771.8). Thus the presence of pink color in the solution retained in the Centricon is an indication of labelling. An additional proof of labelling, is the shift in the maximum absorbance spectra seen after conjugation from 559 nm for free Cy3B to 565 nm after labelling (figure 33). Also a peak at 280 nm corresponding to *Pf*Hsp70 protein can be observed in conjugated and not in free Cy3B, as expected (fig. 33).

4.9 Chip Assay

For proof-of-concept of the competitive chip assay, a drop of partially purified *Pf*Hsp70 (see section 3.7) was immobilized on one side of a nitrocellulose sheet and non-transformed RosettaBlue™ cells (resuspended pellet; see 3.6.2) were immobilized on the other end. After drying and blocking the nitrocellulose strips, normalized NHS/EDC and non-NHS/EDC conjugates (2 nM AuNP-MUA; molar ratio = 70; 1.2 mM and 2.8 mM of NHS and EDC, respectively [for NHS/EDC BNCs]; blocked with BSA) pre-incubation with either buffer (blank) or with excess pure *Pf*Hsp70 (positive) were added to the nitrocellulose strips (section: 3.9). Since the binding sites of 2E6 antibody will be partially/fully saturated in case of positive samples (during pre-incubation), 2E6 will not easily bind to immobilized *Pf*Hsp70 and thus no red color should be seen. However, in blank samples many 2E6 binding sites will be exposed, 2E6 will easily bind to immobilized *Pf*Hsp70 and consequently a red color should be observed (figure 34). As seen in figures 35 and 36, blank samples in case of non-NHS/EDC and NHS/EDC gave a red color while positive samples gave no color. Importantly, NHS/EDC BNCs were found to be less active since the intensity of the red color on the strip of the blank sample of NHS/EDC BNCs was faint as compared to that of blank sample of non-NHS/EDC conjugates. Thus for the fluorescence quenching competitive assay, non-NHS/EDC conjugates were used. Both NHS/EDC and non-NHS/EDC conjugates were specific since the BNCs did not bind to the drop having non-transformed bacterial culture (full of non-target proteins) but only to the drop of the partially purified *Pf*Hsp70.

4.10 Fluorescence quenching competitive assay

As a proof-of-concept for developing a fluorescence quenching competitive assay for the quantification of *Pf*Hsp70, different concentrations of AuNP-MUA particles (0 -

2.75nM) were added to determine their quenching effect over Cy3B-labelled *Pf*Hsp70 diluted in buffer (0.1 M sodium borate pH = 8.3; 150 mM NaCl). A linear relation of fluorescence quenching was achieved in the concentration range from 0 to 0.825 nM of AuNP-MUA (figure 37).

Proof-of-concept for the fluorescence quenching competitive assay for the detection of *Pf*Hsp70 was then established (principle explained in 3.10). As seen in figure 38, positive samples gave a higher fluorescence intensity value than blank in concentrations higher than 87 ng/mL (*Pf*Hsp70). However for lower concentrations, the difference between positives and blank was less than 3X standard deviation (0.67). Thus 87 ng/mL (1.16 pM) was taken as the limit of detection in this study. In figure 38C, fluorescence enhancement (%) was plotted against the concentration of *Pf*Hsp70 in positive samples. Fluorescence enhancement was calculated as follows (equation 3):

$$Fluorescence\ enhancement\,(\%) = \left(1 - \frac{Blank\ FI\ value - average buffer\ FI\ value}{Sample\ FI\ value - average buffer\ FI\ value}\right) \times 100 \quad (3)$$

where FI is the fluorescence intensity; average buffer fluorescence intensity value is the average fluorescence emission value of the borate buffer alone at 574 nm.

CHAPTER 5. DISCUSSION

In this study, two prototype AuNP-based immunoassays for the detection of *Pf*Hsp70 antigen were developed. Production and purification of anti-*Pf*Hsp70 monoclonal antibody (2E6) were performed and specificity for Hsp70 in mouse blood and human blood culture was determined. 2E6 antibodies were conjugated to AuNPs in the presence and absence of NHS/EDC cross-linkers. Characterization of BNCs was performed and assessment of BNC stability was then done. *Pf*Hsp70 was expressed from *E. Coli* system, purified using Ni-NTA agarose and labelled with Cy3B. Finally, a prototype dipstick chip assay and a prototype fluorescence quenching competitive immunoassay for the detection of *Pf*Hsp70 were developed.

5.1 Purification and specificity of 2E6 antibody

2E6 antibody was purified from hybridoma culture in two steps. The first step is purification using Protein G Sepharose 4 Fast Flow column and the second using PD SpinTrap G-25 disposable columns. Protein G is a group G Streptococcal bacterial protein that has high affinity for IgG antibodies[41]. Protein G columns were chosen rather than Protein A since protein G binds to a wider range of IgGs from eukaryotic species as well as to different IgG subtypes [41] (table 1; appendix). The monoclonal antibody 2E6 was only partially purified using the Protein G Sepharose 4 Fast Flow column and the process required further optimization (such as increasing the number of washes before elution). Thus it was decided to use the disposable spin columns to purify the whole batch of partially purified 2E6. When the two bands of 2E6 obtained in the SDS-PAGE were compared with the marker, their molecular weights were ~31 kDa and ~58 kDa, respectively. Theoretical values for IgG antibody sub-units are 25 kDa and 50 kDa, respectively. The 25 kDa band corresponds to the light chains of the antibody and the 50 kDa band corresponds to the heavy chains of the antibody, that were linked together through disulphide linkages (figure 39)[63].

To determine the specificity of 2E6 for parasitic Hsp70 and to prove that Hsp70 is a diagnostic target for the diagnosis of malaria, Western blot analysis was performed. Since *P. falciparum* human infected blood was not available, *P. berghei* infected and non-infected mice blood were analyzed instead since it was proven previously that 2E6 recognizes both *Pf*Hsp70 and *Pb*Hsp70[45]. Western blot analysis for the detection of *Pb*Hsp70 using 2E6 antibody was first performed on plasma and

on whole blood of *P. berghei* infected and non-infected mice blood. Comparison of infected and non-infected mice plasma suggests that *Pb*Hsp70 is not secreted into plasma and thus plasma is not an appropriate specimen for the diagnostic assay. However, in the case of whole blood of infected mice, an additional band at about 75 kDa (corresponding to *Pb*Hsp70) was observed when compared to whole blood of non-infected mice. However, since several bands were seen in non-infected whole blood samples that were very similar to those of non-infected plasma, it was reasoned that 2E6 non-specifically binds to other proteins, mainly in plasma, and thus the most suitable sample will not be whole blood but instead the detection of *Pb*Hsp70 in isolated RBCs. Thus another protocol was followed, where RBCs were separated from whole blood, washed twice with PBS and then lysed by saponin and the pellet after saponin treatment was washed 4 times with PBS[44]. Saponin causes RBC lysis, leading to the release of RBC cytoplasm contents into the lysate (supernatant). *Plasmodium* Hsp70 was proven not to be exported into the RBC cytoplasm; i.e should not be detected in cell lysate but instead should be detected in the saponin pellet that contains parasitic proteins that are localized within the parasitic membrane[44].When the saponin pellet of non-infected mice, infected mice and that of non-infected human were compared, *Pb*Hsp70 was found only in the infected mice saponin pellet, as expected. The 2E6 monoclonal antibody did not bind t o non-infected human saponin pellet even when the undiluted sample was analyzed.

As a loading control, anti-actin primary and anti-rabbit secondary antibodies were added to the lower part of the blotted membrane while the upper part was treated with 2E6 primary antibody and anti-mouse secondary antibody (membrane was cut above the 50 kDa marker band; section 3.2.3). It was found that even when the actin bands were comparable in intensity for both infected and non-infected mice RBC saponin pellets (samples normalized; section 4.2.2), the *Pb*Hsp70 band was only found in the infected blood. After process optimization using mice blood infected with *P. berghei*, a human blood culture infected with *P. falciparum* was provided. The sample was analyzed by Western blot and compared with mice blood infected with *P. berghei*. Although the intensities of the actin bands in both samples were comparable (samples normalized), the band representing *Pf*Hsp70 had a much higher intensity when compared to the band representing *Pb*Hsp70, indicating that the 2E6 monoclonal antibody binds more strongly to *Pf*Hsp70 than to *Pb*Hsp70.

5.2 Synthesis and functionalization of AuNPs and characterization of AuNP-MUA-2E6 BNCs

Gold citrate particles were synthesized and functionalized with MUA. MUA allows the uniformity of negative charge onto the particles and was reported to reduce the aggregation of citrate particles[64]. Proof of functionalization with MUA was proven previously by the simultaneous detection of gold and sulphur using Inductive Coupled Plasma (ICP)[62]. Another peptide functional group (CALNN) was also tested. But since MUA particles were prepared in our laboratory, unlike AuNP- CALNN, and gave stable conjugates, further studies were performed on AuNP-MUA instead of AuNP-CALNN particles.

After functionalization of AuNP with MUA, conjugation with 2E6 was then performed by two strategies. The first strategy was conjugation in the absence of NHS/EDC cross-linkers, where conjugation occurs mainly through electrostatic forces between 2E6 and MUA groups on the surface of AuNPs. The second strategy was conjugation in the presence of NHS/EDC cross-linkers allowing the covalent linkage between 2E6 and MUA and thus should lead to more stable and robust conjugates. EDC is a dehydrating agent that aids the reaction between two compounds, one having an amine group (2E6) and the other having a carboxyl group (MUA). This occurs by the binding of EDC to a carboxyl group forming an O-acylisourea intermediate that can easily react with an amine group on another molecule forming an amide bond. However, if EDC is used alone, the intermediate is susceptible to hydrolysis to give the free carbonyl group again. Thus NHS is added to stabilize the unstable O-acylisourea intermediate by giving a NHS-ester intermediate and thus enhancing the EDC coupling (figure 40)[65-66].

Monoclonal antibody (2E6) conjugation to AuNP-MUA was verified using 3 different techniques, namely: UV-visible spectroscopy, agarose gel electrophoresis and ζ-potential analysis. After conjugation, a shift in absorbance peak maximum occurred (from 521 nm to 530 nm) due to the change in the local refractive index surrounding the AuNPs[67]. Another proof of conjugation is agarose gel electrophoresis where naked AuNP-MUA aggregated in the wells (due to surface charge cancellation caused by the running buffer) while AuNP-MUA-2E6 conjugates were protected from aggregation and migrated through the gel towards the positive pole (negative

particles) according to their size and charge. Gel electrophoresis enabled the choice of the optimum concentration of NHS/EDC needed for the covalent linkage of 2E6 to AuNP-MUA particles, where high concentrations led to aggregations of the particles as seen as a smear on the gel and/or aggregation in the wells; while compact bands were seen at lower concentrations (0.6 mM; 1.4 mM and 1.2 mM; 2.8 mM of NHS and EDC, respectively; the latter was considered optimum conditions).Gel electrophoresis also enabled the comparison between non-NHS/EDC and NHS/EDC conjugates, where NHS/EDC ones were found to be slightly more uniform and robust (seen as a tighter band). This is expected since the type of bond formed is covalent whereas in case of non-NHS/EDC, it is mainly electrostatic attraction. An additional proof of conjugation was the use of ζ-potential measurements. As 2E6 antibody binds to the AuNP-MUA surface, the ζ-potential increases (becomes less negatively charged) due to the change in surface properties of the particles[53]. Stabilization of ζ-potential with the increase in 2E6 to AuNP molar ratio corresponds to a stabilization of the number of antibodies that bind to the AuNP-MUA. It was proven that NHS/EDC allowed a stronger binding between 2E6 and AuNP-MUA, corresponding to a seven- fold increase in the binding constant value (K_L = 0.161 and K_L = 0.023, for NHS/EDC and non-NHS/EDC BNCs, respectively). Thus at low 2E6 to AuNP-MUA molar ratios, NHS/EDC seems to allow more antibody to bind to AuNP-MUA. However, at high 2E6 to AuNP-MUA molar ratios, when no NHS/EDC cross-linking agent was present, a higher ζ-potential plateau value for the non-NHS/EDC samples was achieved, indicating that more 2E6 antibody was bound.

To determine the stability of the BNCs against harsh conditions, an equal volume of 5M NaCl was added to NHS/EDC and non-NHS/EDC BNCs. NHS/EDC conjugates were found to be slightly more stable than non-NHS/EDC conjugates (for molar ratios ≥ 15) and for both conjugates a molar ratio of 2E6 to AuNP-MUA less than 20 couldn't protect conjugates from aggregating. It is important to note that theoretically the number of antibodies needed to form a monolayer on the surface of the AuNP is about 9 according to the following equation[68]:

$$Number\ of\ antibodies\ to\ form\ monolayer = \frac{4\pi r^{2}}{head\ group\ surface\ area\ of\ IgG\ antibody} \quad (4)$$

where $4\pi r^2$ is the surface area of the sphere of AuNP; r is the radius of the AuNP sphere (8.5 nm); head group surface area of IgG antibody was reported[68] to be 100 nm^2.

According to pH aggregation studies, in the pH range of 1 - 11, both NHS/EDC and non-NHS/EDC conjugates had similar behavior, where aggregation was minimal throughout the different pH values. However, AuNP-MUA alone were dramatically aggregated at pH values ≤ 4. Thus this result was an additional proof of conjugation. To conclude, NHS/EDC conjugates were slightly more uniform and stable against NaCl aggregation than non-NHS/EDC conjugates.

5.3 *Pf*Hsp70 expression

Transformation of pQE30/*Pf*Hsp70 into RosettaBlue™ cells was performed through heat shock. In Matambo's study, two plasmids were transformed (pQE30/*Pf*Hsp70 and pRIG) into *E. coli* XLI Blue cells[57]. pRIG plasmid was transformed into the cells as it encodes tRNAs for rare codons to enhance the yield of the full length protein (*Pf*Hsp70) and to inhibit the formation of truncation products. However, in our study, only pQE30/*Pf*Hsp70 was transformed into the cells because RosettaBlue™ cells have the ability to express tRNAs for rare codons as they already have pRARE plasmid[69]. RosettaBlue™ cells resist both chloramphenicol (resistance encoded by pRARE plasmid) and tetracycline (resistance encoded by genome). Transformed cells having the pQE30/*Pf*Hsp70 construct (or positive control) can also resist ampicillin. Thus colonies on LB plates (having chloramphenicol and ampicillin) indicate transformed cells, either having pQE30/*Pf*Hsp70 plasmid or the positive control. Expression of *Pf*Hsp70 from transformed cells was performed under different induction conditions and as illustrated before (section: 4.6.2), induction with IPTG and harvesting the next day was chosen as the optimum conditions for *Pf*Hsp70 expression. Western blot analysis showed that within the impure bands appearing on SDS-PAGE, two bands (at *ca.* 35 kDa and 50 kDa) that are also intense represent either degradation or truncation products of *Pf*Hsp70. Importantly, when SDS-PAGE of resuspended pellets of non-transformed cells were compared with those of transformed ones, the band representing *Pf*Hsp70 was only found in transformed cells. However, a band in non-transformed cells was very close to that representing *Pf*Hsp70 which was suggested to be DnaK (Hsp70 of RosettaBlue™ cells). Western

blot analysis also showed that 2E6 only recognized Hsp70 in transformed cells (*Pf*Hsp70) and not in non-transformed cells (DnaK)[57].

5.4 Purification and Cy3B-labelling of *Pf*Hsp70

Since expressed *Pf*Hsp70 was His-tagged (6x) at the N-terminus, we used Ni-NTA column for purification. Nickel has high affinity for histidine and thus proteins with His-tag can be separated from other proteins via affinity chromatography using Ni-NTA agarose[70]. Purification didn't give a single band on SDS-PAGE and the reason for this was not clear. Possible explanations are rapid degradation of *Pf*Hsp70 and some non-specific binding of impurities to the column. However, the impure bands were less intense compared to *Pf*Hsp70 band (75 kDa) and the second main band (30-35 kDa) seemed to belong to a degradation or truncation product of *Pf*Hsp70 that can bind to 2E6 (as proven by Western blot analysis) and thus is useful for the fluorescence quenching competitive assay. Thus this partially purified protein was labelled with Cy3B as is.

Although FITC has been used in several fluorescence quenching immunoassays with AuNPs (see Chapter 1: introduction) and is inexpensive, we preferred to use Cy3B instead due to the multiple advantages of Cy3B over FITC[71]. Cyanine dyes in general are less influenced by tryptophan quenching than conventional dyes and thus have high signal to noise ratio. Also they are less affected by pH changes and are photostable[71]. Table 2 (appendix) compares the properties of FITC and Cy3B. Cy3B is the backbone-stabilized form of Cy3. Thus due to the rigid structure of Cy3B, Cy3B-labelled proteins have 3-folds brighter fluorescence compared to proteins labelled with Cy3[71]. Importantly, Mayilo *et al*.[39] reported that the sensitivity of the fluorescence quenching competitive assay (the same method used in our study) based on Cy3B was more sensitive than that based on Cy3. Thus Cy3B was chosen as the labelling dye in our study.

In our study, Cy3B-NHS ester was used that allows the linkage with the protein of interest via acylation of amino groups (primary amino groups present at the N- terminus and at ε-amino group of lysine). The reaction is stopped by adding a large amount of free lysine. Cy3B-labelling was proven not only by a shift in peak

maximum of absorbance spectrum (from 559 to 565 nm) upon conjugation but also simply by the fact that labelled *Pf*Hsp70 was not filtered through the 30 kDa Centricon during washing. This is because, the free dye can easily pass through a 30 kDa Centricon due to its small size (mwt 771.8 Da) while labelled *Pf*Hsp70 is more than 75 kDa and thus cannot pass with the filtrate during washing of the Centricons (30 kDa). Molar ratio of Cy3B to *Pf*Hsp70 of 2 : 1 was chosen since this was proven to be optimum for BSA labelling which is similar in size to *Pf*Hsp70 (BSA: about 67 kDa; P*f*Hsp70: about 75 kDa)[39, 72].

5.5 Chip Assay

Proof-of-concept of the competitive chip assay was established where when AuNP-MUA-2E6 conjugates (with or without NHS/EDC) were preincubated with buffer (in blank), the strip gave a red color and when overloaded with *Pf*Hsp70 (positive sample), no color was seen (figures 35, 36). Both NHS/EDC and non-NHS/EDC conjugates were specific since they only recognized the drop of immobilized *Pf*Hsp70 but not the drop of resuspended pellet of non-transformed RosettaBlue™ cells. NHS/EDC BNCs were less active than non-NHS/EDC BNCs since the intensity of the red color produced on the strips was fainter than that produced by non-NHS/EDC conjugates in the blank samples. This may be due to the partial denaturation of 2E6 antibody by its covalent linkage to the surface of AuNP-MUA particles[73].

5.6 Fluorescence quenching competitive assay

A linear relation of fluorescence (of Cy3B) quenching was achieved on the addition of AuNP-MUA within the concentration range of AuNP-MUA of 0 to 0.825 nM. Proof-of-concept for fluorescence quenching competitive assay was established and the detection limit was 87 ng/mL (1.16 pM). Further studies are still needed to enhance sensitivity and determine the quantitative linear range. As stated previously, Mayilo S *et al* [39] reported using the same method that the LOD and limit of quantitation were 0.2 and 0.6 ng/mL, respectively (0.51 and 1.54 pM, respectively) and the quantitative linearity range was between 0.5 - 3 ng/mL (1.28 - 7.69 pM, respectively).

CHAPTER 6. CONCLUSIONS

6.1 Summary

The objectives of the current study were achieved with the establishment of proof-of-concept of two prototype diagnostic assays for malaria based on the detection of *P. falciparum* Hsp70; (i) competitive based chip assay (ii) fluorescence quenching competitive assay. 2E6 monoclonal antibody was produced from hybridoma culture and specificity of 2E6 for parasitic Hsp70 was proven using Western blot analysis where detection of *Pb*Hsp70 in saponin pellet of RBCs of *P. berghei* infected mice and *Pf*Hsp70 in that of *P. falciparum* infected human culture was established. Recombinant *Pf*Hsp70 antigen was expressed using genetically modified *E. coli* RosettaBlue™ cells. To increase the yield and to produce relatively pure *Pf*Hsp70, induction of the culture was done using IPTG and harvesting was performed the next day. Western blot analysis showed that transformed cells, but not non-transformed cells, expressed *Pf*Hsp70 protein that was recognized by 2E6 antibody. Purification of *Pf*Hsp70 was carried out using Ni-NTA column and the partially purified protein was labelled using Cy3B, for intended usage in the fluorescence quenching competitive assay.

Gold citrate nanoparticles were synthesized and functionalized with MUA. Conjugation of 2E6 antibody to AuNP-MUA was then performed either through electrostatic linkage (in the absence of NHS/EDC) or through covalent amide bond (in the presence of NHS/EDC cross linkers). By comparing these conjugates, NHS/EDC BNCs were slightly more uniform (as seen using agarose gel electrophoresis) and stable against aggregation induced by 5 M NaCl. However, 2E6 antibody activity was more preserved in non-NHS/EDC BNCS than in NHS/EDC BNCs as determined using prototype competitive chip assay. Proof-of-concept of the prototype competitive chip assay and prototype fluorescence quenching competitive assay was proven. The prototype fluorescence quenching competitive assay featured a detection limit of 87 ng/mL (1.16 pM). Analysis of clinical specimens is still to be determined.

6.2 Future plans

In this study, we have chosen *Pf*Hsp70 as the diagnostic target for our two prototype competitive assays (chip and fluorescence quenching). However, *Pf*Hsp70 has two

main drawbacks. The first is that it is conserved between different species and thus false positivity is expected to occur if the patient is infected with a disease caused by an agent that has an Hsp70 protein that is recognized by 2E6[12]. An example of such an agent is *Toxoplasma gondii* (causes Toxoplasmosis), since *Tg*Hsp70 has a similarity of 82% with *Pf*Hsp70 (this was known by performing a protein blast [NCBI] of the sequence of *Pf*Hsp70 that binds to 2E6 [365-681 a.a]. It is important to note that *Pb*Hsp70, which was found to bind to 2E6 by Western blot analysis, has a similarity of 83% with *Pf*Hsp70. The second drawback is that, as proven by our Western blot analysis, neither whole blood or plasma can be used as the direct diagnostic specimen for Hsp70 analysis and that RBCs need to be collected, treated with saponin and the saponin pellet washed prior to being analyzed by the diagnostic assay. This is not practical in field assays (assays performed in endemic countries) since it significantly increases the number of analysis steps. However, we used *Pf*Hsp70 as diagnostic target for proof-of-concept of our assays since both the plasmid expressing *Pf*Hsp70 antigen as well as the hybridoma culture expressing 2E6 antibody were supplied by our collaborators (Prof. Gregory Blatch [Rhodes University, South Africa] and Prof. Maria Mota and Dr. Miguel Prudêncio [Instituto de Medicina Molecular, Portugal, respectively). Our group is planning to use both two dimensional gel electrophoresis and mass spectroscopy to search for new *P. falciparum* specific proteins in infected human plasma to make diagnosis more sensitive, more specific, rapid and easy. After selecting the new target, the chip assay will be developed as a competitive assay (concept already proven) using non-NHS/EDC BNCs since they were proven to be more active than NHS/EDC conjugates. For the fluorescence quenching competitive assay, in order to increase the sensitivity of the assay, cubical or decahedral shapes instead of spherical particles will also be tested. Such choice of non-spherical nanoparticles is related to the fact that the emission fluorescence spectra of Cy3B-labelled protein will overlap more fully with absorbance spectra of cubical [74] or decahedral particles[75] than they do with spherical particles (figure 41). This will allow better quenching of the AuNPs to the fluorescence emission of Cy3B-labelled *Pf*Hsp70 and thus should enhance sensitivity. Also determination of the quantitative linear range for the fluorescence quenching competitive assay (for the different AuNPs shapes) will be determined.

CHAPTER 7. REFERENCES

1 Seed, C. R., Kitchen, A. & Davis, T. M. The current status and potential role of laboratory testing to prevent transfusion-transmitted malaria. *Transfus Med Rev* **19**, 229-240 (2005).

2 WHO. http://www.who.int/mediacentre/factsheets/fs094/en/index.html. (Updated January 2009).

3 Hawkes, M. & Kain, K. C. Advances in malaria diagnosis. *Expert Rev Anti Infect Ther* **5**, 485-495 (2007).

4 Trampuz, A., Jereb, M., Muzlovic, I. & Prabhu, R. M. Clinical review: Severe malaria. *Crit Care* **7**, 315-323 (2003).

5 Jones, M. K. & Good, M. F. Malaria parasites up close. *Nat Med* **12**, 170-171 (2006).

6 Hviid L. http://journals.cambridge.org/fulltext_content/ERM/ERM1_04/S1462399498000179sup001.pdf. Expert Reviews in Molecular Medicine ISSN 1462-3994 http://www–ermm.cbcu.cam.ac.uk. Accession date: 1998.

7 Corradin, G. & Kajava, A. V. Malaria vaccine: why is it taking so long? *Expert Rev Vaccines* **9**, 111-114 (2010).

8 Girard, M. P., Reed, Z. H., Friede, M. & Kieny, M. P. A review of human vaccine research and development: malaria. *Vaccine* **25**, 1567-1580 (2007).

9 Behr, C. *et al.* Antibodies and reactive T cells against the malaria heat-shock protein Pf72/Hsp70-1 and derived peptides in individuals continuously exposed to Plasmodium falciparum. *J Immunol* **149**, 3321-3330 (1992).

10 Hoffman, S. L. *et al.* Development of a metabolically active, non-replicating sporozoite vaccine to prevent Plasmodium falciparum malaria. *Hum Vaccin* **6**, 97-106 (2010).

11 Whitley, D., Goldberg, S. P. & Jordan, W. D. Heat shock proteins: a review of the molecular chaperones. *J Vasc Surg* **29**, 748-751 (1999).

12 Shonhai, A., Boshoff, A. & Blatch, G. L. The structural and functional diversity of Hsp70 proteins from Plasmodium falciparum. *Protein Sci* **16**, 1803-1818 (2007).

13 Sharma, Y. D. Structure and possible function of heat-shock proteins in Falciparum malaria. *Comp Biochem Physiol B* **102**, 437-444 (1992).

14 Misra, G. & Ramachandran, R. Hsp70-1 from Plasmodium falciparum: protein stability, domain analysis and chaperone activity. *Biophys Chem* **142**, 55-64 (2009).

15 Radwan, S. H. & Azzazy, H. M. Gold nanoparticles for molecular diagnostics. *Expert Rev Mol Diagn* **9**, 511-524 (2009).

16 Baptista, P. *et al.* Gold nanoparticles for the development of clinical diagnosis methods. *Anal Bioanal Chem* **391**, 943-950 (2008).

17 Seydack, M. Nanoparticle labels in immunosensing using optical detection methods. *Biosens Bioelectron* **20**, 2454-2469 (2005).

18 Microbiology Education Series - Parasitology No. 2. http://www.cosmosbiomedical.com/education/parasitology/parasitology2.shtml.

19 Ohrt, C., Purnomo, Sutamihardja, M. A., Tang, D. & Kain, K. C. Impact of microscopy error on estimates of protective efficacy in malaria-prevention trials. *J Infect Dis* **186**, 540-546 (2002).
20 Payne, D. Use and limitations of light microscopy for diagnosing malaria at the primary health care level. *Bull World Health Organ.* **66**, 621–626 (1988).
21 Chiodini, P. L. *et al.* The heat stability of Plasmodium lactate dehydrogenase-based and histidine-rich protein 2-based malaria rapid diagnostic tests. *Trans R Soc Trop Med Hyg* **101**, 331-337 (2007).
22 Jelinek, T., Grobusch, M. P. & Nothdurft, H. D. Use of dipstick tests for the rapid diagnosis of malaria in nonimmune travelers. *J Travel Med* **7**, 175-179 (2000).
23 Marx A, P. D., Egger M, Nüesch R, Bucher HC, Genton B, Hatz C, Jüni P. Meta-analysis: accuracy of rapid tests for malaria in travelers returning from endemic areas. *Ann Intern Med.* **142**, 836-846 (2005).
24 Ochola LB, V. P., Smith T, Mabaso ML, Newton CR. The reliability of diagnostic techniques in the diagnosis and management of malaria in the absence of a gold standard. *Lancet Infect Dis.* **6**, 582-588 (2006).
25 Snounou, G., Viriyakosol, S., Jarra, W., Thaithong, S. & Brown, K. N. Identification of the four human malaria parasite species in field samples by the polymerase chain reaction and detection of a high prevalence of mixed infections. *Mol Biochem Parasitol* **58**, 283-292 (1993).
26 Snounou, G. *et al.* High sensitivity of detection of human malaria parasites by the use of nested polymerase chain reaction. *Mol Biochem Parasitol* **61**, 315-320 (1993).
27 Hanscheid, T., Pinto, B. G., Cristino, J. M. & Grobusch, M. P. Malaria diagnosis with the haematology analyser Cell-Dyn 3500: What does the instrument detect? *Clin Lab Haematol* **22**, 259-261 (2000).
28 Dromigny, J. A., Jambou, R., Scott, C. S. & Perrier-Gros-Claude, J. D. Performance evaluation of automated depolarization analysis for detecting clinically unsuspected malaria in endemic countries. *Trans R Soc Trop Med Hyg* **99**, 430-439 (2005).
29 de Langen, A. J. *et al.* Automated detection of malaria pigment: feasibility for malaria diagnosing in an area with seasonal malaria in northern Namibia. *Trop Med Int Health* **11**, 809-816 (2006).
30 Demirev, P. A. *et al.* Detection of malaria parasites in blood by laser desorption mass spectrometry. *Anal Chem* **74**, 3262-3266 (2002).
31 Tanaka, M., Matsuo, K., Enomoto, M. & Mizuno, K. A sol particle homogeneous immunoassay for measuring serum cystatin C. *Clin Biochem* **37**, 27-35 (2004).
32 Liu, X. & Huo, Q. A washing-free and amplification-free one-step homogeneous assay for protein detection using gold nanoparticle probes and dynamic light scattering. *J Immunol Methods* **349**, 38-44 (2009).
33 Shen, G. & Zhang, Y. Highly sensitive electrochemical stripping detection of hepatitis B surface antigen based on copper-enhanced gold nanoparticle tags and magnetic nanoparticles. *Anal Chim Acta* **674**, 27-31 (2010).
34 Commercially available rapid tests for malaria. www.rapid-diagnostics.org/files/rdtinfo-comava-malaria-200804.rtf
35 Ao, L., Gao, F., Pan, B., He, R. & Cui, D. Fluoroimmunoassay for antigen based on fluorescence quenching signal of gold nanoparticles. *Anal Chem* **78**, 1104-1106 (2006).

36 Mayilo, S. *et al.* Long-range fluorescence quenching by gold nanoparticles in a sandwich immunoassay for cardiac troponin T. *Nano Lett* **9**, 4558-4563 (2009).
37 Peng, Z. *et al.* A novel immunoassay based on the dissociation of immunocomplex and fluorescence quenching by gold nanoparticles. *Anal Chim Acta* **583**, 40-44 (2007).
38 Matveeva, E. G., Shtoyko, T., Gryczynski, I., Akopova, I. & Gryczynski, Z. Fluorescence Quenching/Enhancement Surface Assays: Signal Manipulation Using Silver-coated Gold Nanoparticles. *Chem Phys Lett* **454**, 85-90 (2008).
39 Mayilo, S. *et al.* Competitive homogeneous digoxigenin immunoassay based on fluorescence quenching by gold nanoparticles. *Anal Chim Acta* **646**, 119-122 (2009).
40 Ammonium Sulphate Precipitation Procedure. http://www.protein-chem.com/Resources/Ammonium.pdf.
41 GE Healthcare. Antibody Purification Handbook. www.gelifesciences.com/protein-purification.
42 GE Healthcare. Protein G HP SpinTrap / Ab SpinTrap. http://www.gelifesciences.co.jp/tech_support/manual/pdf/28906772.pdf.
43 Krohn, R. I. The colorimetric detection and quantitation of total protein. *Curr Protoc Cell Biol* **Appendix 3**, Appendix 3H, (2002).
44 Banumathy, G., Singh, V. & Tatu, U. Host chaperones are recruited in membrane-bound complexes by *Plasmodium falciparum*. *J Biol Chem* **277**, 3902-3912 (2002).
45 Tsuji, M., Mattei, D., Nussenzweig, R. S., Eichinger, D. & Zavala, F. Demonstration of heat-shock protein 70 in the sporozoite stage of malaria parasites. *Parasitol Res* **80**, 16-21 (1994).
46 Bordin, L., Ion-Popa, F., Brunati, A. M., Clari, G. & Low, P. S. Effector-induced Syk-mediated phosphorylation in human erythrocytes. *Biochim Biophys Acta* **1745**, 20-28 (2005).
47 Baptista, P., Doria, G., Henriques, D., Pereira, E. & Franco, R. Colorimetric detection of eukaryotic gene expression with DNA-derivatized gold nanoparticles. *J Biotechnol* **119**, 111-117 (2005).
48 P. C. Lee, D. M. Adsorption and surface-enhanced Raman of dyes on silver and gold sols. *J. Phys. Chem.* **86** 3391–3395 (1982).
49 Zhou, Y. *et al.* Colloidal gold probe-based immunochromatographic assay for the rapid detection of brevetoxins in fishery product samples. *Biosens Bioelectron* **24**, 2744-2747 (2009).
50 Anthony J. Di Pasqua, R. E. M. I., Yan-Li Ship, James C. Dabrowiak, and Tewodros Asefa. Preparation of antibody-conjugated gold nanoparticles *Materials Letters* **63**, 1876-1879 (2009).
51 Rayavarapu, R. G. *et al.* Synthesis and bioconjugation of gold nanoparticles as potential molecular probes for light-based imaging techniques. *Int J Biomed Imaging* **2007**, 29817 (2007).
52 Sandanaraj, B. S. *et al.* Noncovalent modification of chymotrypsin surface using an amphiphilic polymer scaffold: implications in modulating protein function. *J Am Chem Soc* **127**, 10693-10698 (2005).
53 Gomes, I, Santos, N.C., Oliveira, L.M.A., Quintas, A., Eaton, P., Pereira, E., Franco, R. Probing Surface Properties of Cytochrome c at Au Bionanoconjugates. *J. Phys. Chem. C* **112** 16340–16347 (2008).

54 Shim, W. B. *et al.* Development of immunochromatography strip-test using nanocolloidal gold-antibody probe for the rapid detection of aflatoxin B1 in grain and feed samples. *J Microbiol Biotechnol* **17**, 1629-1637 (2007).
55 Zhu, Y. *et al.* Development of an immunochromatography strip for the rapid detection of 12 fluoroquinolones in chicken muscle and liver. *J Agric Food Chem* **56**, 5469-5474 (2008).
56 Novagen. Competent Cells. User Protocol TB009 Rev. G 0609. www.novagen.com.
57 Matambo, T. S., Odunuga, O. O., Boshoff, A. & Blatch, G. L. Overproduction, purification, and characterization of the Plasmodium falciparum heat shock protein 70. *Protein Expr Purif* **33**, 214-222 (2004).
58 Roche Applied Science. The Complete Guide for Protease Inhibition. http://www.roche-applied-science.com/ProteaseInhibitor/pdf/proteaseinhibition_guide.pdf.
59 GE Healthcare. Amersham Cy™3B mono-reactive dye. http//www.gehealthcare.com/lifesciences.
60 Tanaka, R. *et al.* A novel enhancement assay for immunochromatographic test strips using gold nanoparticles. *Anal Bioanal Chem* **385**, 1414-1420, doi:10.1007/s00216-006-0549-4 (2006).
61 Kriebardis, A. G. *et al.* Storage-dependent remodeling of the red blood cell membrane is associated with increased immunoglobulin G binding, lipid raft rearrangement, and caspase activation. *Transfusion* **47**, 1212-1220 (2007).
62 Gomes, I. I. F. PhD Thesis, UNL, Lisboa, Portugal,. (2009).
63 Gilbert, S. F. A companion to developmental biology. Regulation of Transcription From Immunoglobin Light Chains. Edition 8 (2006).
64 Yang, Y., Matsubara, S., Nogami, M., Shi, J. Controlling the aggregation behavior of gold nanoparticles *Materials Science and Engineering B* **140**, 172–176 (2007).
65 Pierce. NHS and Sulfo-NHS. Improve the efficiency of EDC coupling or create amine-reactive reagents. http://www.piercenet.com/products/browse.cfm?fldID=02040114.
66 Fischer, M. J. Amine coupling through EDC/NHS: a practical approach. *Methods Mol Biol* **627**, 55-73 (2010).
67 Sokolov, K. *et al.* Real-time vital optical imaging of precancer using anti-epidermal growth factor receptor antibodies conjugated to gold nanoparticles. *Cancer Res* **63**, 1999-2004 (2003).
68 Melancon, M. P. *et al.* In vitro and in vivo targeting of hollow gold nanoshells directed at epidermal growth factor receptor for photothermal ablation therapy. *Mol Cancer Ther* **7**, 1730–1739 (2008).
69 News Letter Of Novagen, I. Overcoming the codon bias of E. coli for enhanced protein expression. Advanced Products And Protocols For Molecular Biology Research. Number 12. http://wolfson.huji.ac.il/expression/rosetta.pdf (2001).
70 Qiagen. The QIAexpressionist™. A handbook for high-level expression and purification of 6xHis-tagged proteins. www.qiagen.com (2003).
71 Amersham biosciences. Fluorescence screening reagents guide. http://www.apczech.cz/pdf/BR-Fluorescence-Screening-Reagents-Guide.pdf.
72 BSA (Bovine Serum Albumin). http://www.pbcpeptide.com/BSA.htm.

73 Di Marco, M. *et al.* Overview of the main methods used to combine proteins with nanosystems: absorption, bioconjugation, and encapsulation. *Int J Nanomedicine* **5**, 37-49 (2010).
74 Wu, X. *et al.* High-photoluminescence-yield gold nanocubes: for cell imaging and photothermal therapy. *ACS Nano* **4**, 113-120 (2010).
75 Jianhua Sun, M. G., Tongming Shang, Cuiling Gao, Zheng Xu, and & Zhu, J. Selective Synthesis of Gold Cuboid and Decahedral Nanoparticles Regulated and Controlled by Cu2+ Ions. *Crystal Growth & Design* **8**, 906–910 (2008).

CHAPTER 8. LIST OF FIGURES

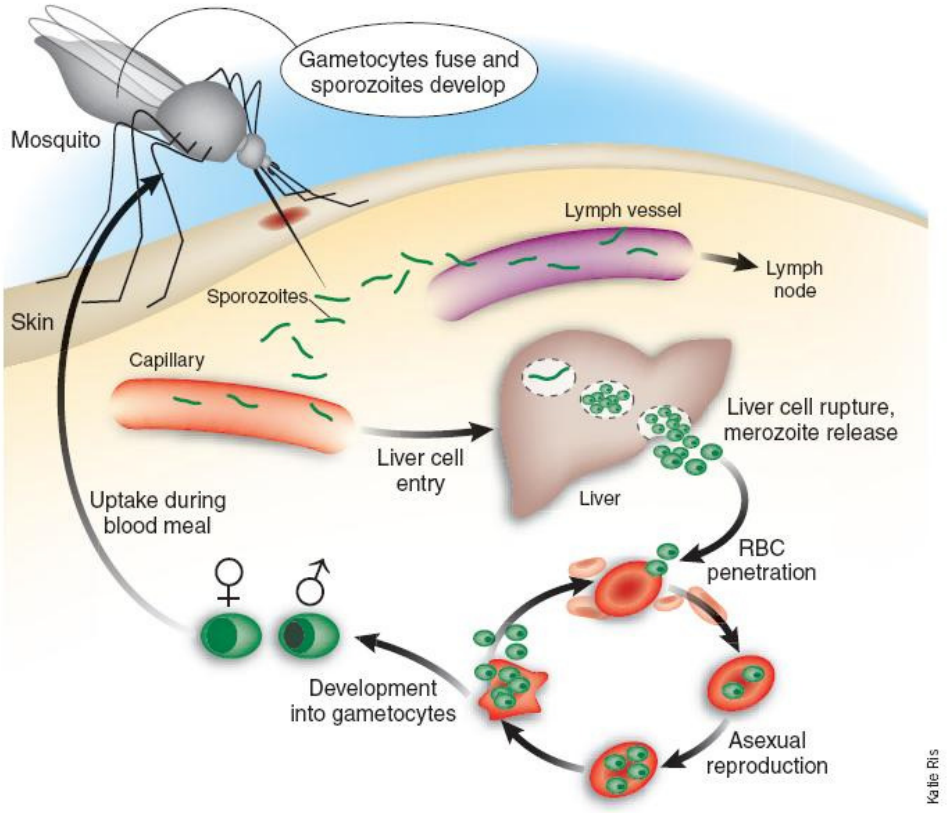

Figure 1. Malaria life cycle. In mammals (including humans), the life cycle starts with a bite of the individual by an infected mosquito. Sporozoites are released from the saliva of the mosquito into the patient's blood and then reach the liver where asexual reproduction occurs, leading to the production of merozoites. Infected hepatocytes then rupture, leading to the release of merozoites into the blood stream and then into red blood cells (RBCs) and starting the erythrocytic cycle. Another asexual replication then takes place leading to the production of more merozoites that are then released from ruptured RBCs to invade more RBCs. Some of the merozoites start to form male and female sexual forms in the blood of the infected patient. During the feeding of a female *Anopheles* mosquito, these sexual forms are taken up by the mosquito leading to the formation of the zygote in its midgut. The zygote formed matures to generate ookinetes that divide within oocysts to generate thousands of sporozoites. Sporozoites then migrate to the salivary gland ready to be injected with the next mosquito blood meal. Figure reproduced from [5].

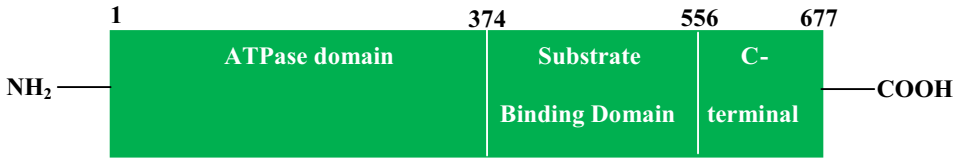

Figure 2. Structure of Hsp70-1. Figure modified from [14].

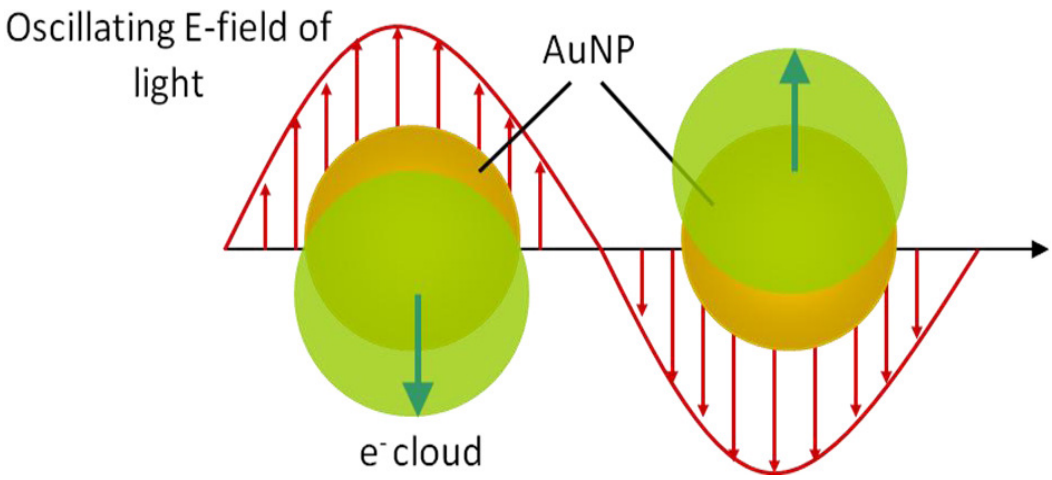

Figure 3. Surface Plasmon Resonance of AuNPs. Figure reproduced from[15].

Figure 4. Giemsa stained RBCs of *Plasmodium falciparum* infected patient showing several *P. falciparum* ring structures. Figure reproduced from [18].

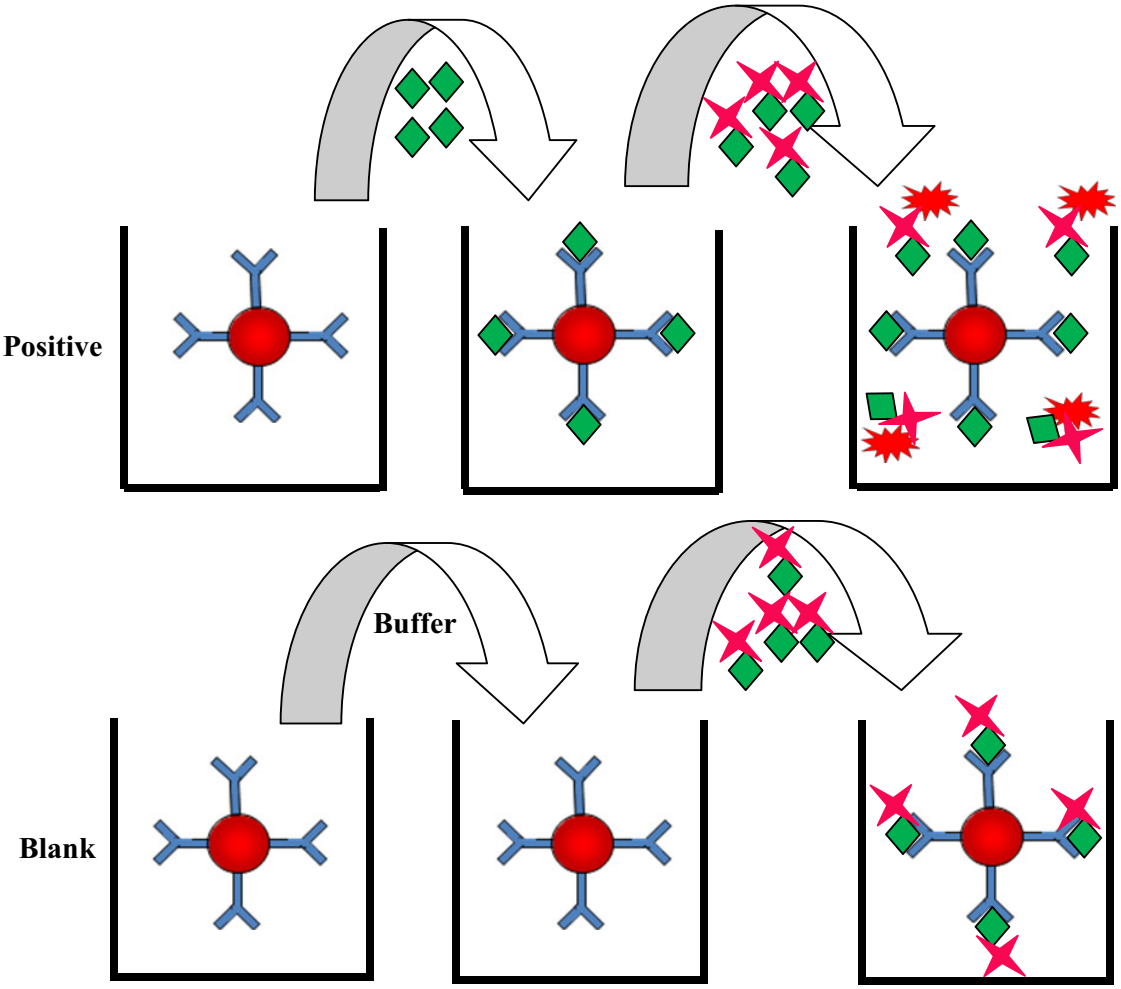

Figure 5. Principle of the fluorescence quenching competitive assay for detection of *Pf*Hsp70.

: AuNP-MUA-2E6

: *Pf*Hsp70

: Cy3B

: Fluorescence Emission

Buffer: 0.1 M borate buffer pH = 8.3; 150 mM NaCl.

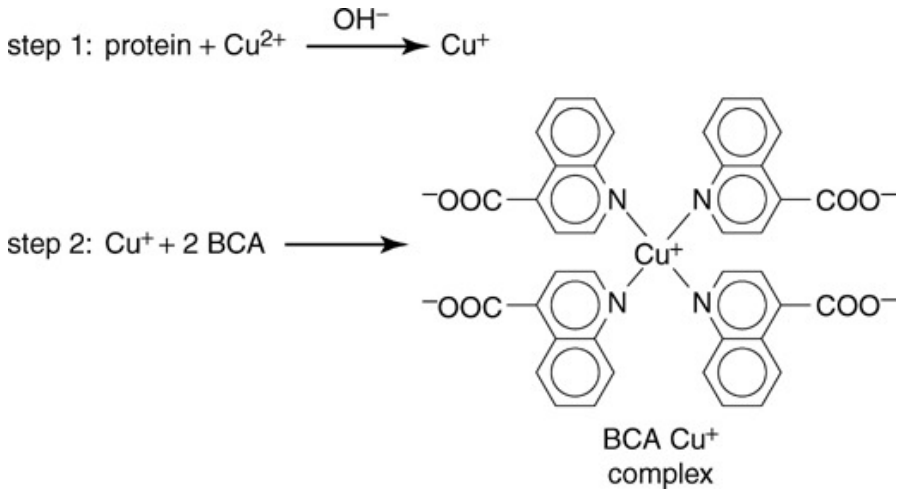

Figure 6. BCA protein assay principle. Reproduced from [43].

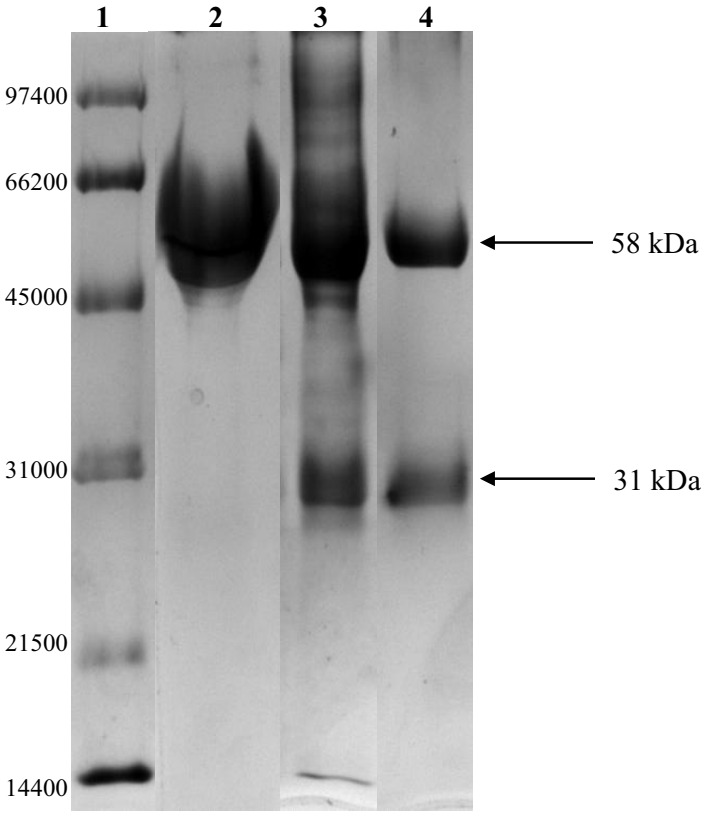

Figure 7. SDS-PAGE (12.5%) analysis of 2E6 antibody purified using two step Protein G affinity chromatography columns.

- Lane 1. Marker
- Lane 2. 2E6 containing solution before purification (sample diluted 1 : 15)
- Lane 3. Protein G Sepharose 4 Fast Flow column purified 2E6 (sample undiluted)
- Lane 4. PD SpinTrap G-25 columns purified 2E6 (sample undiluted)
- Arrows show positions of upper (corresponding to heavy chain; about 58 kDa) and lower bands (corresponding to light chain; about 31 kDa) of 2E6 antibody.
- The reason why a single band was seen in lane 2 (impure 2E6) is perhaps due to overloading excess proteins that retarded the migration of bands through the gel.

A

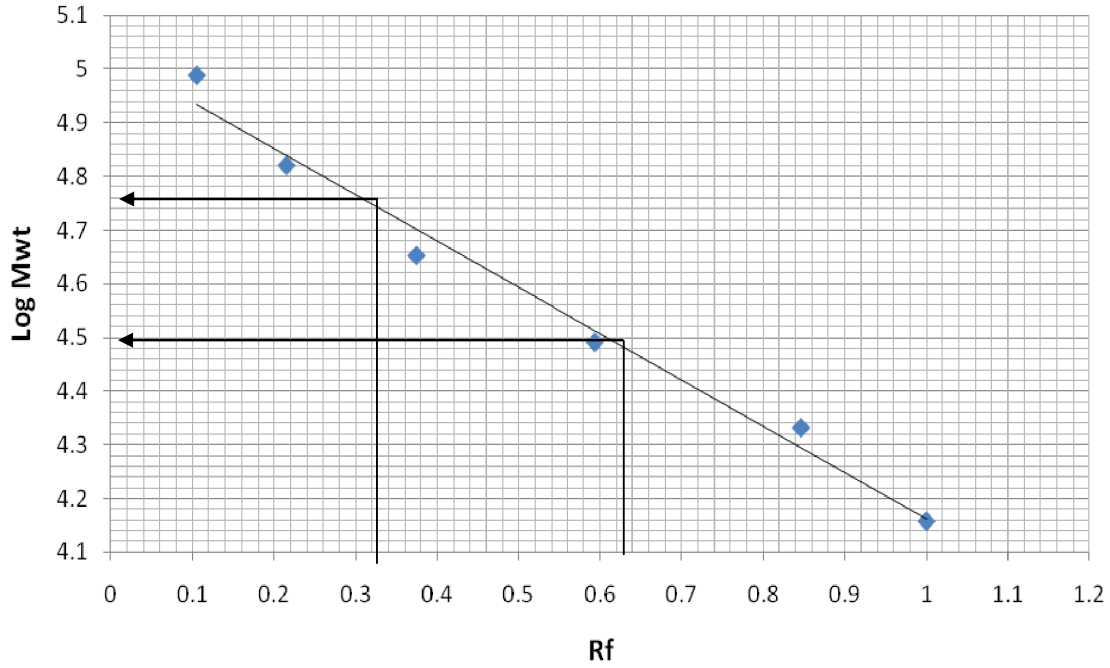

B

Band	Migration of band	Dye migration	R_f	Log Mwt from curve	Calculated Mwt (Da)	Theoretical Mwt (Da)
Lower	5.6	9.1	0.615	4.49	30,902	25,000
Upper	2.8	9.1	0.308	4.76	57,543	50,000

Figure 8. Molecular weight values of the two bands of 2E6 (corresponding to heavy and light chains) shown on SDS-PAGE, as calculated based on calibration curve. A: Calibration curve of Log Molecular weight *vs*. R_f (ratio of length of migration of sample on gel divided by migration of loading dye). B: Calculation of practical molecular weight values of the two bands of 2E6 antibody and comparing results with theoretical values.

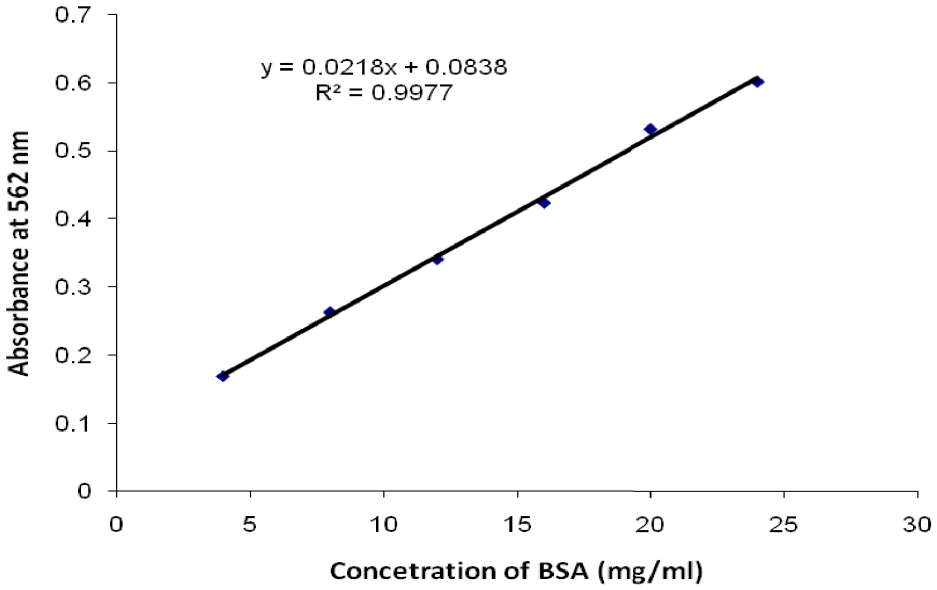

Figure 9. Standard curve of BCA test for determining concentration of purified 2E6 antibody.

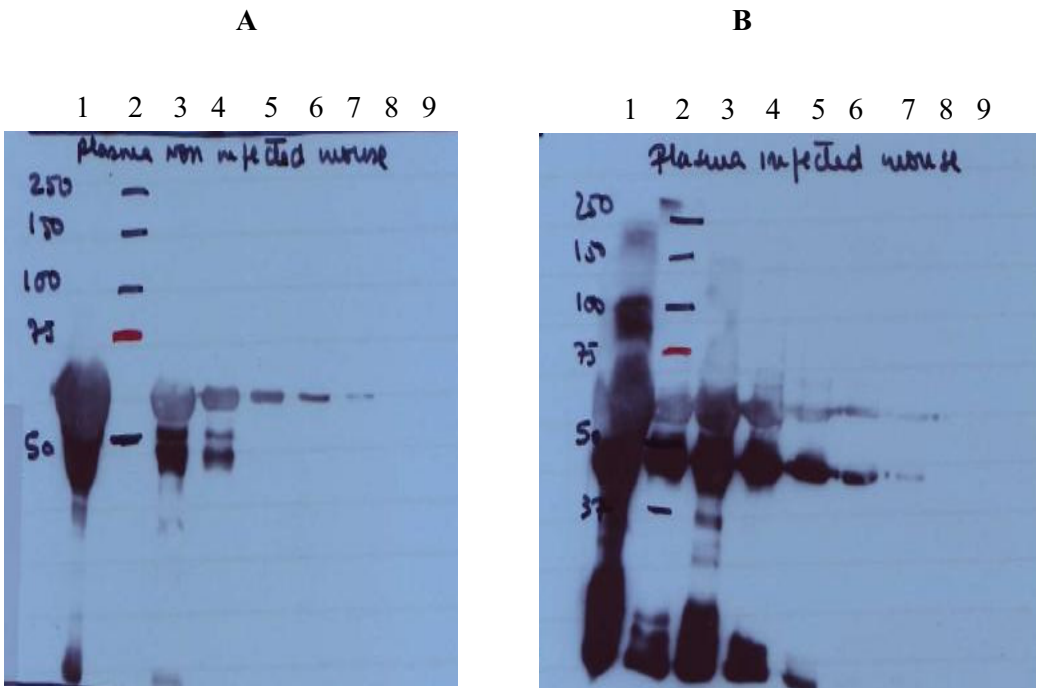

Figure 10. Western blot analysis of plasma of non-infected mice (A) and of mice blood infected with *Plasmodium berghei* (B) using 2E6 antibody. As seen in the figure, no difference can be seen between infected and non-infected plasma. Samples are in the following sequence for figures A and B: Lane 1) Undiluted plasma; Lane 2) MW markers; Lanes 3-9 Plasma at different dilutions: 3) 1 : 5; 4) 1 : 25; 5) 1 : 125; 6) 1 : 625; 7) 1 : 3125; 8) 1 : 15625; 9) 1 : 78125.

- SDS-PAGE: 10%
- Primary antibody: 2E6
- Secondary antibody: HRP-labelled anti-mouse antibody

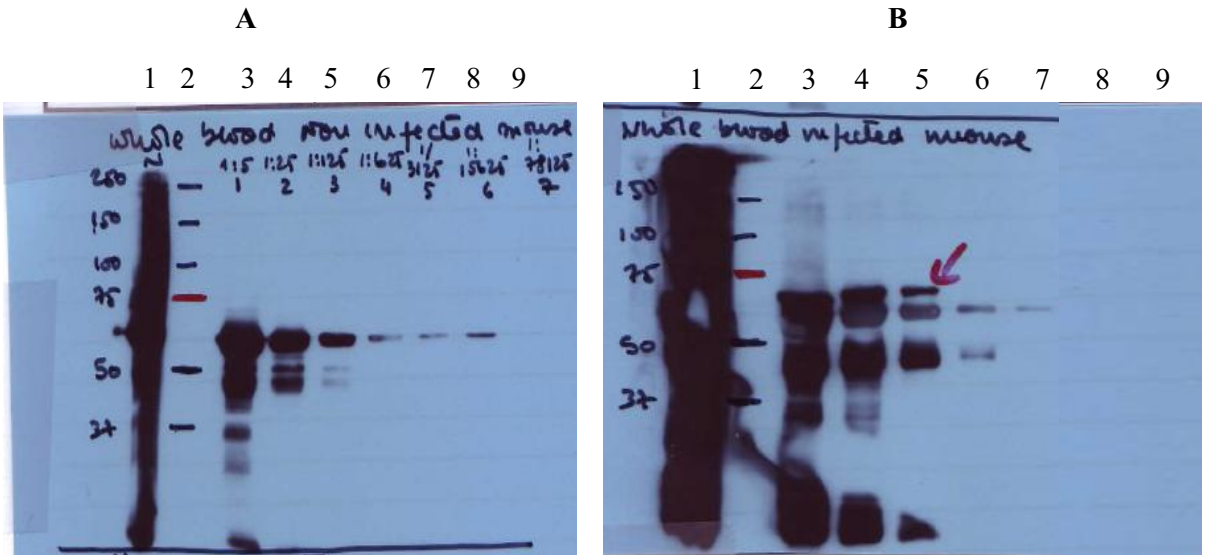

Figure 11. Western blot analysis of whole blood of non-infected mice (A) and of mice infected with *Plasmodium berghei* (B) using 2E6 antibody. This figure shows that there is an extra band (lanes 3, 4 and 5) at about 75 kDa in infected (B) but not in non-infected whole blood (A).

- Arrow shows the band of *Pb*Hsp70.
- Samples are in the following sequence for figures A and B: Lane 1) Undiluted whole blood; Lane 2) MW markers; Lane 3-9 Whole blood with different dilutions: 3) 1 : 5; 4) 1 : 25; 5) 1 : 125; 6) 1 : 625; 7) 1 : 3125; 8) 1 : 15625; 9) 1 : 78125.
- SDS-PAGE: 10%.
- Primary antibody: 2E6.
- Secondary antibody: HRP-labelled anti-mouse antibody.

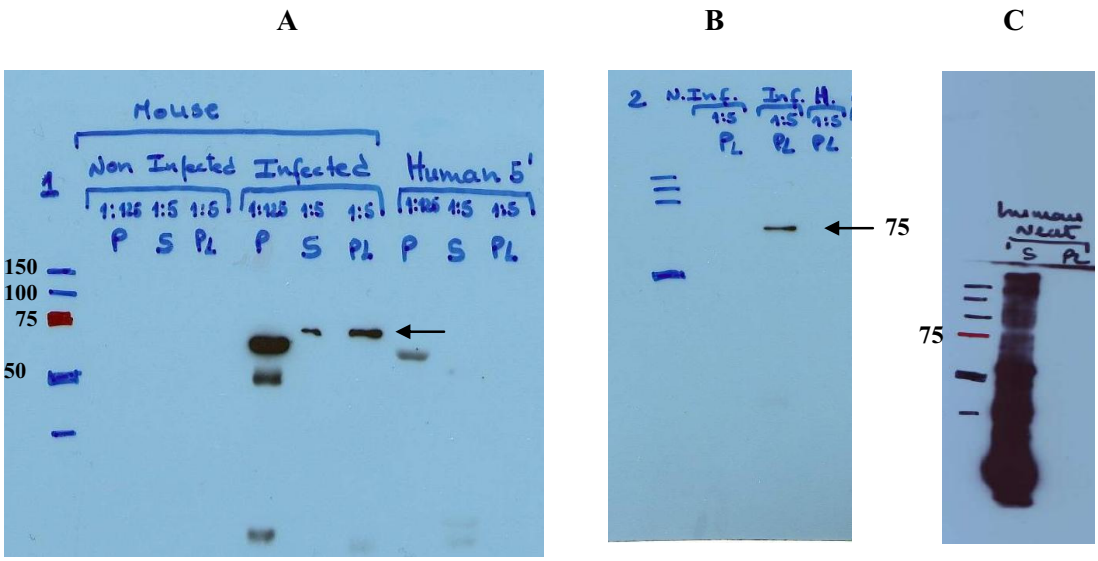

Figure 12. A: Western blot analysis comparing plasma, saponin supernatant (RBC lysate) and saponin pellet of non-infected mice; mice infected with *Plasmodium berghei*; and non-infected human blood, using 2E6 antibody. The figure shows that the saponin pellet of treated RBC of infected mice showed the band corresponding to *Pb*Hsp70. **B: Western blot analysis comparing saponin pellet of non-infected mice; mice infected with *Plasmodium berghei*; and non-infected human blood, using 2E6 antibody.** The figure shows that the saponin pellet of treated RBC of infected mice only showed the band corresponding to *Pb*Hsp70 but this band was not seen for non infected mice and human. **C: Western blot analysis showing undiluted saponin supernatant and saponin pellet of non-infected human blood, using 2E6 antibody.** The figure shows that no bands were seen when undiluted saponin pellet of non-infected human blood was analyzed.

- Arrows show the band of *Pb*Hsp70.
- SDS-PAGE: 10%.
- Primary antibody: 2E6.
- Secondary antibody: HRP-labelled anti-mouse antibody.
- P: plasma; PL: saponin pellet; S: saponin supernatant.

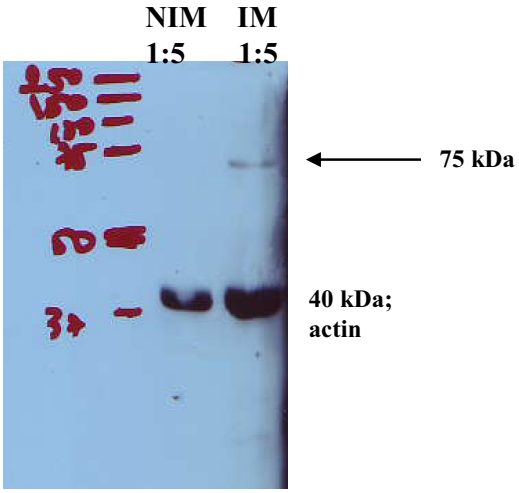

Figure 13. Western blot analysis of non-infected mice saponin pellet and of mice infected with *Plasmodium berghei*, using actin as loading control. The figure shows that the actin band intensities were comparable (lower bands; samples normalized) and that the *Pb*Hsp70 band was seen in infected mice saponin pellet and not in non-infected mice saponin pellet.

- Arrow shows the band of *Pb*Hsp70.
- SDS-PAGE: 10%.
- Primary antibody: 2E6.
- Secondary antibody: HRP-labelled anti-mouse antibody.
- IM: infected mice saponin pellet; NIM: non-infected mice saponin pellet.
- Numbers represent dilution.

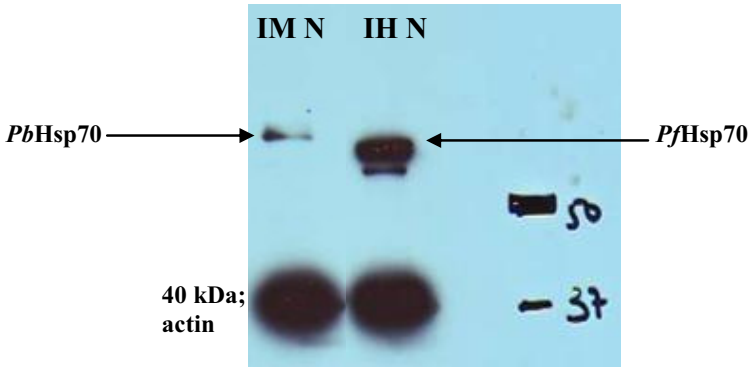

Figure 14. Western blot analysis of saponin pellets of RBCs of mice infected with *Plasmodium berghei* and of human blood culture infected with *Plasmodium falciparum*. This figure shows that the actin band intensities were comparable (samples normalized) and that the band corresponding to *Pf*Hsp70 was larger than that corresponding to *Pb*Hsp70 (2E6 recognizes *Pf*Hsp70 more than *Pb*Hsp70).

- SDS-PAGE: 10%.
- Primary antibody: 2E6.
- Secondary antibody: HRP-labelled anti-mouse antibody.
- IH: infected human; IM: infected mouse; N: neat (undiluted).

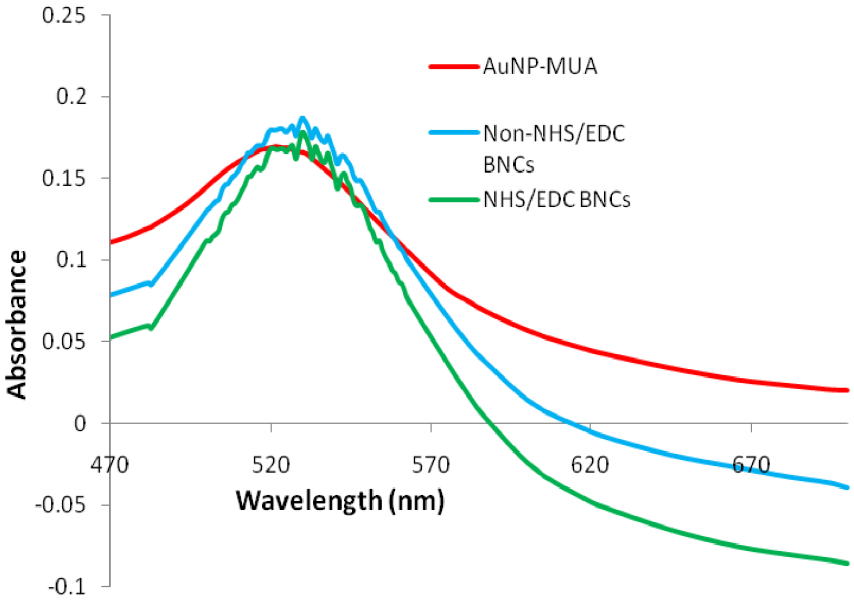

Figure 15. Absorbance spectrum of AuNP-MUA before and after 2E6 conjugation showing a shift in peak maximum from 521 nm to 530 nm for both NHS/EDC and non-NHS/EDC BNCs.

- Molar ratio of 2E6 to AuNP-MUA for both NHS/EDC and non-NHS/EDC conjugates was 100.
- BNCs: bionanoconjugates.

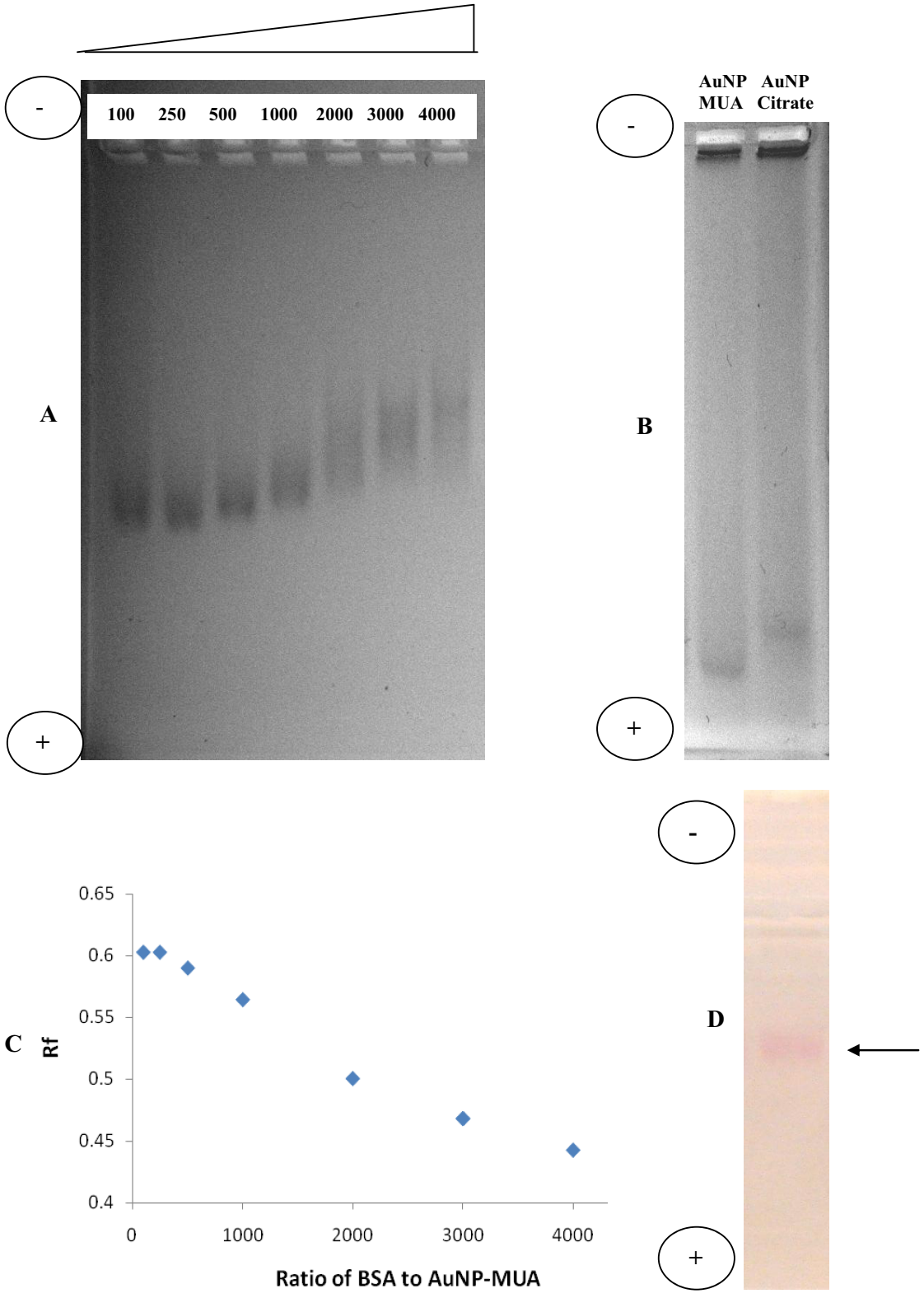

Figure 16. Unstained agarose gel electrophoresis of AuNPs and bionanoconjugates (BNCs) prepared with different molar ratios of BSA to AuNP-MUA. A: BSA BNCs; B: unconjugated AuNPs alone; C: Rf values (distance migrated by sample to total distance till end of gel) *vs*. molar ratio of

BSA to AuNP-MUA; D: digital photograph showing the appearance of the band of a BSA BNC on the agarose gel.

- BSA bionanoconjugates migrate according to size and charge (fig. 15 A). Unconjugated AuNPs were stuck in wells due to charge cancellation and/or aggregation caused by running buffer (fig. 15 B).
- Numbers represent molar ratios of BSA to AuNP-MUA (fig. 15A).
- Agarose concentration: 1% in 5 mM sodium phosphate buffer (pH = 7)
- Running buffer: 5 mM sodium phosphate buffer (pH = 7).
- All bands appeared red in color as seen in “D”, however the available camera with high resolution was only black and white.

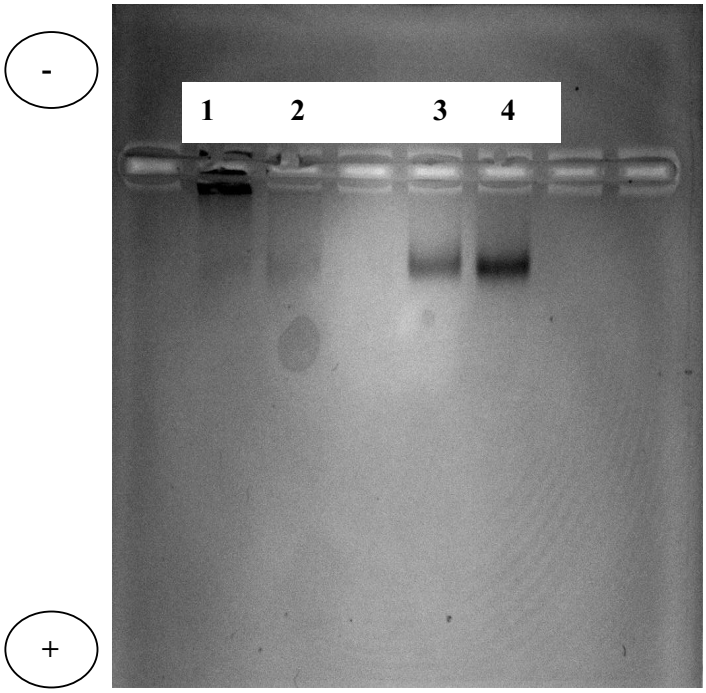

Figure 17. Unstained agarose gel electrophoresis of AuNP-MUA-2E6 conjugates prepared with different NHS/EDC concentrations showing that 0.6 - 1.2 mM and 1.4 - 2.8 mM concentration of NHS and EDC, respectively, were found to be optimal for cross-linking (compact bands seen).

- Lane 1. 6 mM and 14 mM of NHS and EDC, respectively.
- Lane 2. 3 mM and 7 mM of NHS and EDC, respectively.
- Lane 3. 1.2 mM and 2.8 mM of NHS and EDC, respectively.
- Lane 4. 0.6 mM and 1.4 mM of NHS and EDC, respectively.
- The molar ratio of 2E6 to AuNP-MUA was 250.
- Agarose concentration: 1% in 5 mM sodium phosphate buffer (pH = 7).
- Running buffer: 5 mM sodium phosphate buffer (pH = 7).
- All bands appeared red in color, however the available camera with high resolution was only black and white.

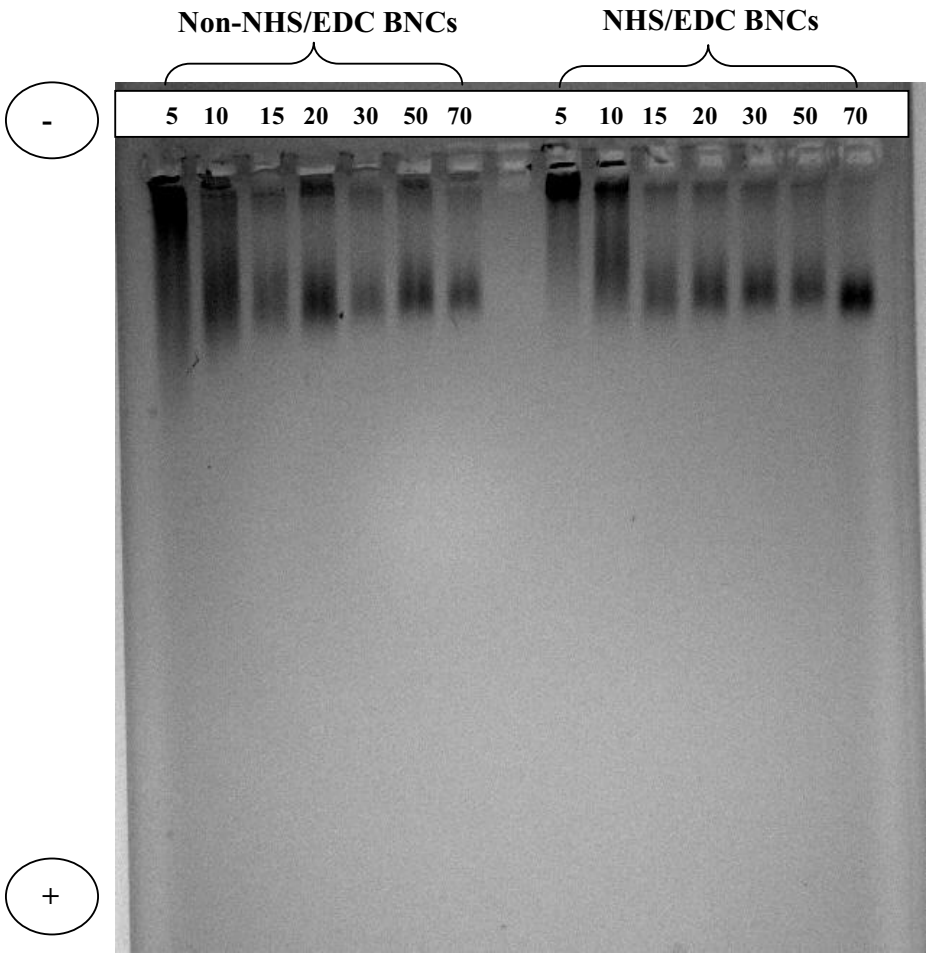

Figure 18. Unstained agarose gel electrophoresis of AuNP-MUA-2E6 conjugates (with and without NHS/EDC) prepared with different molar ratios of 2E6 to AuNP-MUA. This figure shows that NHS/EDC BNCs are slightly more uniform (more compact bands) than non-NHS/EDC BNCs.

- Numbers represent molar ratios of 2E6 to AuNP-MUA.
- Agarose concentration: 1% in 5 mM sodium phosphate buffer (pH = 7)
- Running buffer: 5 mM sodium phosphate buffer (pH = 7).
- All bands appeared red in color, however the available camera with high resolution was only black and white.

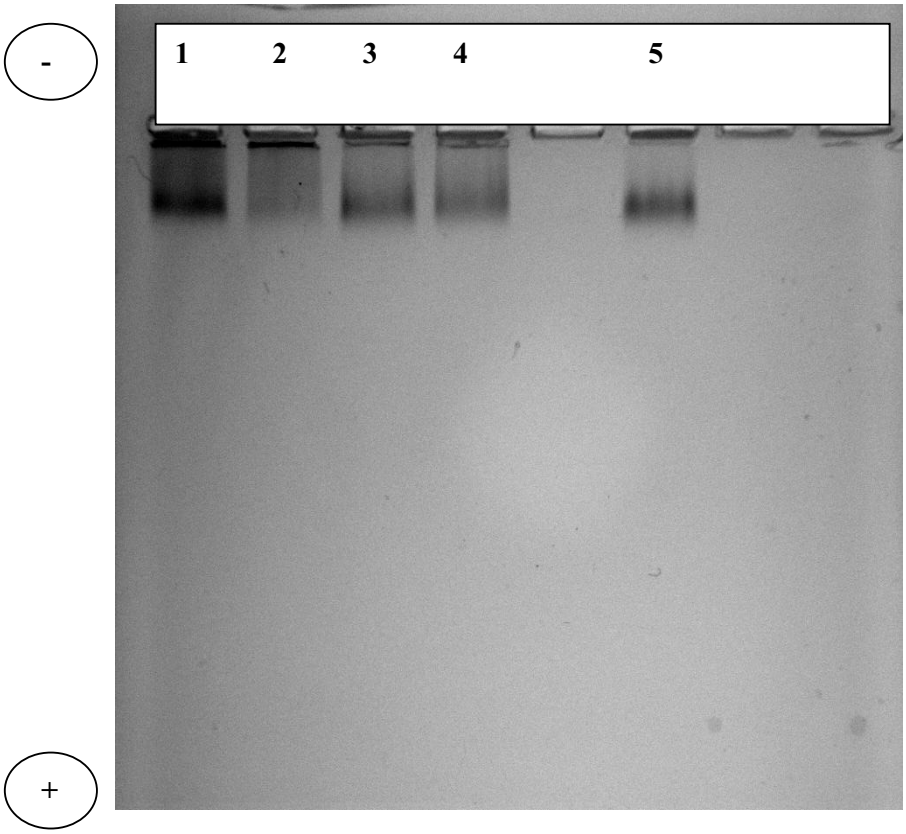

Figure 19. Unstained agarose gel electrophoresis of AuNP-CALNN-2E6 conjugates prepared with different NHS/EDC concentrations. This figure shows that 3 mM and 7 mM concentration of NHS and EDC, respectively, was optimal for cross-linking (compact band).

- Lane 1: buffer alone
- Lane 2: 0.3 mM and 0.7 mM of NHS and EDC, respectively.
- Lane 3: 0.6 mM and 1.4 mM of NHS and EDC, respectively.
- Lane 4: 1.2 mM and 2.8 mM of NHS and EDC, respectively.
- Lane 5: 3 mM and 7 mM of NHS and EDC, respectively.
- The molar ratio of 2E6 to AuNP-MUA was 100.
- Agarose concentration: 1% in 5 mM sodium phosphate buffer (pH = 7)
- Running buffer: 5 mM sodium phosphate buffer (pH = 7)
- All bands appeared red in color, however the available camera with high resolution was only black and white.

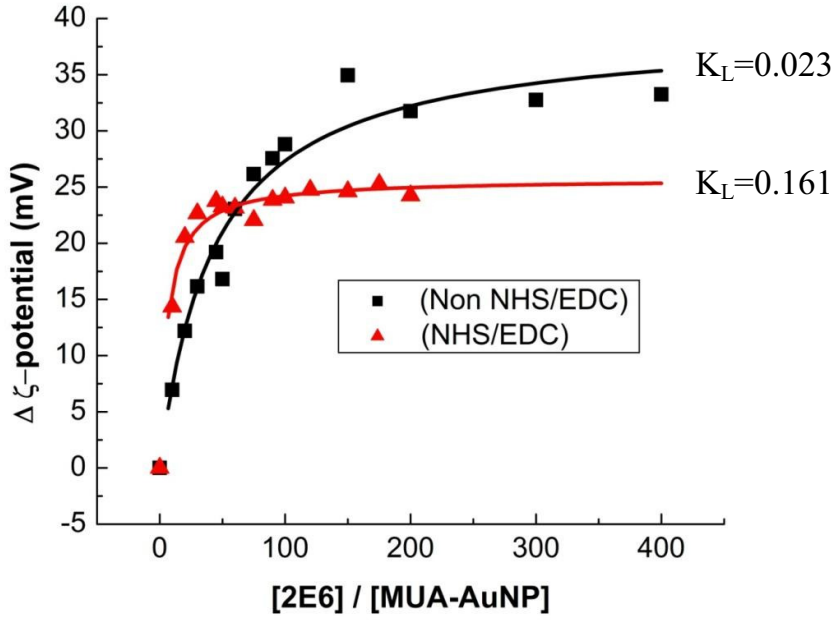

Figure 20. ζ-potential of non-NHS/EDC and NHS/EDC AuNP-MUA-2E6 bionanoconjugates. This figure shows that NHS/EDC coupling increases the binding between 2E6 and AuNP-MUA by about 7 folds for low 2E6/AuNP-MUA molar ratios.

- Zeta-potential measurements were performed in a Zetasizer Nano-ZS from Malvern Instruments. A 4 mW He-Ne laser (633 nm) was used with a fixed 173 º (DLS) or 17 º (ζ-potential) scattering angle. The software was adjusted as follows: material: protein; dispersant: water; temperature: 25^{o}C; equilibration time: 900 sec; measurement: monomodal; number of measurements: 4; number of runs: 100.

A

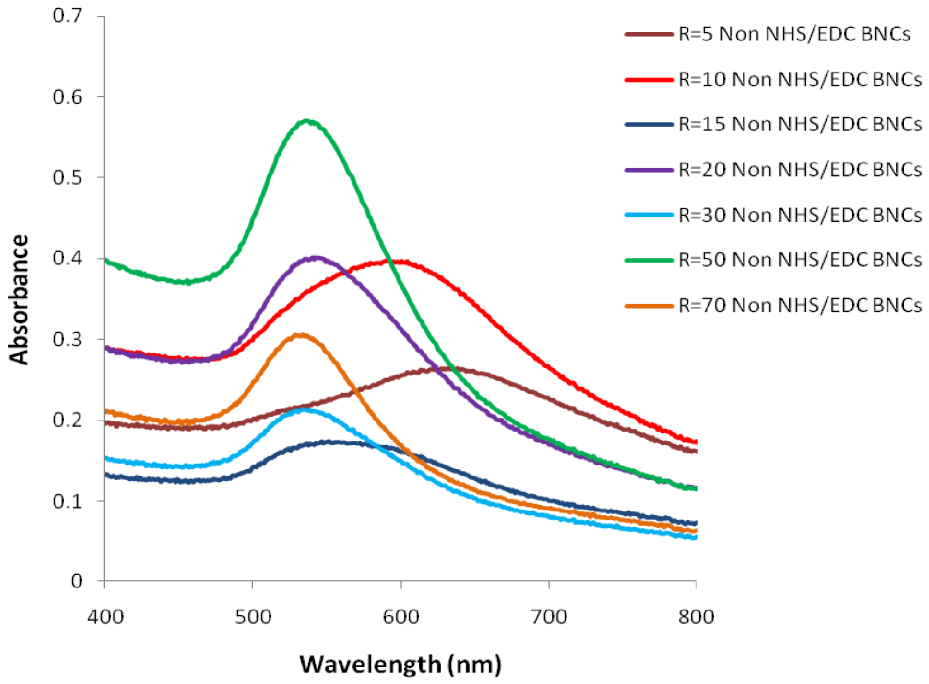

B

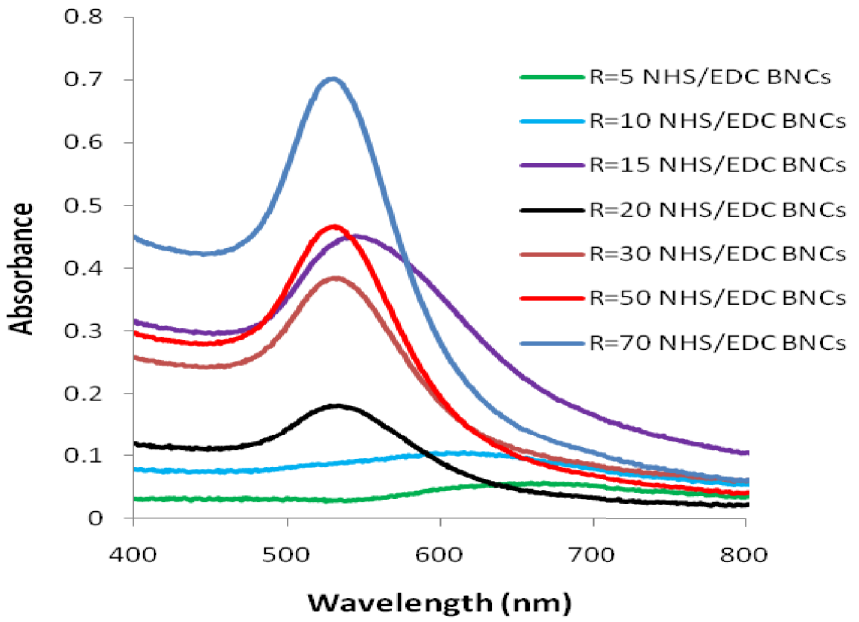

Figure 21. Absorbance spectra of non-NHS/EDC (A) and NHS/EDC (B) AuNP-MUA-2E6 BNCs after adding an equal volume of 5 M NaCl. This figure shows that a molar ratio of 2E6 to AuNP-MUA less than 20 could not protect the BNCs (with or without NHS/EDC) from NaCl-induced aggregation as shown by shifts in peak maxima.

- BNCs: bionanoconjugates; R: molar ratio of 2E6 to AuNP-MUA.

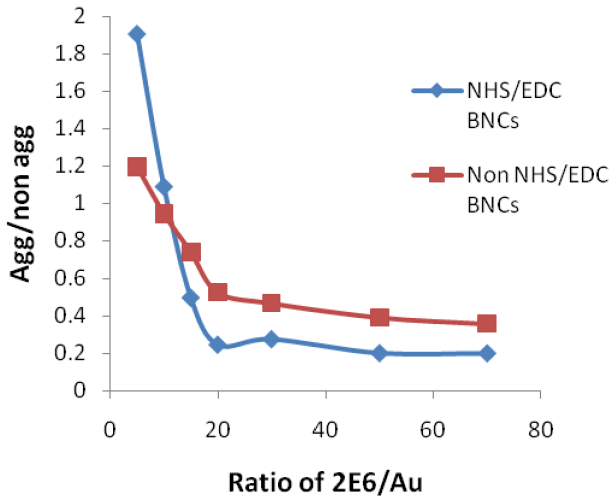

Figure 22. Ratio of absorbance of aggregated (agg.) forms (659 nm) to non-aggregated (non-agg.) forms (530 nm) after adding an equal volume of 5 M NaCl *vs*. the molar ratio of 2E6 to AuNP-MUA of BNCs prepared with and without NHS/EDC. This figure shows that a molar ratio of 2E6 to AuNP-MUA less than 20 could not protect the BNCs (with or without NHS/EDC) from NaCl-induced aggregation. Also NHS/EDC BNCs seemed to be slightly more stable against NaCl-induced aggregation compared to non-NHS/EDC BNCs (value of agg./non-agg. was less for molar ratios ≥ 15 in case of NHS/EDC BNCs).

- BNCs: bionanoconjugates.

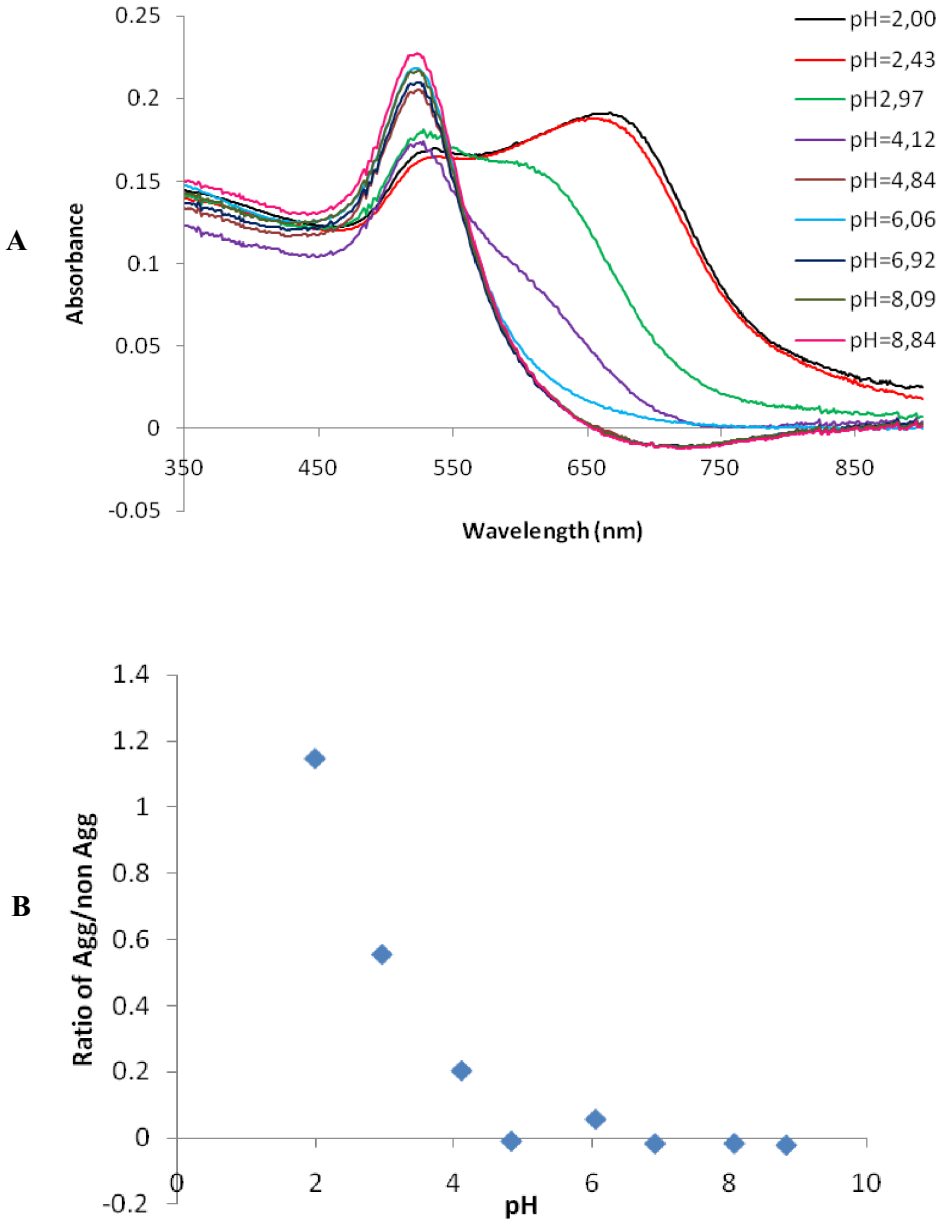

Figure 23. A: Visible absorbance spectra of 1nM AuNP-MUA at different pH values. B: Ratio of absorbance of aggregated forms of 1nM AuNP-MUA (666 nm) to that of non-aggregated forms (523 nm) at different pH values. This figure shows that AuNP-MUA aggregate at pH values ≤ 4.

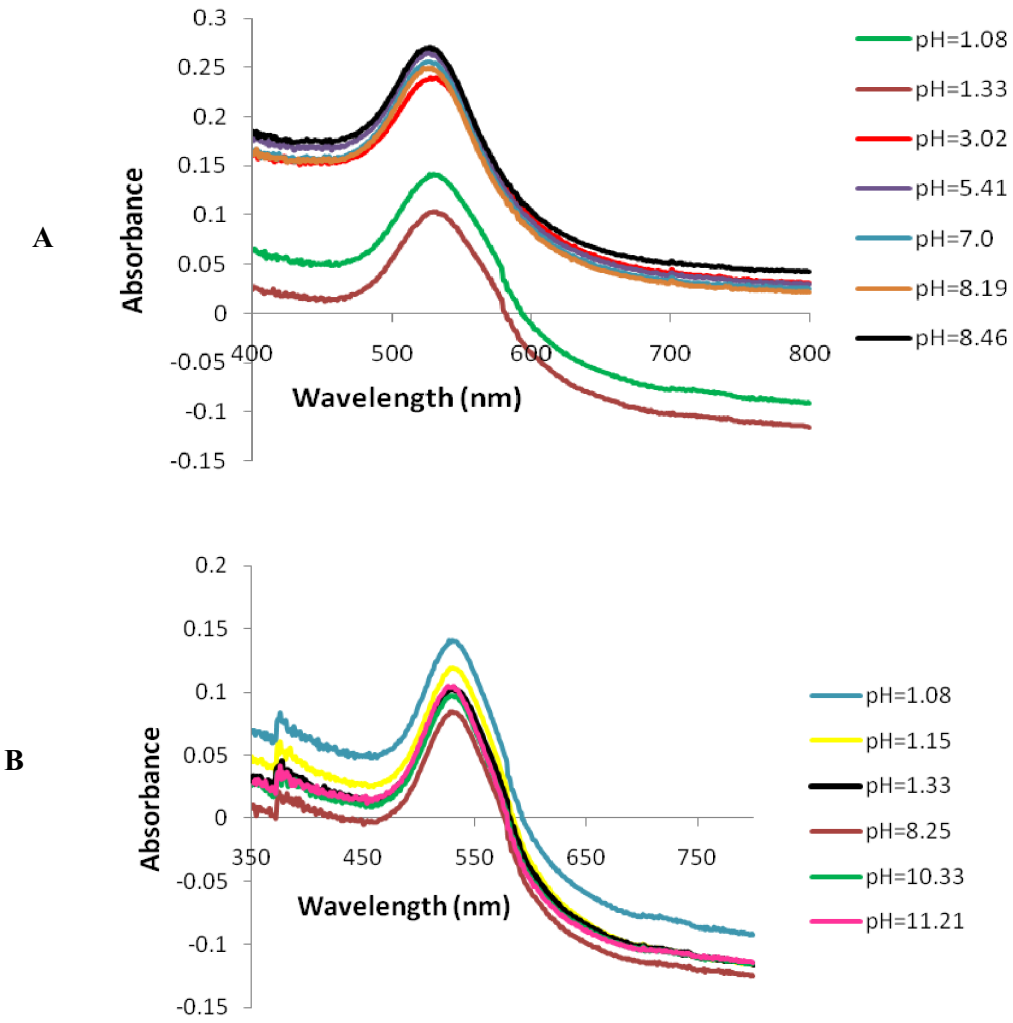

Figure 24. Absorbance spectra of AuNP-MUA-2E6 BNCs prepared in the presence of NHS/EDC at different pH values. A. pH was decreased using 0.1 M HCl (in the same tube); B: pH was increased using 0.1 M NaOH (in the same tube). NHS/EDC BNCs show minimal aggregation at pH values ranging from 1 - 11. This is a proof of conjugation since BNCs behave differently from unconjugated AuNP-MUA (fig. 23 A).

- Molar ratio of 2E6 to AuNP-MUA for both NHS/EDC and non-NHS/EDC conjugates was 70.

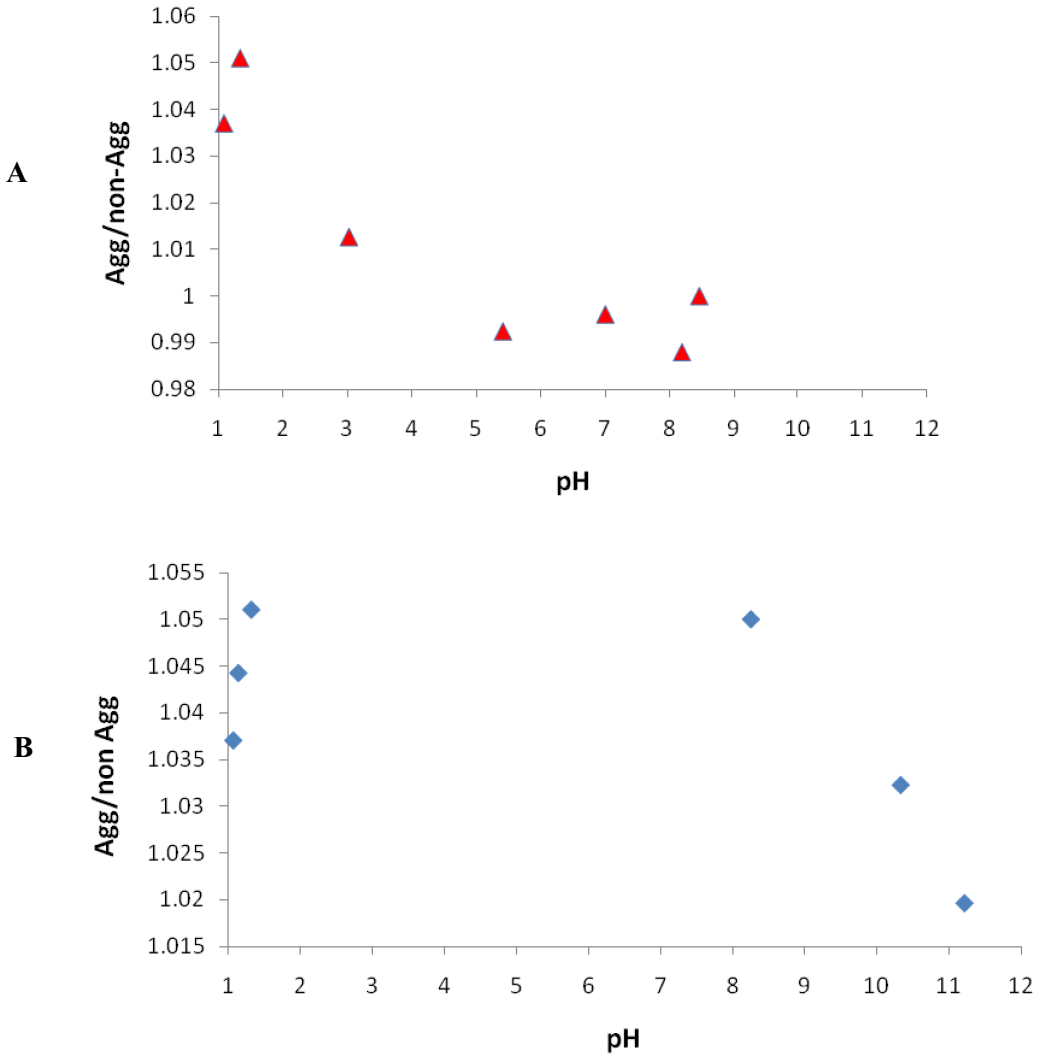

Figure 25. pH aggregation study of AuNP-MUA-2E6 BNCs prepared in the presence of NHS/EDC showing ratio of absorbance of aggregated forms of BNCs to that of non-aggregated forms at different pH values. A: pH was decreased using 0.1 M HCl in the same tube (aggregated form 532 nm; non aggregated form: 523 nm); B: pH was increased using 0.1 M NaOH in the same tube (aggregated form 562 nm; non aggregated form: 528 nm). This figure shows that NHS/EDC BNCs show minimal aggregation at pH values ranging from 1 - 11. This is a proof of conjugation since BNCs behave differently from unconjugated AuNP-MUA (fig. 23 B).

- Molar ratio of 2E6 to AuNP-MUA for both NHS/EDC and non-NHS/EDC conjugates was 70.

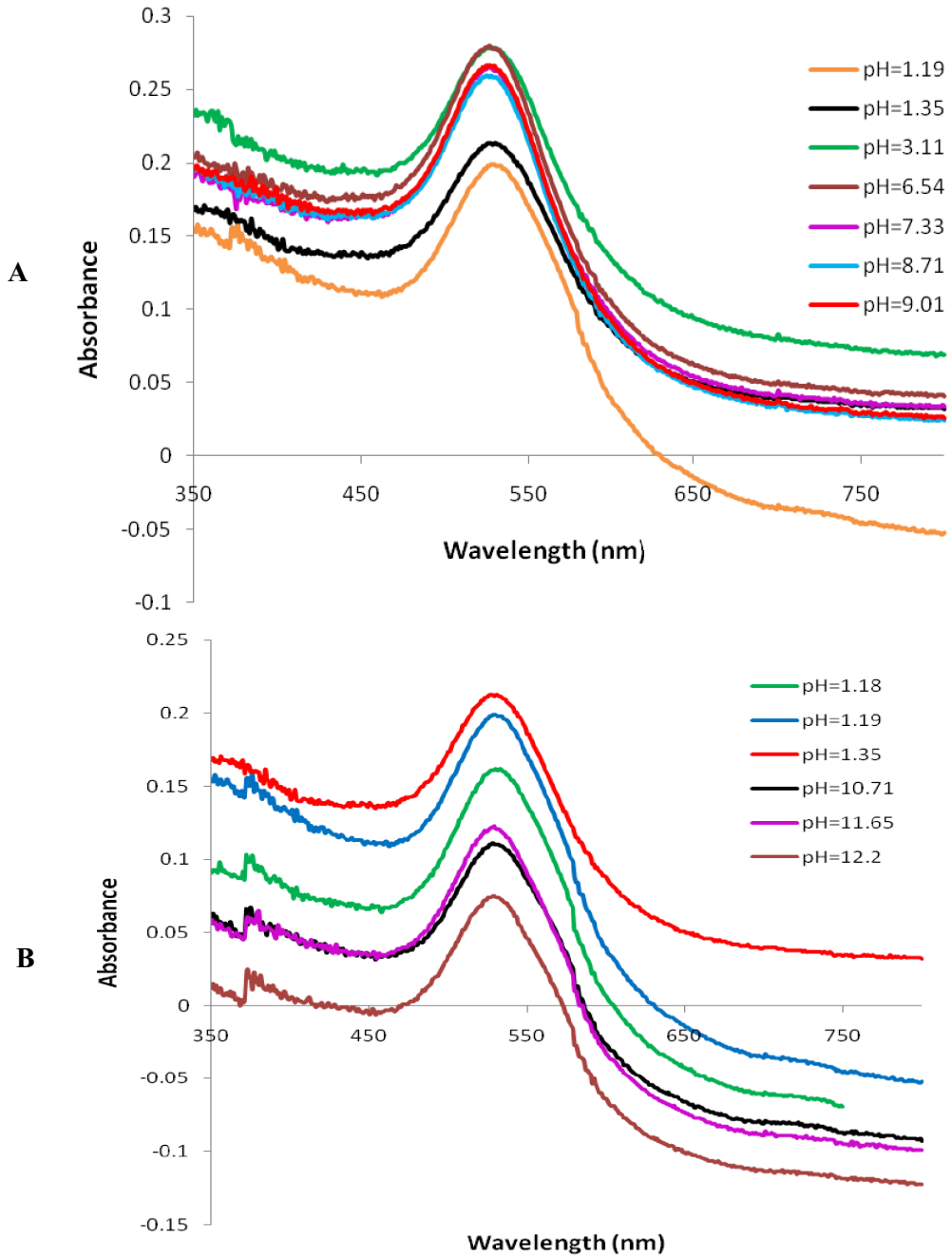

Figure 26. Absorbance spectra of AuNP-MUA-2E6 BNCs prepared in the absence of NHS/EDC at different pH values. A. pH was decreased using 0.1 M HCl (in the same tube); B: pH was increased using 0.1 M NaOH (in the same tube). Non-NHS/EDC BNCs show minimal aggregation at pH values ranging from 1 - 11. This is a proof of conjugation since BNCs behave differently from unconjugated AuNP-MUA (fig. 23 A).

- Molar ratio of 2E6 to AuNP-MUA for both NHS/EDC and non-NHS/EDC conjugates was 70.

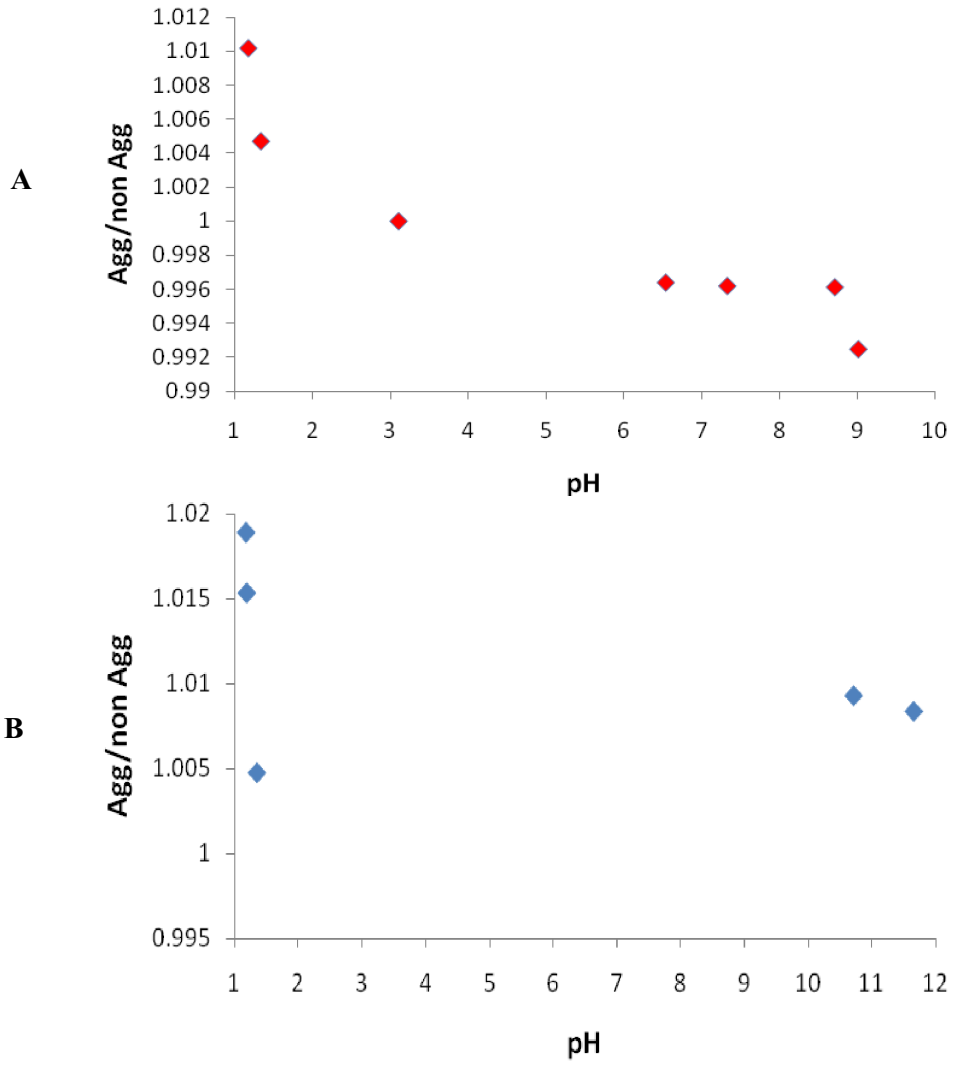

Figure 27. pH aggregation study of AuNP-MUA-2E6 BNCs prepared in the absence of NHS/EDC showing ratio of absorbance of aggregated forms of BNCs to that of non-aggregated forms at different pH values. A: pH was decreased using 0.1 M HCl in the same tube (aggregated form 531 nm; non-aggregated form: 525 nm); B: pH was increased using 0.1 M NaOH in the same tube (aggregated form 562 nm; non-aggregated form: 528 nm). Non-NHS/EDC BNCs show minimal aggregation at pH values ranging from 1 - 11. This is a proof of conjugation since BNCs behave differently from unconjugated AuNP-MUA (fig. 23 B).

- Molar ratio of 2E6 to AuNP-MUA for both NHS/EDC and non-NHS/EDC conjugates was 70.

A

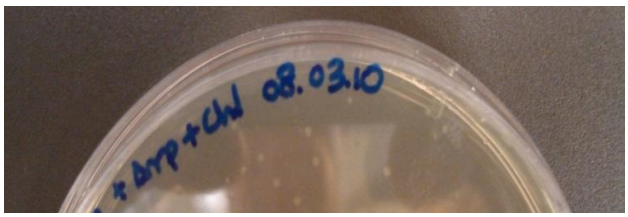

B

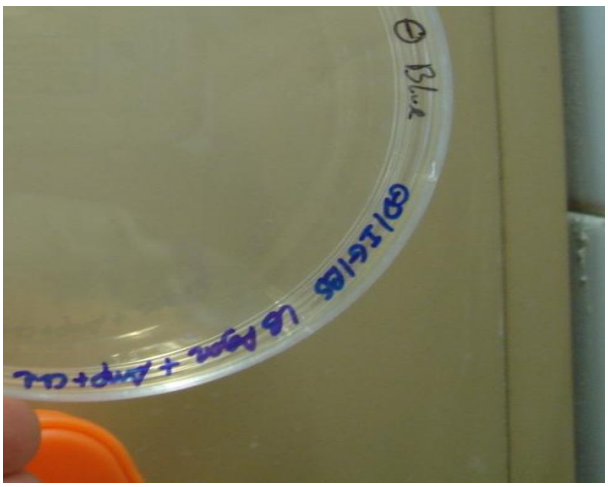

C

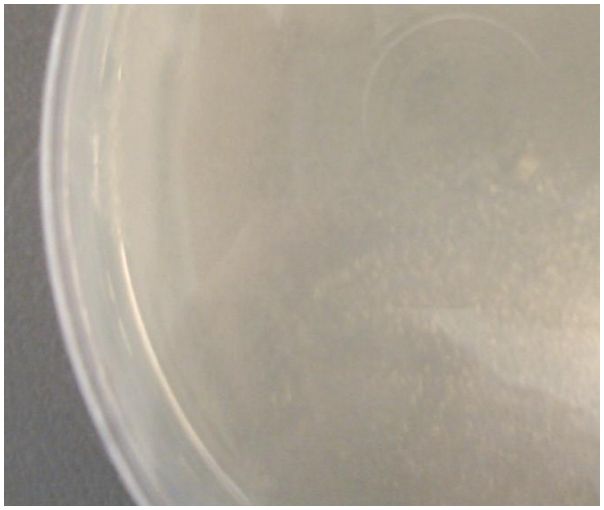

Figure 28. LB agar plates having ampicillin and chloramphenicol showing RosettaBlue™ transformed cells. A. RosettaBlue™ cells transformed with pQE30/*Pf*Hsp70 plasmid. B: Negative control prepared with autoclaved water instead of plasmid; C: Positive control "Test Plasmid" (supplied by manufacturer with cells).

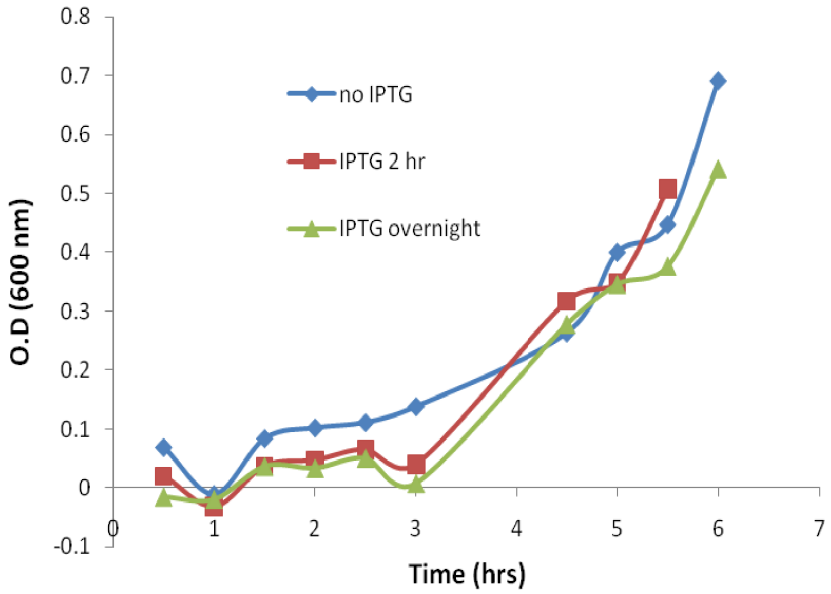

Figure 29. Bacterial growth curve showing optical density ($O.D_{600nm}$) *vs* time under different induction conditions. This figure proves the growth of RosettaBlue™ cells over time. Bacterial growth till O.D values ranging from 0.5 - 0.6 was performed after which cultures were either induced using IPTG (and harvesting performed after 2 hrs or the next day) or not induced and harvested the next day.

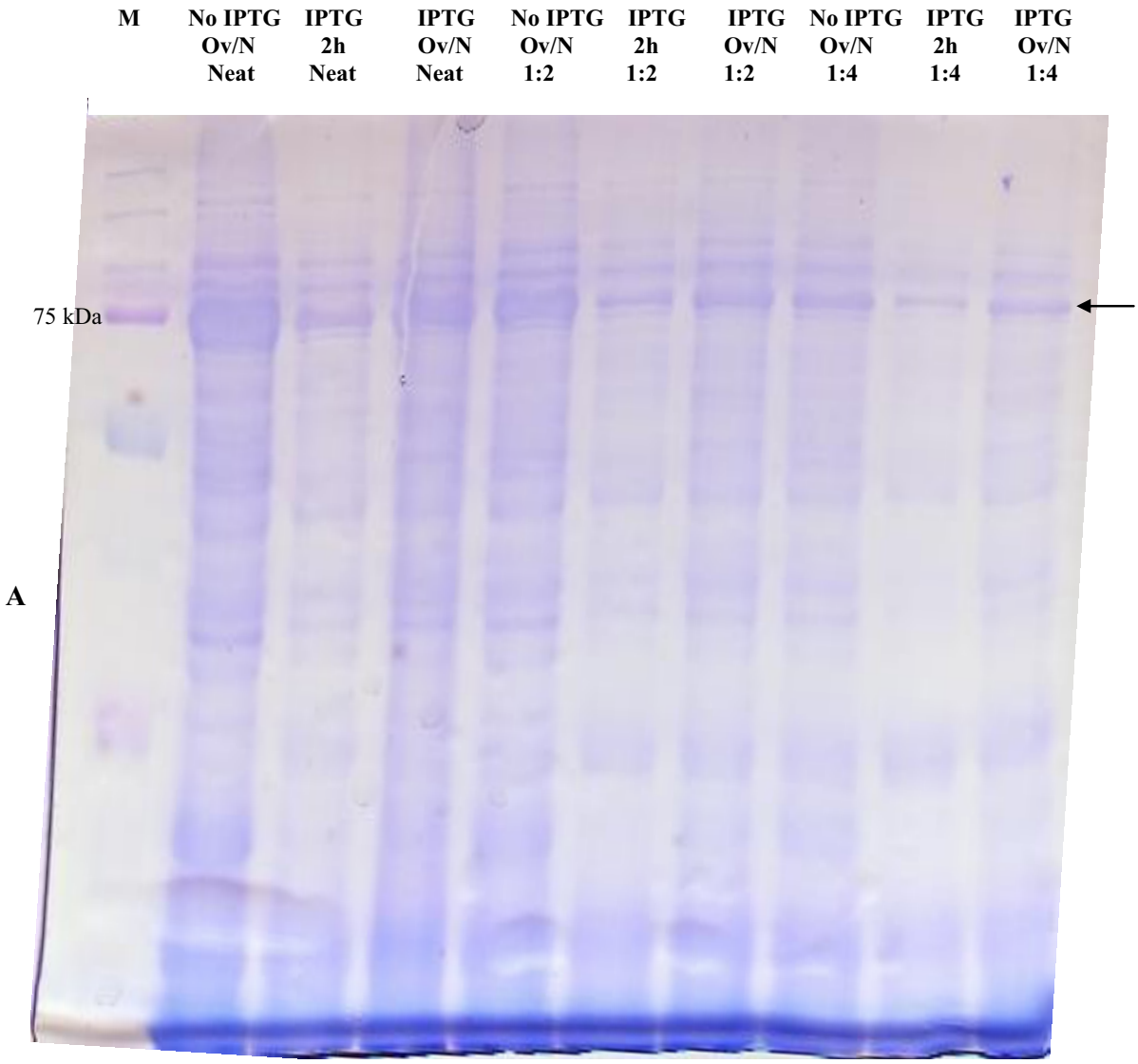

Figure 30 A. SDS-PAGE (10%) analysis of pellets after resuspension in lysis buffer of cultures under different induction conditions.

- To prevent sample overloading, neat (undiluted) samples for "IPTG 2hr" and "IPTG OV" were prepared by diluting in lysis buffer by 1 : 2.5 and 1 : 1.7, respectively. These were named neat samples. However "no IPTG" neat solution was used as is without diluting. Then 1 : 2 and 1 : 4 dilutions were performed using lysis buffer from these neat solutions.
- Arrow shows the band of *Pf*Hsp70.
- 2: 2 hrs; OV/N: overnight; W/O: without.

B

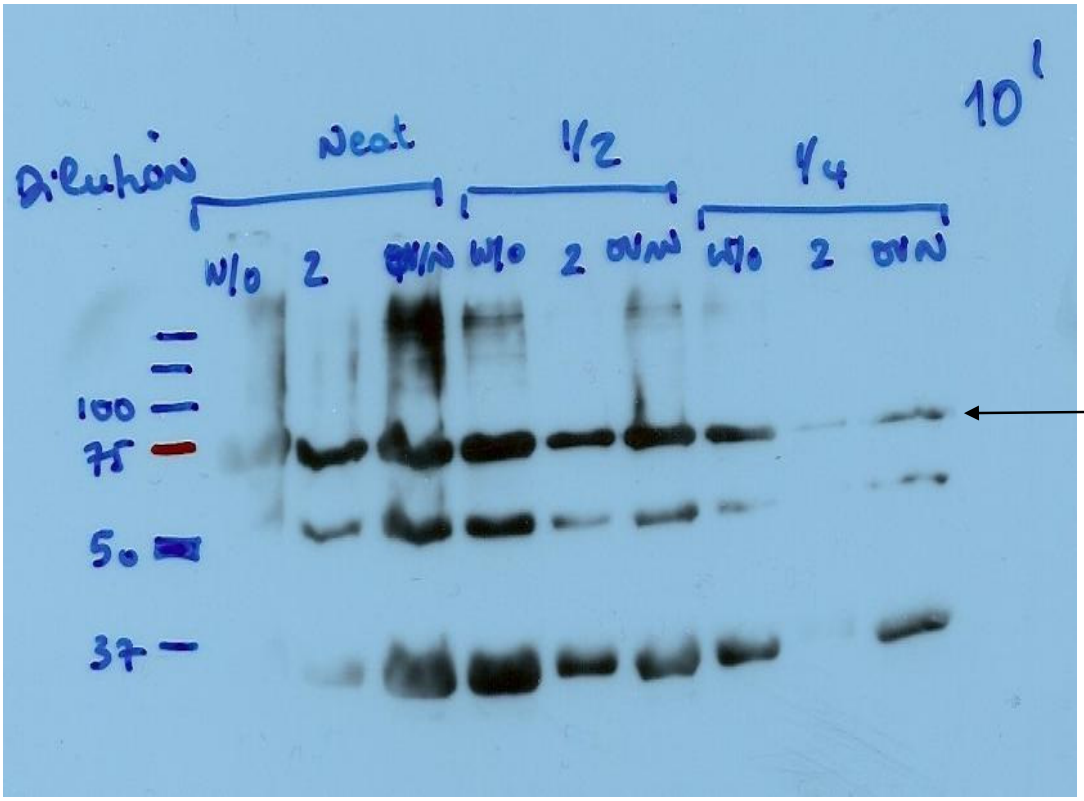

Figure 30 B. Western blot analysis of pellets after resuspension in lysis buffer of cultures under different induction conditions.

- Note to Fig. 29: to prevent sample overloading, neat (undiluted) samples for "IPTG 2 hr" and "IPTG OV" were prepared by diluting in lysis buffer by 1 : 2.5 and 1 : 1.7, respectively. These were named neat samples. However "no IPTG" neat solution was used as is without diluting. Then 1 : 2 and 1 : 4 dilutions were performed using lysis buffer from these neat solutions.
- Arrows show the band of *Pf*Hsp70.
- Primary antibody: 2E6.
- Secondary antibody: HRP-labelled anti-mouse antibody.
- 2: 2 hrs; OV/N: overnight; W/O: without.

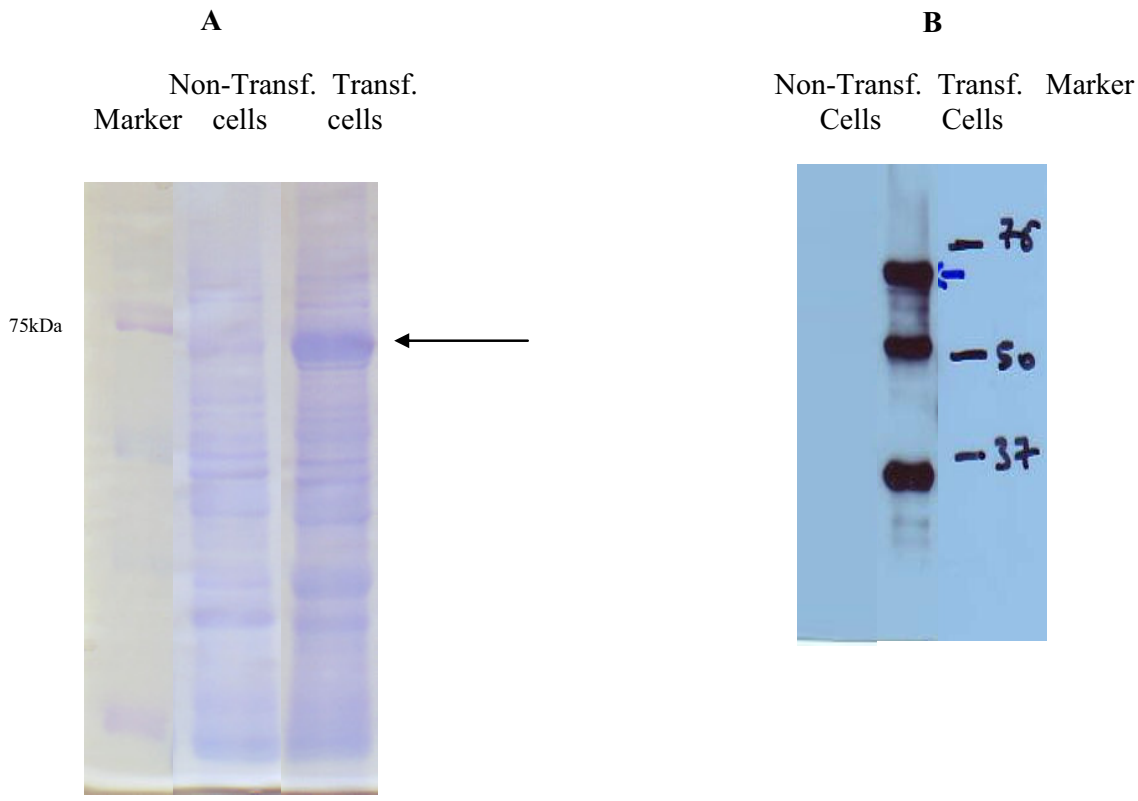

Figure 31. SDS-PAGE (10%) and Western blot analysis of pellets after resuspension in lysis buffer of transformed and non-transformed RosettaBlue™ cells. A: Commasie-blue stained SDS-PAGE. B: Western blot analysis. This figure shows that *Pf*Hsp70 band (at 75 kDa) was seen only in transformed and not in non-transformed cells (negative control). There was however a band in non-transformed cell lane very close to *Pf*Hsp70 band (found in transformed cells at 75 kDa) that was suggested to be DnaK (Hsp70 of *E. coli*). Western blot analysis showed that 2E6 recognizes *Pf*Hsp70 (75 kDa) but not DnaK. In transformed cells, two bands (*ca*. 35 kDa and 50 kDa) were also seen suggested to be possible degradation or truncation products of *Pf*Hsp70.

- Arrows show the band of *Pf*Hsp70.
- To prevent sample overloading, transformed cell pellet was diluted 1 : 1.7. Non-transformed cell pellet was diluted 1 : 2.
- Transf: Transformed; Transformed cells are the “IPTG overnight” sample.
- SDS-PAGE: 10%.
- Primary antibody: 2E6.
- Secondary antibody: HRP-labelled anti-mouse antibody.

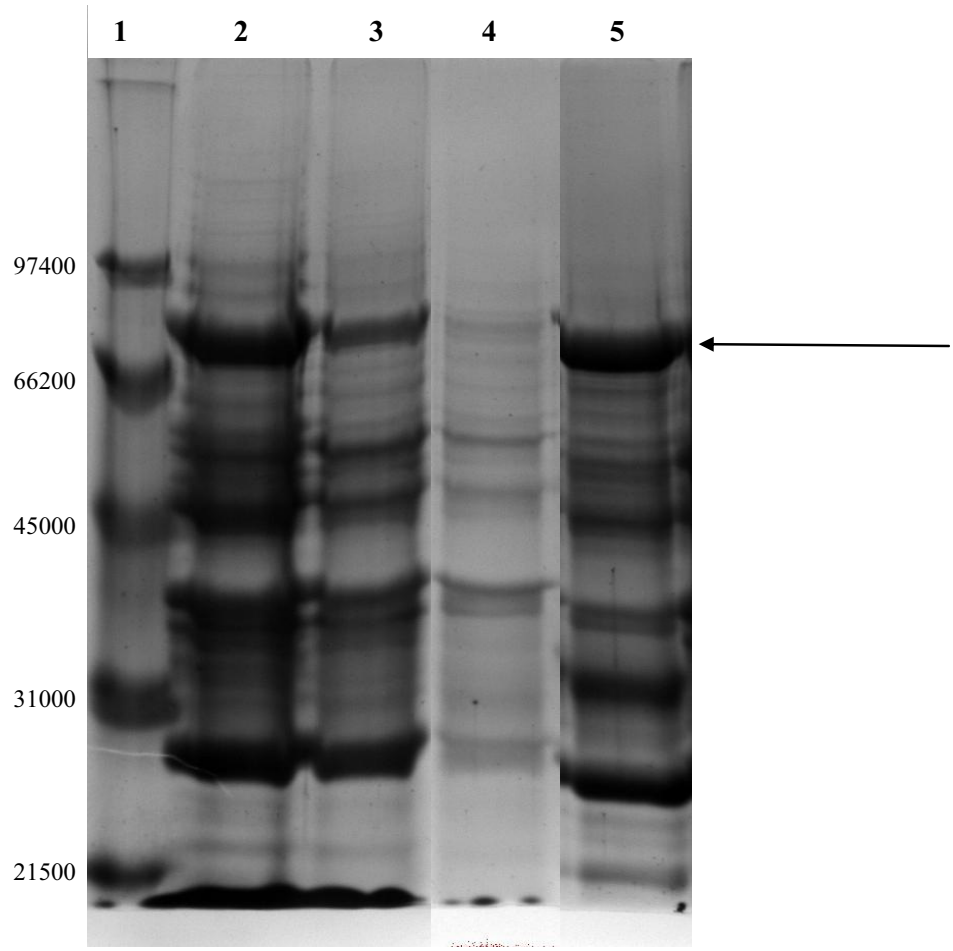

Figure 32. SDS-PAGE (10%) analysis of bacterial culture containing *Pf*Hsp70 before and after Ni-NTA purification. Lane 1) Marker; 2) sample after French-press and before loading on column (1 : 5); 3) flow through (1 : 5); 4) wash; 5) concentrated eluate (1 : 1.5)

- Arrow shows the band of *Pf*Hsp70.
- Although the eluted *Pf*Hsp70 (lane 5) was only partially pure, the protein was labelled with Cy3B as is. This is because the intensity of the *Pf*Hsp70 band was much higher than the impurities and that the second intense band at *ca*. 30-35 kDa was a probable degradation or truncation product of *Pf*Hsp70 that can bind to 2E6 (verified by Western blot analysis) and is useful for the fluorescence quenching competitive assay.

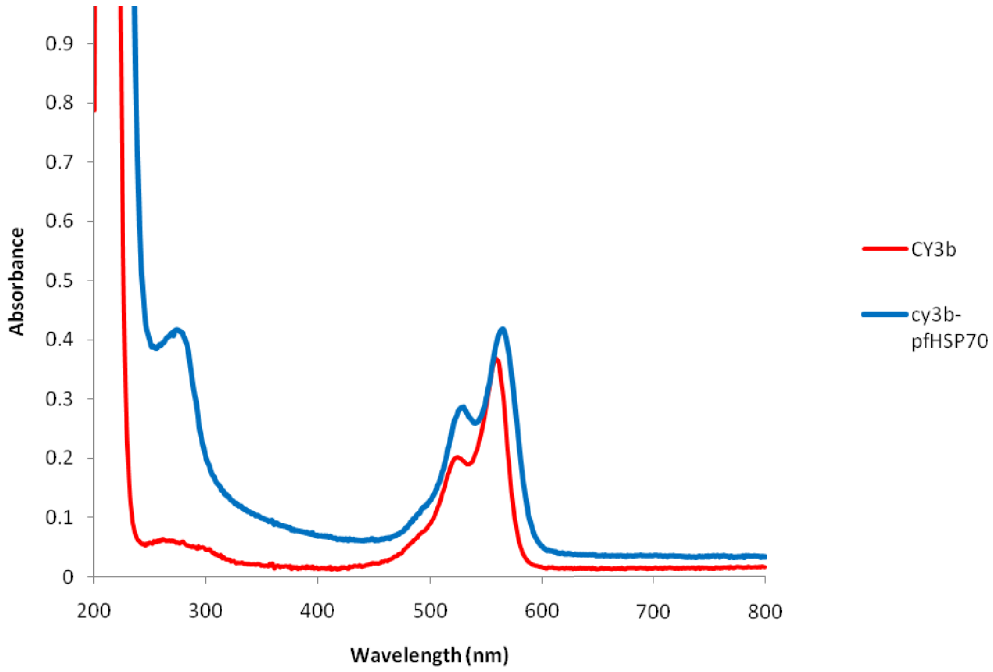

Figure 33. Absorbance spectra of free Cy3B (red trace) and of Cy3B-labelled *Pf*Hsp70 (blue trace). Shift in peak maximum occurred from 559 nm to 565 nm upon labelling. An additional band at 280 nm was found in case of Cy3B-labelled *Pf*Hsp70 but not in case of free Cy3B.

- Molar ratio of Cy3B to *Pf*Hsp70 was 2 : 1.

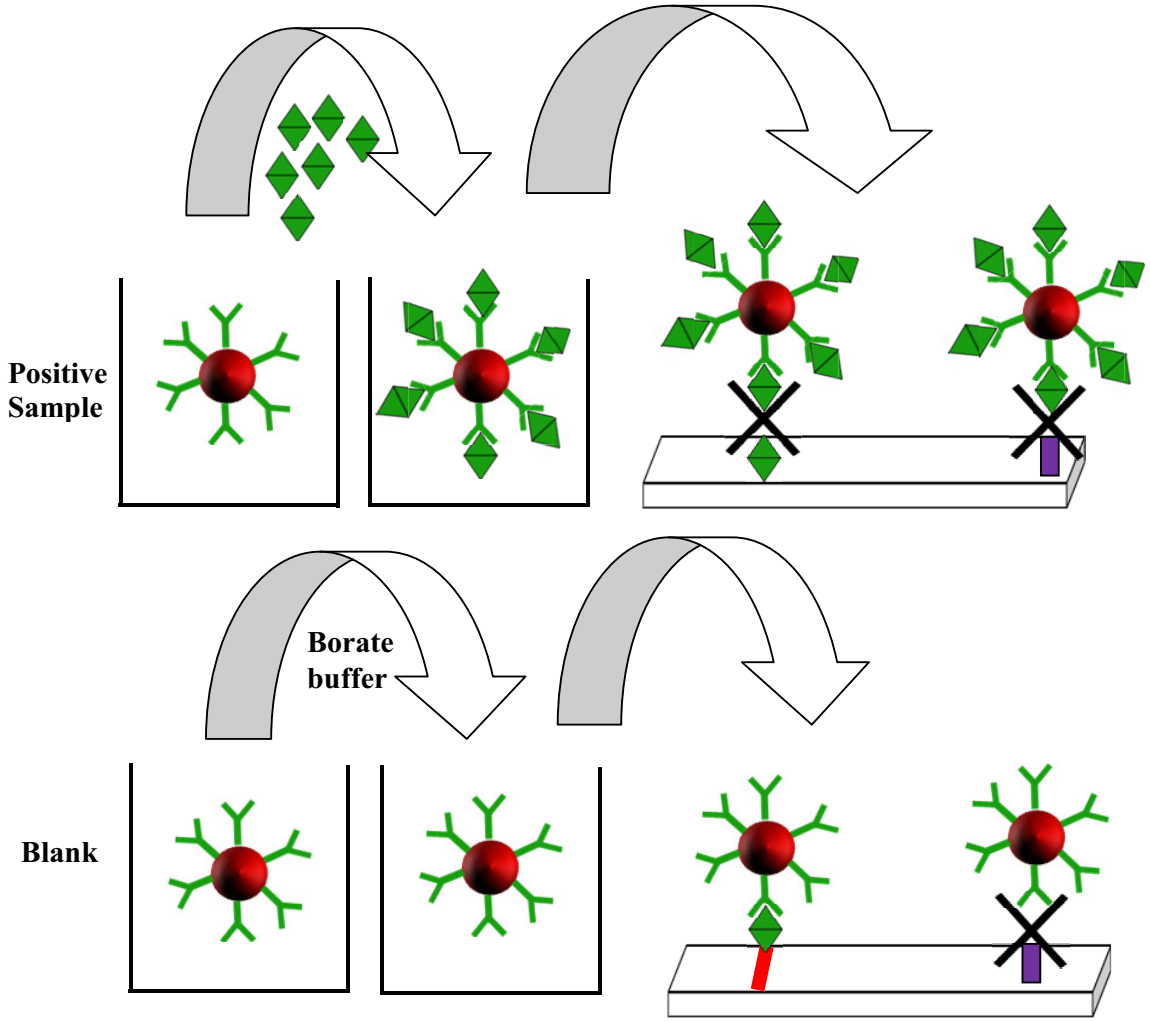

Figure 34. Chip competitive assay principle.

: AuNP-MUA-2E6

: Non-transformed RosettaBlue™ cells (negative control)

: *Pf*Hsp70

: red color produced on chip assay

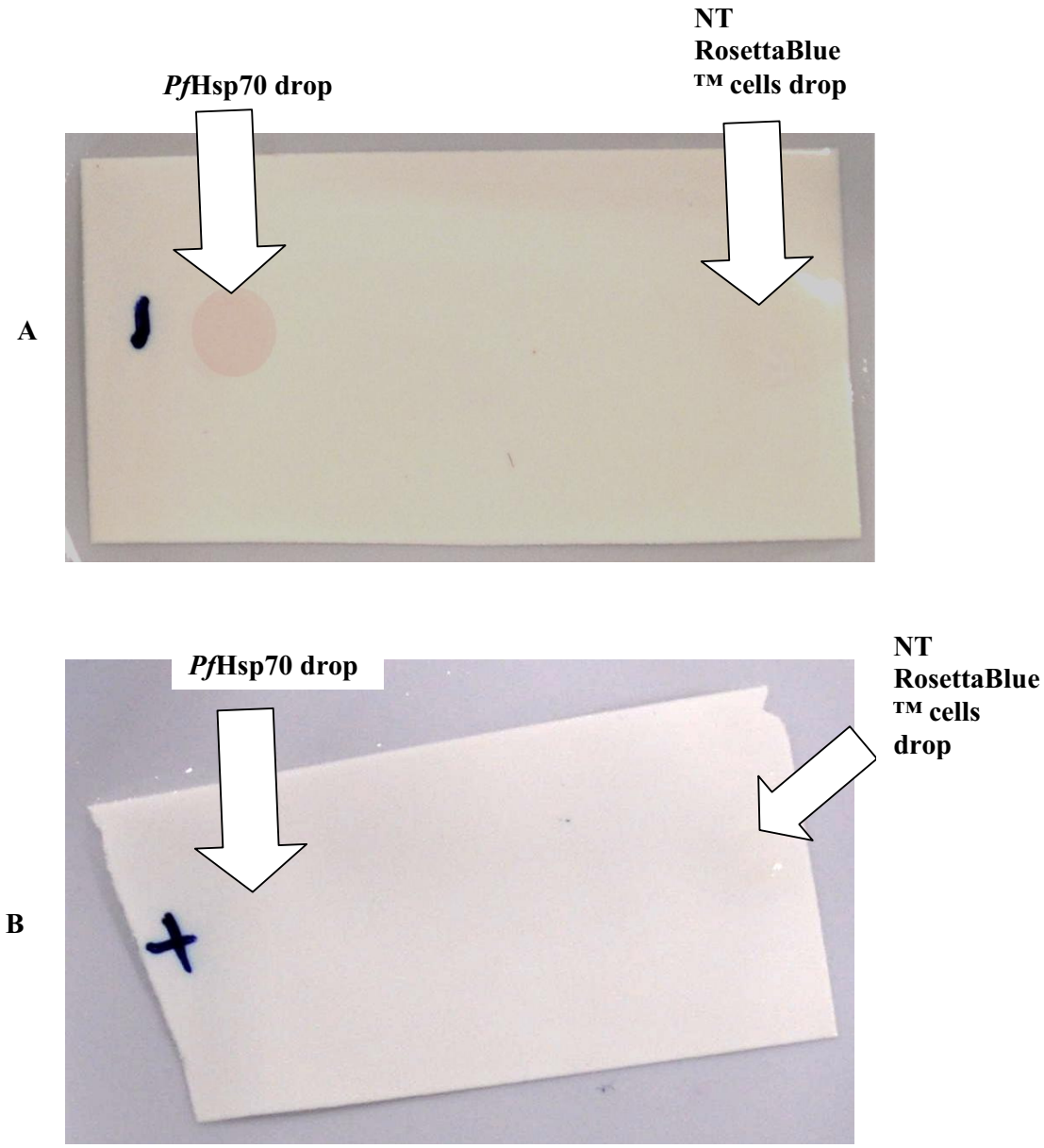

Figure 35. Prototype chip assay utilizing non-NHS/EDC bionanoconjugates. Non-NHS/EDC conjugates pre-incubated with either buffer (blank) or an overload of *Pf*Hsp70 (positive) were added to nitrocellulose strips having two spots of immobilized proteins: on the left, purified *Pf*Hsp70 was immobilized while on the right non-transformed RosettaBlue™ cells were immobilized. A. Blank sample; B: Positive sample.

- This figure shows that no red color was produced for the negative control. Since the chip assay is a competitive assay, a red color on immobilized *Pf*Hsp70 was produced in blank sample (binding sites of 2E6 are free) but not for positive sample.
- NT: non-transformed.

A

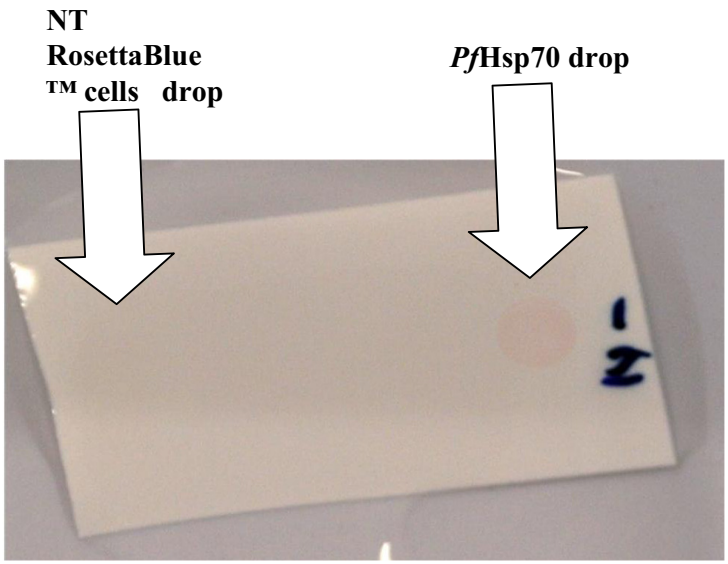

B

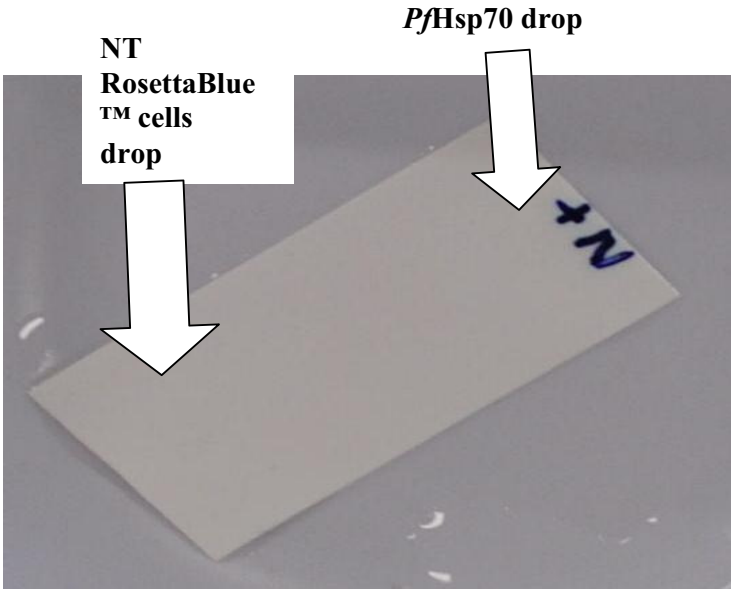

Figure 36. Prototype chip assay utilizing NHS/EDC bionanoconjugates. NHS/EDC conjugates pre-incubated with either buffer (blank) or an overload of *Pf*Hsp70 (positive) were added to nitrocellulose strips having two spots of immobilized proteins: on the right, purified *Pf*Hsp70 was immobilized while on the left non-transformed RosettaBlue™ cells were immobilized. A. Blank sample; B: Positive sample. This figure shows that no red color was produced for the negative control. Since the chip assay is a competitive assay, a red color on immobilized *Pf*Hsp70 was produced in blank sample (binding sites of 2E6 are free) but not for positive sample. Red color intensity on blank was found to be fainter compared to non-NHS/EDC BNCs (fig. 34).

- NT: non-transformed.

A

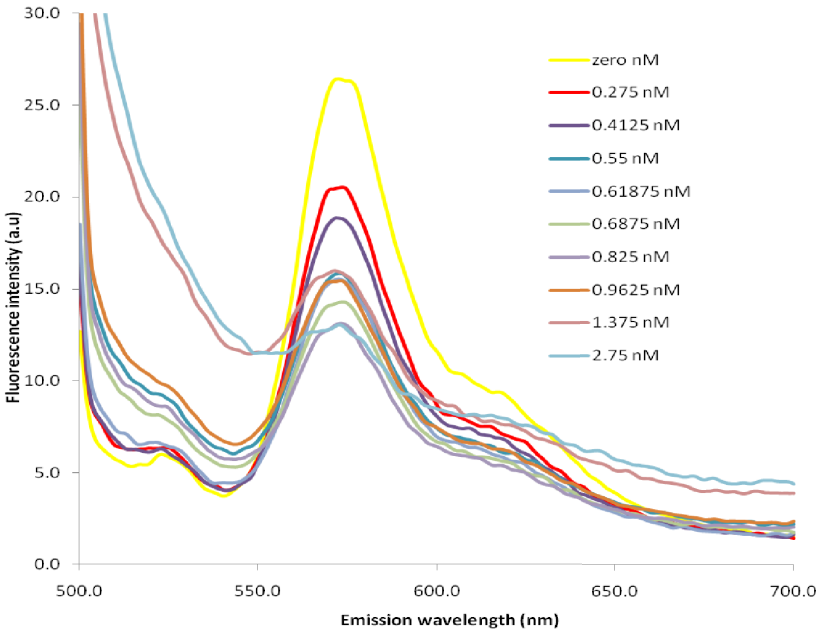

B

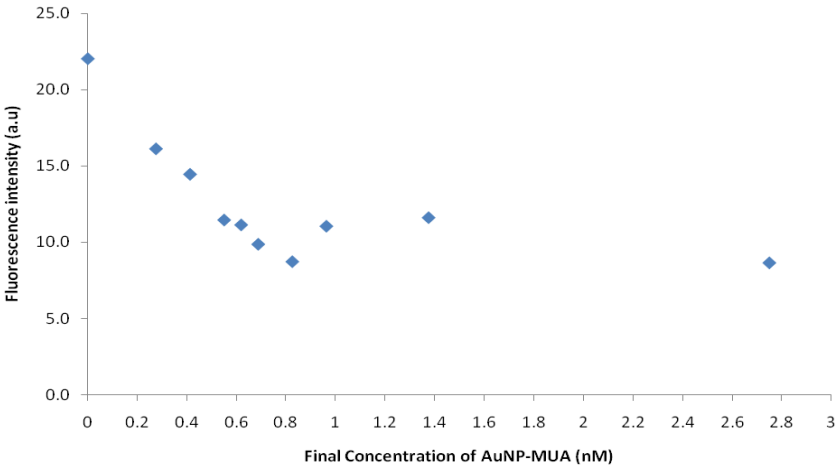

Figure 37. Quenching effect of AuNP-MUA on fluorescence emission of Cy3B-labelled *Pf*Hsp70. A: Fluorescence spectra of Cy3B-labelled *Pf*Hsp70 after adding different concentrations of AuNP-MUA. B: Fluorescence intensity at the peak maximum (after subtraction of the average buffer value) *vs*. the final AuNP-MUA concentrations. Linearity was achieved from concentration of AuNP-MUA ranging from 0 - 0.825 nM.

- Average buffer fluorescence intensity value is the average fluorescence emission value of the borate buffer alone at 572 nm; Excitation wavelength used was 480 nm.

A

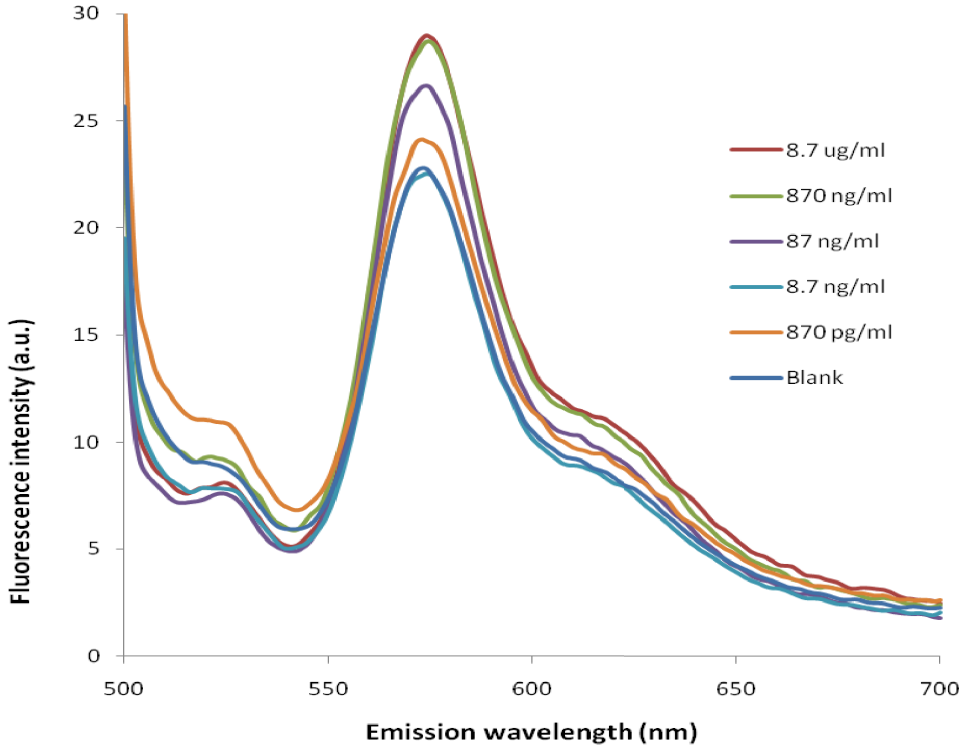
30
25
20
15
10
5
0
500
550
600
650
700
Fluorescence intensity (a.u.)
Emission wavelength (nm)
8.7 ug/ml
870 ng/ml
87 ng/ml
8.7 ng/ml
870 pg/ml
Blank

B

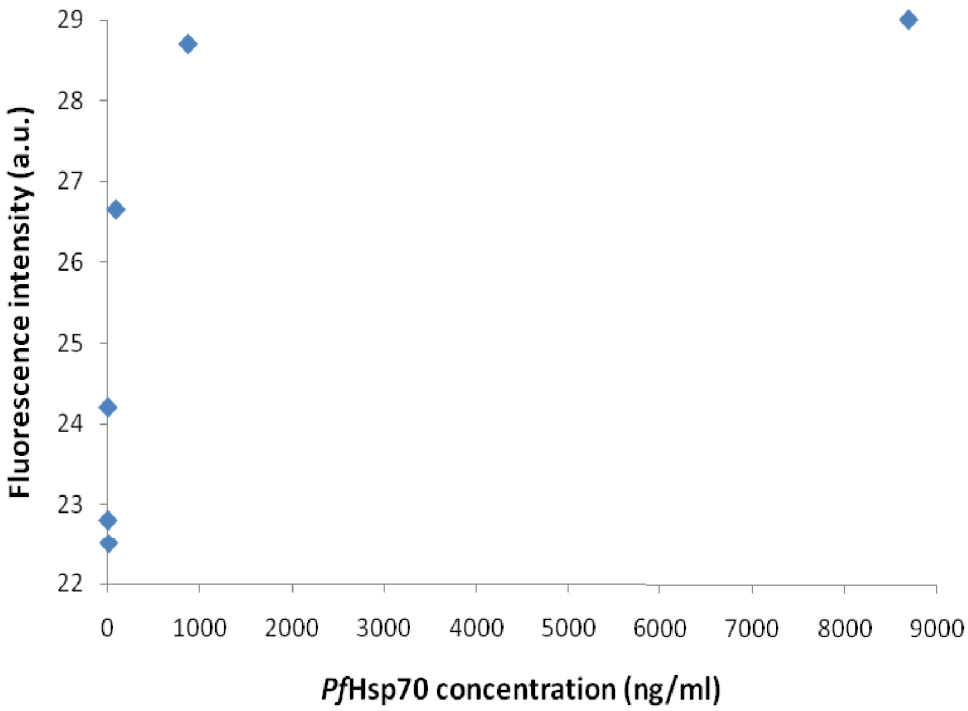
29
28
27
26
25
24
23
22
0
1000
2000
3000
4000
5000
6000
7000
8000
9000
Fluorescence intensity (a.u.)
*Pf*Hsp70 concentration (ng/ml)

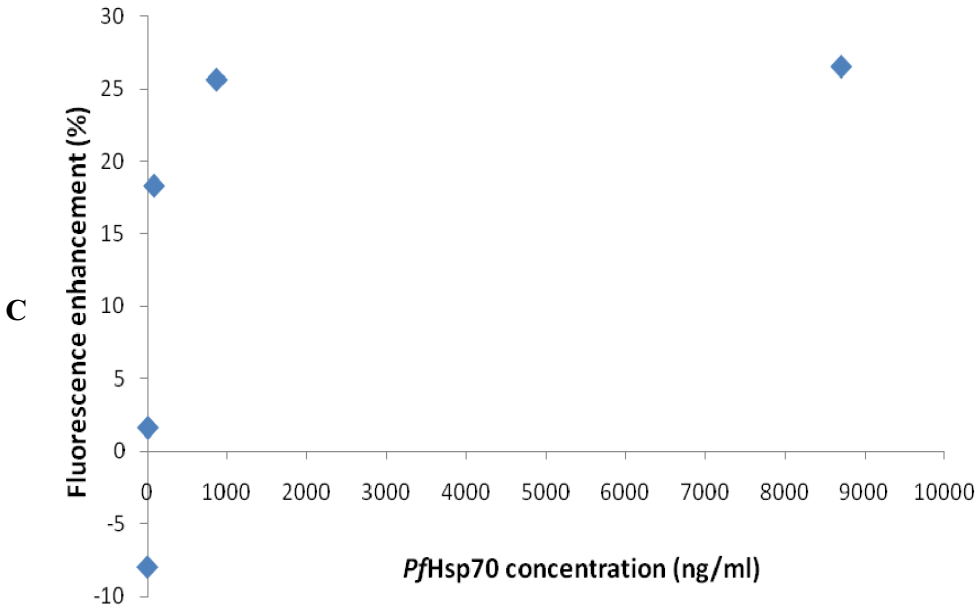

Figure 38. Fluorescence quenching competitive assay. Positive samples with different *Pf*Hsp70 concentrations (8.7 µg/mL; 870 ng/mL; 87 ng/mL; 8.7 ng/mL; 870 pg/mL) were analyzed by adding AuNP-MUA-2E6 (pre-incubated with different *Pf*Hsp70 concentrations) to Cy3B-labelled *Pf*Hsp70 and measuring fluorescence emission immediately. A: Fluorescence spectra of blank and positive samples. B: Fluorescence intensity at peak maximum for blank and positive samples. C: Fluorescence enhancement (%) for the 5 positive samples.

- Fluorescence enhancement was calculated as follows:

$$Fluorescence\ enhancement\,(\%) = \left(1 - \frac{Blank\ FI\ value - average buffer\ FI\ value}{Sample\ FI\ value - average buffer\ FI\ value}\right) \times 100$$

FI: fluorescence intensity; average buffer fluorescence intensity value is the average fluorescence emission value of the borate buffer alone at 574 nm; Excitation wavelength: 480 nm.

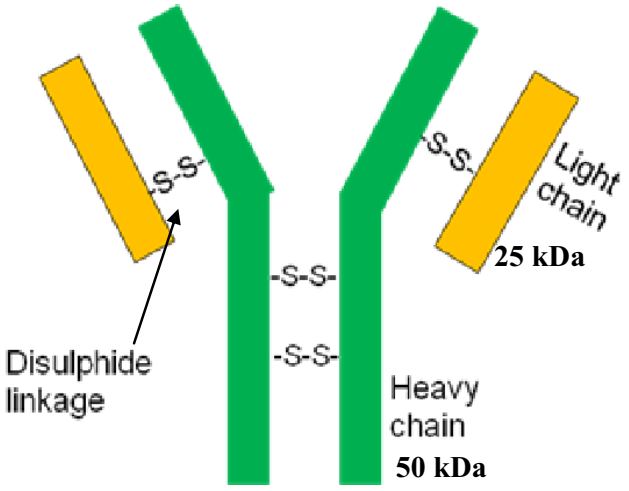

Figure 39. Structure of IgG antibody. Figure modified from[63].

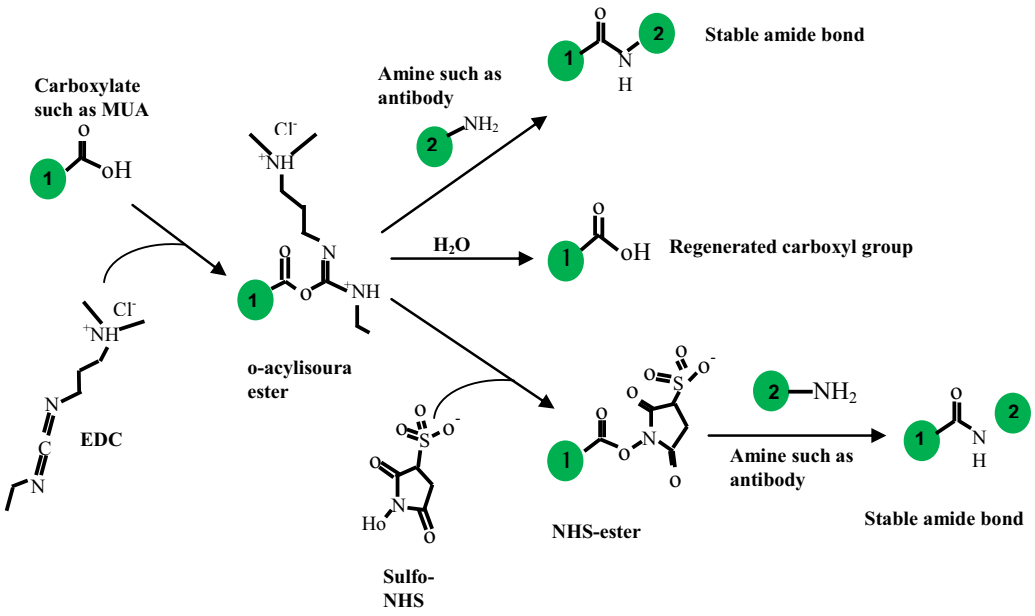

Figure 40. Principle of NHS/EDC cross-linking. EDC is a dehydrating agent that links a carboxyl-containing compound (such as MUA) to an amine-containing compound (such as 2E6) through the formation of an O-acylisourea intermediate. Although O-acylisourea intermediate is reactive with amine groups and gives an amide bond, it is susceptible to hydrolysis to give the free carbonyl group again. If Sulfo-NHS is added in the reaction media, it reacts with the unstable O-acylisourea intermediate forming an NHS-ester intermediate that is more stable and is also reactive with amine groups. Thus NHS enhances the cross-linking efficacy of EDC. Figure modified from [65-66].

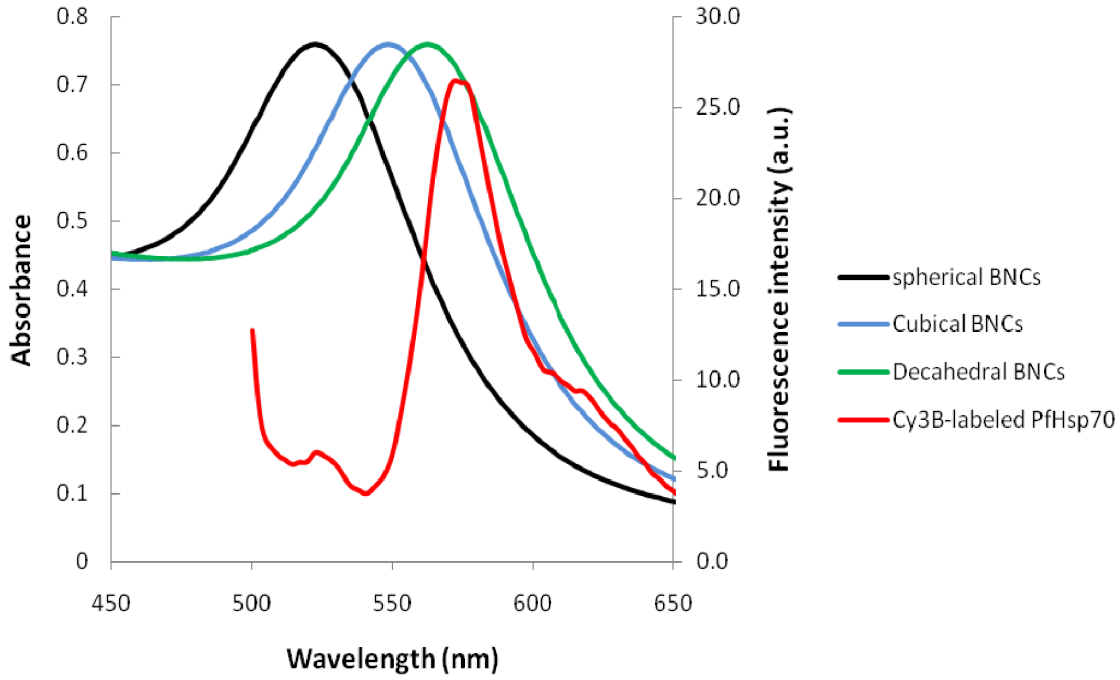

Figure 41. Fluorescence emission band of the Cy3B-labelled antigen overlaps with the absorbance spectra of antibody-conjugated AuNPs (different AuNP shapes: spherical, cubical and decahedral) [74-75]. Antibody-conjugated cubical and decahedral AuNPs absorbance spectra overlap better with the fluorescence emission spectra of Cy3B-labelled antigen compared to spherical particles.

CHAPTER 9. LIST OF TABLES

Table 1. The advantages and disadvantages of the different diagnostic assays for malaria. Table modified from[3]

Method	Type	Sensitivity	Advantages	Disadvantages
Light microscopy	Direct	• 50 - 100 parasites/µL • Can reach 10 parasites/µL in expert centres	• Standard method • Differentiates *Plasmodium spp* • Determines parasitemia level • Low direct cost	• Labour intensive • Requires technical expertise • Low turn-around time
Rapid diagnostic tests (RDTs)	Direct	100 parasites/µL	• Simple • Easy • Rapid • Requires minimal infrastructure and expertise • Cost effective	• Affected by field conditions such as heat and humidity • False positives with rheumatoid factor
Polymerase chain reaction (PCR)	Direct	1 - 5 parasites/µL	• Sensitive • Rapid • High throughput analysis • Method standardized • Differentiates *Plasmodium spp*	• High capital and operating costs • Advanced infrastructure needed • Trained personnel required
Flow cytometry	Indirect	Not applicable	• Uses standard hematology analyzers • Especially potentially useful for diagnosing clinically un-suspected imported malaria	• Expensive • Diagnosis should be confirmed via other methods
Laser desorption mass spectroscopy	Indirect	10 parasites/µL	• Rapid • Easy	• Very expensive equipment • Not availble in routine labs • Until now cannot differentiate between the different *P. sp*

¶: Sensitivity ranges from 49 - 98%. Sensitivity differs between semi-immune and non-immune populations.

Table 2. Composition of SDS-PAGE.

Resolving gel

Reagent	*Volume added for a 10% gel*	*Volume added for a 12.5% gel*
Water	2.01 mL	1.65 mL
Acrylamide 30%	1.665 mL	2.08 mL
1.5 M tris pH = 8.8	1.25 mL	1.25 mL
10% sodium dodecyl sulfate [SDS]	100 µL	100 µL
10% ammonium persulfate [APS]	15 µL	15 µL
Tetramethylethylenediamine [TEMED]	10 µL	15 µL

Stacking gel

Reagent	*Volume added for a 4%gel*
Water	1.525 mL
Acrylamide 30%	0.325 mL
0.5 M tris pH = 6.8	0.625 mL
10% sodium dodecyl sulfate [SDS]	25 µL
10% ammonium persulfate [APS]	12.5 µL
Tetramethylethylenediamine [TEMED]	2.5 µL

Table 3. Volume/concentration of AuNP-MUA added to quench fluorescence emitted by Cy3B-labelled *Pf*Hsp70.

Final concentration of AuNP-MUA (nM)	Volume of AuNP-MUA (11.03nM) added (µL)	Milli-Q water (µL)
0	0	200
0.275	10	190
0.41	15	185
0.55	20	180
0.61875	22.5	177.5
0.6875	25	175
0.825	30	170
0.9625	35	165
1.375	50	150
2.75	100	100

Table 4. Determination of the concentration of 2E6 antibody using BCA

µL of 2E6 added[¶]	Absorbance (562 nm)	(Absorbance - intersection with y axis) [¶¶] /gradient	Conc. (mg/mL) [¶¶¶] by dividing DF	Average conc. (mg/mL)	Average conc. (µM)
10	0.4309	15.9	3.18 by dividing by DF (5)	3.13	20.9
10	0.4507	16.8	3.36 by dividing by DF (5)		
20	0.7338	29.8	2.98 by dividing by DF (10)		
20	0.7394	30	3 by dividing by DF (10)		
30	0.9382	Off limit (outside standard curve)	NA	NA	NA
30	0.9763	Off limit	NA	NA	NA

[¶]: diluted 1 : 2 in sodium phosphate buffer

[¶ ¶]: of standard curve

[¶¶¶]: after adjusting dilution factor

Conc: concentration; DF: dilution factor; NA: not applicable

CHAPTER 10. APPENDIX

Table 1. Comparison between antibody binding to protein A and G. Table reproduced from [42].

2.4 Antibody binding to Protein A and protein G

Relative binding strengths for protein A and protein G

Species	Subclass	Protein A binding	Protein G binding
Human	IgA	variable	-
	IgD	-	-
	IgD	-	-
	IgG_1	++++	++++
	IgG_2	++++	++++
	IgG_3	-	++++
	IgG_4	++++	++++
	IgM	variable	-
Avian egg yolk	IgY	-	-
Cow		++	++++
Dog		++	+
Goat		-	++
Guinea pig	IgG_1	++++	++
	IgG_2	++++	++
Hamster		+	++
Horse		++	++++
Koala		-	+
Llama		-	+
Monkey (rhesus)		++++	++++
Mouse	IgG_1	+	++++
	IgG_{2a}	++++	++++
	IgG_{2b}	+++	+++
	IgG_3	++	+++
	IgM	variable	-
Pig		+++	+++
Rabbit		++++	+++
Rat	IgG_1	-	+
	IgG_{2a}	-	++++
	IgG_{2b}	-	++
	IgG_3	-	++
Sheep		+/-	++

++++ = strong binding
++ = medium binding
- = weak or no binding

Table 2. Comparison between FITC and Cy3B. Table reproduced from [71].

	Fluorescein isothiocyanate (FITC)	Cy3B-NHS
M_r	388	658
Wavelength of excitation	488 nm	558 nm
Wavelength of emission	525 nm	572 nm
Fluorescence lifetime	~ 4 ns	~ 2.8 ns
Fluorescence quantum yield	~ 0.5	> 0.67
pH sensitivity	pKa 6.4	Minimal
Non-specific binding	Binds to BSA	Minimal
Photostability	60% photobleached over 60 s	< 10% photobleached over 60 s
Purity	Mixed 5/6-ITC isomers	> 99% purity